DTU Wind

Overall design optimization of offshore wind farms

Videep Goverdhan Kamath

DTU Wind-M-0593
July 2023

Author: Videep Goverdhan Kamath

Title:
Overall design optimization of offshore wind farms

DTU Wind-M-0593
July 2023

Project period:
November 2022 - July 2023

ECTS: 45

Education: Master of Science

Supervisor(s):
Ju Feng
DTU Wind and Energy Systems

Simon Watson
TU Delft

Remarks:
This report is submitted as partial fulfillment of the requirements for graduation in the above education at the Technical University of Denmark.

DTU Wind and Energy Systems is a department of the Technical University of Denmark with a unique integration of research, education, innovation and public/private sector consulting in the field of wind and energy. Our activities develop new opportunities and technology for the global and Danish exploitation of wind and energy. Research focuses on key technical-scientific fields, which are central for the development, innovation and use of wind energy and provides the basis for advanced education.

Technical University of Denmark
Department of Wind and Energy Systems Frederiksborgvej 399
DK-4000 Roskilde
www.wind.dtu.dk

Overall design optimization of offshore wind farms

by

Videep Goverdhan Kamath

to obtain the degrees of

Master of Science
in Wind Energy
at Technical University of Denmark

Master of Science
in Aerospace Engineering
at Delft University of Technology

To be defended on the 26th of July 2023

Supervisors:	Simon Watson	TU Delft
	Ju Feng	DTU
Defence committee:	Michiel Zaayer	TU Delft
	Andrea Sciacchitano	TU Delft
Start date:	November 1st, 2022	
End date:	June 28, 2023	
Student numbers:	TU Delft:	5607515
	DTU:	s213777

An electronic version of this thesis is available at
`https://repository.tudelft.nl` and `https://findit.dtu.dk`

The code written for this thesis is available at
`https://github.com/videepgk/Overall-design-optimization-of-offshore-wind-farms`

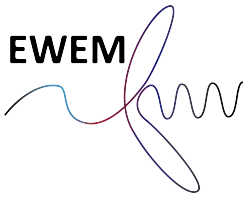

Abstract

The objective of this thesis is to build an optimization algorithm with the aim of optimizing layouts for two objective functions - Annual Energy Production (AEP) and Levelized Cost of Energy (LCoE), for large offshore wind farms. The algorithm considers the four main factors that are taken into account when creating a preliminary system design for an offshore wind farm. They are - the geographical location of the turbines, the hub height of the turbines, the type of the turbine, and the total number of turbines in the design space.

The annual energy production (AEP) of the wind farm is calculated using PyWake which uses the simple NOJDeficit wake model combined with the required superposition and blockage models to resolve wind turbine wakes. This AEP is then fed into TOPFARM, an economic solver developed at DTU which uses scaling factors to derive the total cost of the wind farm. Constant factors such as the discount rate, distance from shore, foundation type, and drivetrain type are also considered when deriving the total cost of the wind farm.

The results of this process are used to determine whether a system design is better than another. Several constraints are applied when changing each optimization variable to keep each iteration as realistic as possible. The boundary is assumed to be a square. Both algorithms arrive at similar results, with random search providing a much better solution with approximately a 40% reduction in LCoE.

Acknowledgements

I would like to express my deepest gratitude to all those who have supported and guided me throughout the journey of completing this thesis. Your invaluable contributions have been instrumental in shaping both my academic and personal growth.

First and foremost, I am indebted to my thesis advisors, Simon Watson and Ju Feng, for their unwavering guidance, patience, and expertise. If I can aspire to achieve even half the level of expertise that they have attained, I would consider it a significant accomplishment and a testament to their invaluable mentorship. Their insightful feedback and constant encouragement have played a pivotal role in shaping the direction and quality of this work.

I would like to extend my sincere appreciation to the faculty members of both TU Delft Aerospace and DTU Wind, whose profound wisdom and dedication to education have provided me with a solid foundation for my research. Their passion for knowledge and commitment to excellence have been a constant source of inspiration throughout my academic journey.

I am profoundly grateful for the invaluable assistance and unwavering friendship of my friends. Their support and guidance were utterly indispensable, and I can emphatically state that my successful completion of this program would not have been possible without their tremendous help. From helping me navigate the logistics of moving between Denmark and the Netherlands to their unwavering support in finding suitable housing, they have been there every step of the way.

Furthermore, I would like to express my gratitude to my mother and my girlfriend for their unwavering support and encouragement. Their belief in my abilities, love, and understanding have been the driving force behind my accomplishments. I would also like to pay tribute to my late father. Though he passed away last year, his memory and influence continue to inspire me every day. His unwavering belief in my potential and his constant encouragement to pursue my dreams will forever be etched in my heart. I am immensely grateful for the values he instilled in me and for his unwavering support throughout my academic journey.

Lastly, I want to express my sincere gratitude to the researchers, scholars, and authors whose work has laid the foundation for my thesis. Their groundbreaking contributions have been instrumental in shaping my research. I am eager to utilize the skills and knowledge gained through this thesis in my professional journey.

Videep Goverdhan Kamath
July 20, 2023

Contents

List of Figures

List of Tables

Nomenclature

AC	Alternating Current
ACO	Ant Colony Optimization
AEP	Annual Energy Production
AWEA	American Wind Energy Association
BNEF	Bloomberg New Energy Finance
CFD	Computational Fluid Dynamics
CN	China
CO2	Carbon Dioxide
COE	Cost of Energy
DC	Direct Current
DE	Differential Evolution
EUR	Euro
GA	Genetic Algorithms
GER	Germany
GHG	Greenhouse Gas
GW	Gigawatt
H	Hour
J	Joule
kg	Kilogram
km	Kilometer
kW	Kilowatt
LCOE	Levelized Cost of Energy
m	Meter
MILP	Mixed-Integer Linear Programming
NREL	National Renewable Energy Laboratory
PPA	Power Purchase Agreement
PSO	Particle Swarm Optimization
RPM	Revolutions Per Minute
s	Second
TWh	Terawatt-hour
UK	United Kingdom
USA	United States of America
V	Volt
WTG	Wind Turbine Generator

CHAPTER 1

Introduction

This chapter introduces the main topic and objectives of this thesis project. Some relevant information regarding the tools used is provided, and the section concludes with the final aim of the project, along with the research questions.

1.1 Importance of wind energy

According to Gielen et al. [41], carbon emissions will rise from 33 gigatons in 2015 to 35 gigatons in 2050 under current and planned policies as seen in Figure 1.1. According to Petrović et al. [76], the main reason for this increase in emissions is the accelerated development of the global economy is leading to increasing consumption of natural resources. If the Paris agreement were to be followed, these emissions need to fall to 9.7 gigatons and renewable energy will be responsible for 94% of these reductions according to [41], and the share of renewable energy in total primary energy supply would rise from 14% in 2015 to 63% in 2050.

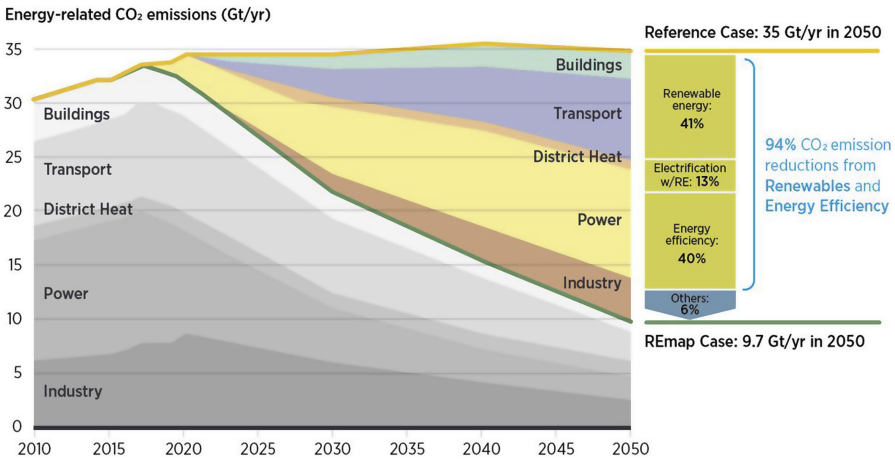

Figure 1.1: Projected increase in emissions [41]

According to Kumar et al. [56], in regions like Europe, wind energy is a much more reliable source of renewable energy (compared to solar) and around 50% of Europe's electricity is projected to be from wind by 2050. Due to recent geopolitical tensions, this notion of wind being very important in Europe has been solidified even further. According to Siemens Gamesa Renewable Energy S.A. et al. [92], wind can provide Europe with energy security and independence through domestic, clean and competitive sources. The importance of this has certainly been highlighted with Russia's war of aggression against Ukraine. It is also important to note that between 2011 and 2021, the wind industry reduced the global average cost of electricity from wind turbines by more than 70%, making wind energy one of the world's cheapest energy sources.

1.2 Offshore wind power

According to Kumar et al. [56], the renewable energy industry in Europe is turning to offshore wind to meet global demand. The amount of offshore wind being installed in Europe is rising every year as evidenced by Figure 1.2. There are several advantages of placing wind turbines offshore. This includes better and stronger wind resource, negligible visual impact, and lower noise pollution for humans. Offshore wind farms also present certain challenges such as tougher installation and maintenance procedures(in most cases), larger CAPEX requirement, and more endangerment to human life due to unpredictable conditions in the ocean.

Figure 1.2: Wind power installation statistics, taken from [56]

Wind energy, highlighted by the North Sea wind power hub project in Efi Koutsokosta et al.'s work [33], has taken center stage in terms of global renewable energy goals. As the global populace continues to expand, it has resulted in a 2% annual rise in global energy demands. Surprisingly, despite the evident environmental impacts, fossil fuels are still responsible for over 70% of worldwide energy consumption. Especially necessary for achieving our objectives is higher implementation of renewable energy sources, such as wind. This requires more wind farms, as well as more refining of current procedures to better harness the available wind reserves.

The consequences of going offshore, both positive and negative, contribute to certain differences between onshore and offshore turbines. According to Muhammad Arshad et al. [4], offshore turbines are larger and have a lower hub height due to better wind resource at lower altitudes compared to onshore turbines. According to Muhammad Arshad et al. [4], the turbines are also exponentially larger than their onshore counterparts since it allows for greater power generation. This also means that a lower amount of turbines are required to reach the same capacity which leads to lower costs. The cost of these wind farms is calculated using a term known as the Levelized Cost of Energy (LCOE) which tells us the cost per kWh generated. In conclusion, offshore wind farms are much more efficient due to higher wind speeds, greater reliability and lower visual and noise impact.

1.3 Wind farm design problem

The design of a wind farm includes several defining choices that need to be made. According to Naima Charhouni et al. [17], seeking for an appropriate design of wind farm (WF) layout

constitutes a complex task in a wind energy project. Designing a wind farm layout refers to the optimal placement of each wind turbine within the boundary to maximize or minimize a certain objective function.

The system and layout design is essential to the planning and operation of all wind farms. The system design of a wind farm involves providing the overall design of a wind farm. According to Naima Charhouni et al. [17], parameters such as the geographical layout, inter-array cabling, transformer location, boundaries, total number of turbines, types of turbines, etc are defined in the system design phase of the project. Although, offshore wind came into existence much later than onshore wind, the former results in various additional challenges when it comes to system design. According to Bosko Rasuo et al. [82], additional parameters such as marine soil conditions, wave loading, wave depth, distance to shore, installation vessels, foundation types, etc are also investigated. But, due to higher and more reliable wind resource coupled with the lack of land for onshore wind farms, offshore wind farms are becoming increasingly dominant in the wind energy sector.

The performance of an offshore wind farm is affected by several factors, with the geographical layout of the WTG's being one of the most important. According to N. Moskalenko et al. [71], wind turbine wakes have a detrimental effect on downstream wind turbines, creating a velocity deficit leading to a lower power production. Wind farm wakes lead to large velocity deficits in the near wake and mixing layers in the intermediate wake regions (as seen in Figure 1.3), leading to power loss. Wind farm optimization aims to provide an optimal layout with minimized wake losses. There are many wind farm optimization techniques such as random search, genetic algorithm, particle swarm optimization (PSO), firefly algorithm, etc. These are elaborated in section 2.2. According to Ying Chen et al [18], the overall power produced by a turbine also inherently depends on it's hub height, since a higher hub height means greater wind resource leading to higher power production. This can also be used to minimize wake losses since turbines at a higher hub height will produce wakes that are higher than turbines at a lower hub height, leading to lower wake losses.

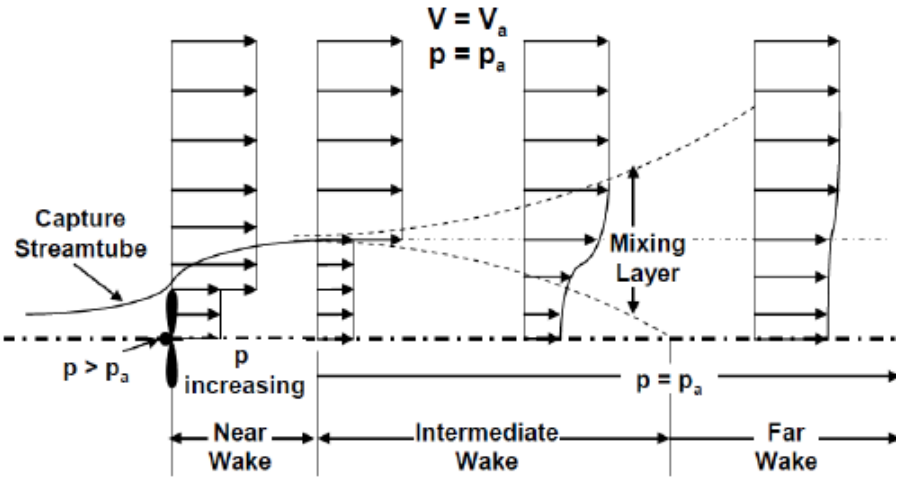

Figure 1.3: Different regions of a wind turbine wake, image taken from [71]

According to Ju Feng et al. [34], wind farm power production also depends on the type of turbine used, along with the total number of wind turbines used. Obviously, a larger number of wind turbines that have an inherently larger rated power will lead to greater power production,

but will also lead to a much higher cost in other aspects such as transport and installation.

1.4 Aim of project

According to Atul Khan Kumar et al. [56], the need for the shift towards renewable energy, with wind power being at the forefront of the transition has led to an increase in the amount of research required in optimizing wind farm designs. By defining certain optimization variables such as turbine positions and hub heights, a wind farm design problem can be developed, which when solved within realistic constraints leads to lower costs and higher power. Therefore, this thesis aims to define a set of optimization variables and constraints, formulate a wind farm design problem and solve it, arriving at an optimal wind farm design.

1.5 Research Questions and objectives

In this section, broad research questions have been formulated according to the project in mind.

1. **How can an optimal windfarm layout design be derived using the defined variables and constraints using the random search and PSO based algorithms?**
    a) How much of a decrease in the LCOE can be observed?
    b) What are the similarities and differences between random search and PSO? Which one gives better results?
2. **Considering the criteria defined in the problem, how is the LCOE defined as an objective function for an offshore wind farm?**
    a) What impact does varying the hub height have on the value of the cost model function?
    b) Can a higher number of WTG's lead to a lower LCOE? If yes, is the LCOE objective function valid?
3. **Can an optimal design have the lowest LCOE while also having the highest AEP?**
    a) What are the main design variables for an increase in AEP which cause a detrimental increase in LCOE, and vice versa?
    b) Which design variables are neglected and when can they have large impacts on the layout design?

It should be kept in mind that Question number 3 can only be successfully answered when a global maximum is found. As suggested in previous sections and in Ju Feng et al. [34], it is quite difficult to arrive at a global maximum for such highly constrained problems. Therefore, project completion is dependent solely on the first 2 questions.

CHAPTER 2
Literature Review

This literature review was conducted over the course of the project. It includes the history of developing wind turbines, wind farms and the accompanying design problems. This is followed up by a section on optimization algorithms, their types and their uses. The section concludes by describing the two case studies used in this thesis, and previous work conducted on each.

2.1 History of Wind Farms

Wind power has been harnessed for centuries, with early evidence of windmills dating back to ancient Persia in the 7th century [3]. Nevertheless, the making of contemporary wind farms - defined by centralized wind turbine installations - gained momentum in the latter part of the 20th century. The account of wind farms is classifiable into many critical phases, each marked by notable advances and important points.

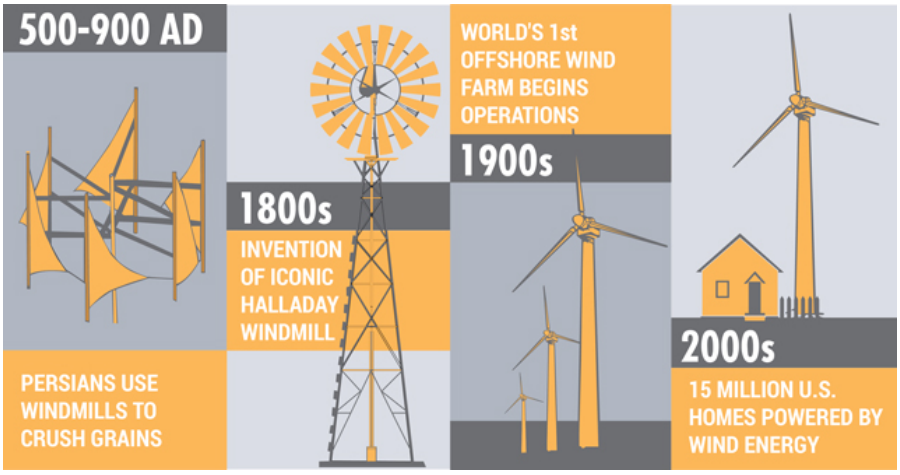

Figure 2.1: History of wind turbines [96]

2.1.1 Early Experiments and the Birth of Wind Power Generation

The concept of generating electricity from wind was first explored in the late 19th century. In 1888, Charles F. Brush installed the first automatic wind turbine for electricity generation in Cleveland, Ohio, USA [65]. This early design featured a large, multi-blade rotor and produced electricity for local lighting. Although the capacity of these early wind turbines was modest, typically ranging from a few kilowatts to a few hundred kilowatts, they laid the foundation for the development of larger-scale wind power generation.

2.1.2 Rise of Wind Farms: 1970s to 1990s

Due to mounting concerns regarding environmental pollution and depletion of fossil fuels, wind farms became a focal point during the 1970s. This era signified a crucial period for the industry, with a renewed interest in generating electricity through wind power. In 1975, the first commercial wind farm, consisting of 20 turbines with a total capacity of 4.5 MW, was installed in New Hampshire, USA [65].

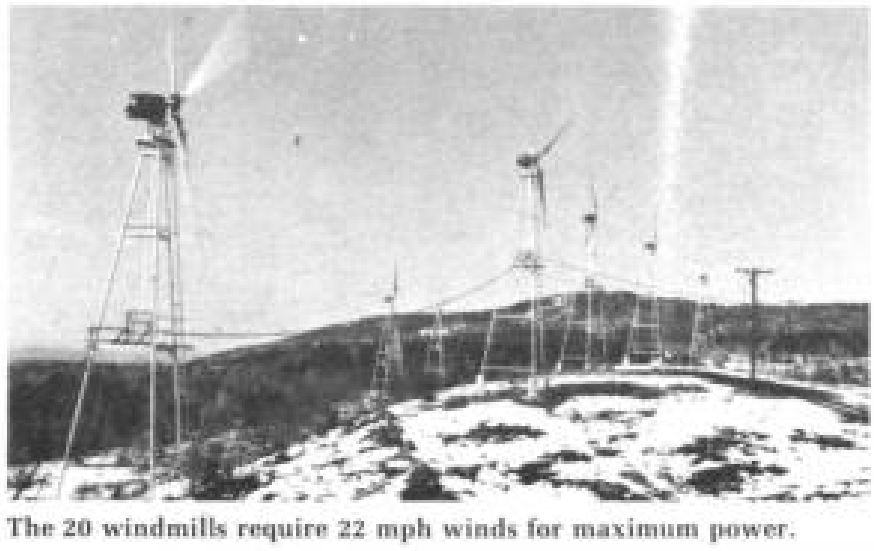

Figure 2.2: First commercial wind farm in New Hampshire [91]

During the 1980s and 1990s, wind farms began to emerge on a larger scale, particularly in Europe. In Denmark, government support and favorable wind conditions facilitated the establishment of several wind farms. Notable examples include Vindeby Offshore Wind Farm, commissioned in 1991, and the larger Middelgrunden Offshore Wind Farm, commissioned in 2000 [60]. These early wind farms demonstrated the feasibility and potential of large-scale wind power generation.

(a) Vindelby wind farm **(b)** Middelgrunden wind farm

Figure 2.3: Newer wind farms

2.1.3 Technological Advancements and the Modern Era

The turn of the 21st century witnessed significant technological advancements that propelled the growth of wind farms. One notable advancement was the introduction of horizontal-axis, three-blade wind turbines. This design, which became prevalent in the 1980s, significantly improved efficiency and reliability, leading to increased adoption of wind farms worldwide [3].

The capacity of wind turbines also continued to increase during this period. In 2002, the first 2 MW turbine, the Vestas V80, was introduced, showcasing significant improvements in energy conversion efficiency and reliability. Subsequently, larger turbines with capacities exceeding 5 MW and rotor diameters reaching 150 meters or more became feasible [39].

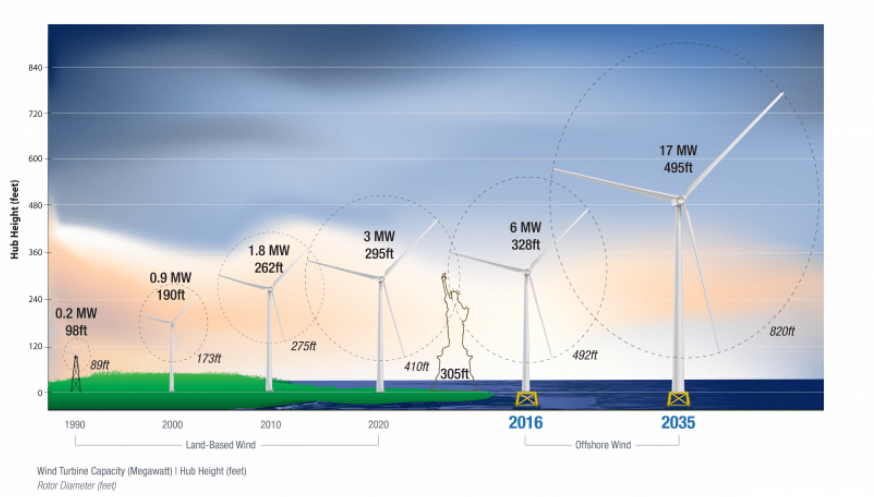

Figure 2.4: Development of wind turbines [104]

Moreover, advancements in blade design, materials science, and control systems played a crucial role in the optimization of wind farm performance. Innovative aerodynamic designs, such as the use of airfoil shapes and curved blade profiles, improved energy capture and conversion efficiency [15]. The incorporation of advanced materials, such as carbon fiber composites, made turbine blades lighter, stronger, and more resistant to fatigue, enabling them to withstand harsh environmental conditions and operate for longer duration [95]. Additionally, advanced control systems and sensors allowed for optimal operation and protection of wind turbines, optimizing power production and ensuring safe and reliable performance [15].

2.1.4 Optimization of Wind Turbines

The optimization of wind turbine design has been a continuous focus in the history of wind farms. Early wind turbines were relatively simple in design, featuring fixed-speed operation and stall-regulated rotor control. However, researchers and engineers recognized the need to enhance turbine performance and improve energy capture.

In the 1990s, the development of variable-speed wind turbines with pitch-regulated control systems revolutionized the industry. These turbines offered improved efficiency and better control over power output, enabling them to operate optimally in varying wind conditions. The introduction of power electronics and advanced control algorithms further enhanced turbine performance by reducing loads and increasing reliability [15].

Furthermore, advancements in aerodynamics and materials science have led to the design of more aerodynamically efficient rotor blades and lighter, yet durable, turbine components. The integration of advanced sensors and data analytics has enabled condition monitoring and predictive maintenance strategies, improving the reliability and lifespan of wind turbines.

2.1.5 Optimization of Wind Farm Layouts

As wind farms grew in size and complexity, researchers and industry professionals recognized the importance of optimizing wind farm layouts to maximize energy production and minimize wake effects. Early wind farm designs were often based on intuitive or ad hoc placement of turbines, without considering the intricate aerodynamics involved.

In the late 1990s, research efforts focused on developing optimization algorithms and methodologies to address the challenges of wind farm layout optimization. These approaches aimed to find the most efficient arrangement of turbines considering factors such as wind flow patterns, wake effects, and land constraints.

The use of computational models, such as the Jensen wake model [50], and optimization algorithms, such as genetic algorithms [70], particle swarm optimization [31], and simulated annealing [54], revolutionized wind farm layout design.

Researchers began exploring different optimization objectives, including maximizing power output, minimizing wake losses, reducing installation costs, and optimizing maintenance accessibility. Furthermore, optimization algorithms were extended to consider uncertainties in wind conditions, turbine performance, and other variables to enhance the robustness of the optimized layouts.

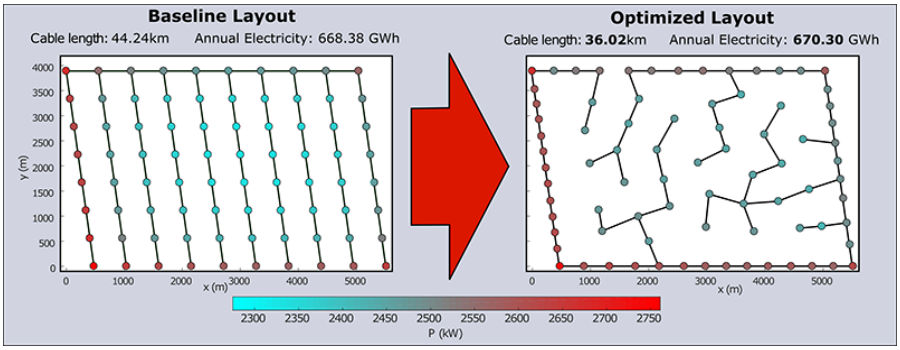

Figure 2.5: Wind farm layout optimization [57]

The field of wind farm layout optimization continues to evolve rapidly, with ongoing research focusing on advanced modeling techniques, optimization algorithms, and real-time control strategies. The ultimate goal is to design wind farm layouts that maximize energy capture, minimize environmental impacts, and ensure long-term economic viability.

2.1.6 Offshore Wind Farms and Global Expansion

In harnessing ample wind resources and creating minimal impact on the onshore environment, offshore wind farms have progressively gained popularity. Development of these farms has been pioneered by countries such as Germany, China, and the UK.The London Array, commissioned in 2013 in the United Kingdom, boasts a capacity of 630 MW and was the world's largest

offshore wind farm at the time [69]. Furthermore, China has rapidly expanded its offshore wind sector, with the installation of the Guangdong Yangjiang Offshore Wind Farm, boasting a capacity of 2,000 MW [108].

One notable offshore wind farm that played a pivotal role in the advancement of offshore wind energy is Horns Rev 1. Located in the North Sea, approximately 14 kilometers off the coast of Denmark, Horns Rev 1 holds historical significance as the first large-scale offshore wind farm to be commissioned in 2002 [101]. The site was carefully selected due to its favorable wind conditions and proximity to existing transmission infrastructure, facilitating efficient power delivery to the onshore grid.

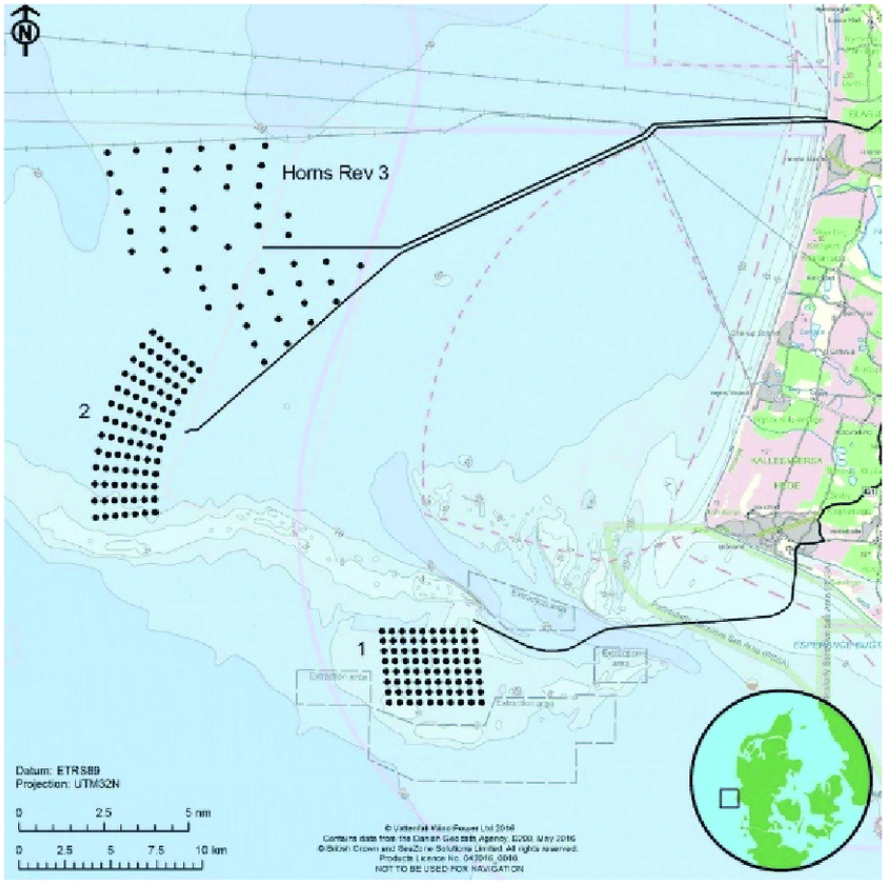

Figure 2.6: Horns Rev phases and layouts [21]

Horns Rev 1 was developed in multiple phases and demonstrated significant technological advancements in offshore wind energy. The initial phase consisted of 80 wind turbines, each with a capacity of 2 MW, resulting in a total capacity of 160 MW. The turbines were installed on monopile foundations firmly anchored to the seabed [101]. The wind farm covers an area of approximately 20 square kilometers and operates at water depths ranging from 5 to 17 meters.

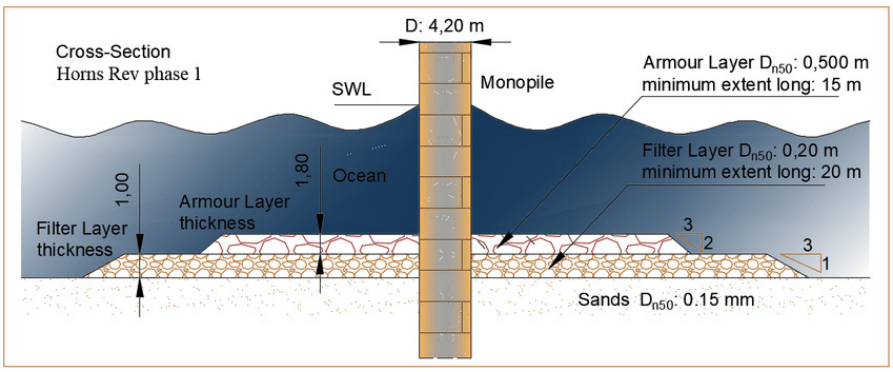

Figure 2.7: Horns Rev 1 foundation and scour protection [32]

The success of Horns Rev 1 paved the way for subsequent offshore wind farm projects, both in Denmark and globally. It served as a testbed for exploring the technical and economic feasibility of offshore wind energy, contributing to the growth and maturation of the industry. The experience gained from Horns Rev 1, including lessons on installation, grid integration, maintenance, and environmental impact assessment, played a crucial role in shaping the development of future offshore wind farms.

Figure 2.8: Vestas V80, turbine used in Horns Rev 1 [12]

Horns Rev 1 continues to operate today, showcasing the long-term reliability and economic viability of offshore wind energy. The site also serves as an important research and innovation hub, facilitating ongoing studies and technological advancements in offshore wind farm design, operation, and maintenance.

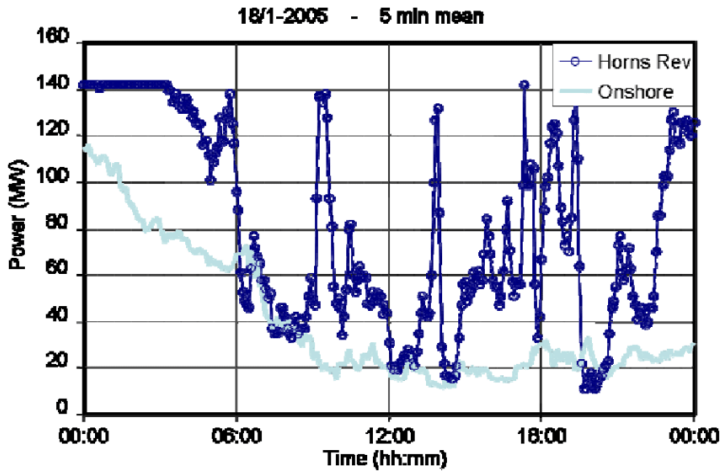

Figure 2.9: Power generation statistics on a random day for Horns Rev 1 [93]

Offshore wind energy has taken off globally, with Horns Rev 1 leading the way. From government to industry, everyone sees the potential for offshore wind power to reduce greenhouse gas emissions and clean up our energy production. As offshore wind farms evolve through technological advancements and increased scale, they'll become even more vital to a sustainable, low-carbon future.

For this thesis, Horns Rev 1 is chosen as the case study due to its historical significance and contributions to the advancement of offshore wind energy. Horns Rev 1 is the first large-scale offshore wind farm to be commissioned in 2002 [101]. Offshore wind farm development showcases its technical, economic, and environmental aspects ideally, as exemplified by its being situated 14 kilometers from Denmark's coast, in the North Sea.

Throughout its lifespan, the Horns Rev 1 has been subject to in-depth analysis of its design, construction, operation, and lessons learned, making it a prime case study for selection. By studying the historical development and performance of Horns Rev 1, valuable insights can be gained regarding the challenges and opportunities associated with offshore wind energy deployment. Additionally, the case study provides a basis for evaluating the effectiveness of optimization techniques in enhancing the energy production and cost-efficiency of offshore wind farms.

The experience gained from Horns Rev 1, including lessons on installation, grid integration, maintenance, and environmental impact assessment, can be used to inform future offshore wind farm projects. By examining the success factors and challenges encountered in the development and operation of Horns Rev 1, this thesis aims to contribute to the knowledge and understanding of offshore wind energy and provide practical recommendations for the design and optimization of future offshore wind farms.

Horns Rev 1 is a long-term operating offshore wind farm. This presents an opportunity to assess offshore wind's reliability, performance, and economics over time. The case study serves as a real-world example of offshore wind farms' feasibility and sustainability as a key component of the global energy transition.

By focusing on Horns Rev 1 as the case study, this thesis aims to contribute to the body of knowledge surrounding offshore wind farm development, optimization, and long-term operation. Through the analysis of this landmark project, valuable insights can be gained to further advance the deployment of offshore wind energy on a global scale.

2.1.7 Current Trends and Future Prospects

Wind energy has become an integral part of the global energy mix, with the cumulative installed wind capacity exceeding 700,000 MW by the end of 2021 [81]. Ongoing research focuses on enhancing turbine efficiency, integrating wind power into existing grids, exploring innovative floating wind farms, and advancing the optimization of wind farm layouts.

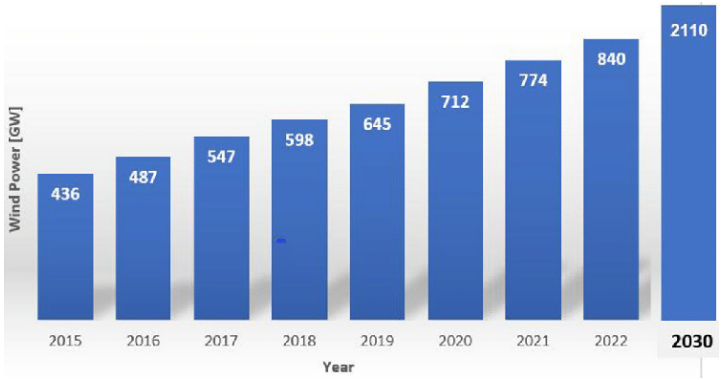

Figure 2.10: Projected growth of installed wind capacity [23]

With the advent of machine learning, artificial intelligence, and big data analytics, wind farm layout optimization is expected to benefit from more sophisticated and data-driven approaches. The incorporation of real-time data, advanced wake modeling techniques, and multi-objective optimization algorithms will enable the design of wind farms that maximize energy production while considering environmental, social, and economic factors.

Wind farms hold a tremendous capability for meeting the world's increasing electricity needs in a sustainable and environmentally friendly manner. Continued studies and innovation in wind turbine layout and optimization, in addition to wind farm layout optimization, will play a crucial position in realizing this ability.

2.2 Optimization Algorithms in Wind Farm Layout Design

Wind farm layout design involves determining the optimal arrangement of wind turbines within a given area to maximize energy production while considering various constraints. Optimization algorithms play a crucial role in this process by exploring the design space efficiently. In this section, we will discuss the history of wind farm optimization, optimization algorithms commonly used in wind energy, Random Search, and Particle Swarm Optimization (PSO).

2.2.1 History of Wind Farm Optimization

The optimization of wind farm layouts has gained significant attention over the years. Early studies focused on simplistic approaches such as grid-based layouts or regular arrangements of turbines. However, it became clear that these approaches did not fully capture the complexities of wind flow patterns and resulted in suboptimal energy production.

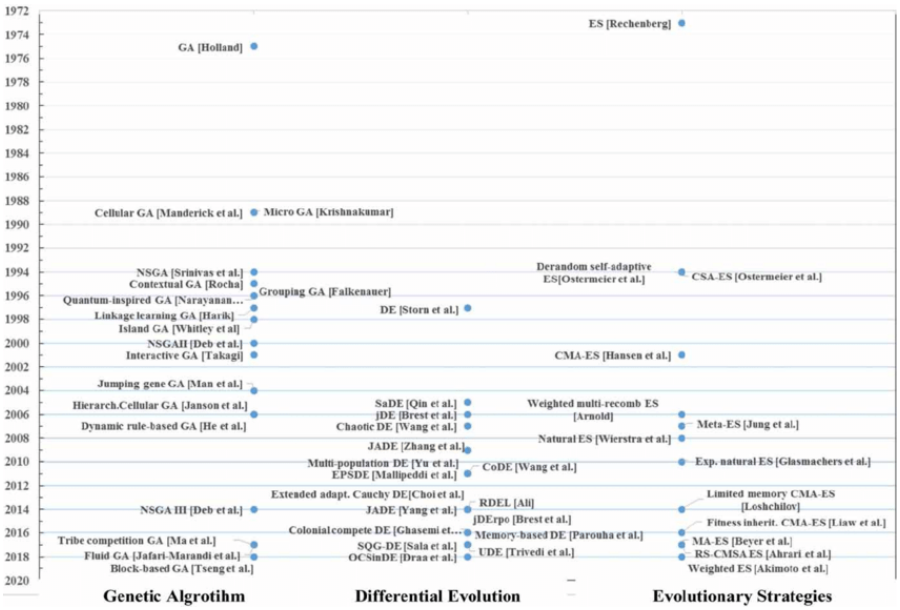

Figure 2.11: History of optimization algorithms [49]

As computational power increased, researchers began developing more sophisticated optimization techniques. Evolutionary algorithms, such as Genetic Algorithms (GA), became popular for wind farm layout optimization due to their ability to handle multiple objectives and complex constraints. These algorithms employ concepts inspired by natural evolution, such as selection, crossover, and mutation, to iteratively improve the layout designs.

2.2.2 Optimization Algorithms Used in Wind Energy

Various optimization algorithms have been applied to wind farm layout design, each with its advantages and limitations. These algorithms include gradient-based methods, heuristic algorithms, metaheuristic algorithms, and evolutionary algorithms.

Gradient-based methods, such as gradient descent, aim to find the optimal layout by iteratively adjusting the turbine positions based on the gradient of the objective function. However, these methods can often get trapped in local optima and struggle with the nonlinearity and complexity of wind flow simulations.

Heuristic algorithms, such as random search and simulated annealing, explore the design space by iteratively sampling turbine locations. While simple to implement, these algorithms can require a large number of iterations to converge and may struggle to find globally optimal solutions. For instance, Feng et al. [36] used a random search algorithm to optimize wind turbine layouts considering wake effects and wind resource variability. Their results demonstrated that random search can efficiently explore the design space and provide near-optimal solutions.

Metaheuristic algorithms, such as Ant Colony Optimization (ACO) and Tabu Search, are inspired by natural phenomena or problem-solving strategies. They offer a balance between exploration and exploitation of the design space, often achieving good results in wind farm layout optimization.

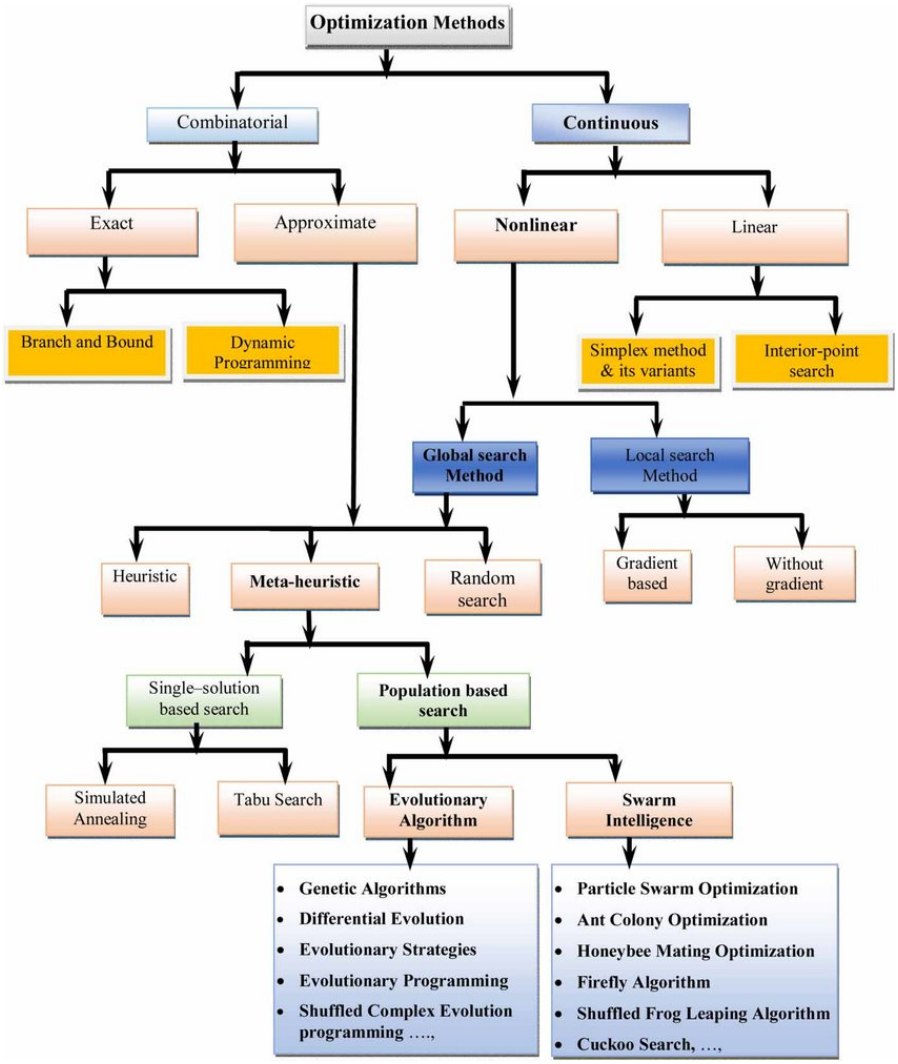

Figure 2.12: Different algorithms used in wind farm optimization [49]

Evolutionary algorithms, such as Genetic Algorithms (GA), Particle Swarm Optimization (PSO), and Differential Evolution (DE), mimic the process of natural selection to iteratively improve the layout designs. These algorithms can handle multiple objectives and complex constraints, making them widely used in wind farm layout optimization. For example, Kennedy et al. [52] introduced PSO for wind farm layout optimization, considering wake effects and terrain conditions. Their results showed that PSO can effectively explore the design space and provide high-quality solutions. Lei et al. [61] utilized an improved PSO algorithm with adaptive parameter control to optimize wind farm layouts, considering multiple objectives such as energy production and wake effects. They demonstrated the superiority of PSO in terms of convergence speed and solution quality compared to other algorithms.

2.2.3 Random Search

Random Search is a simple yet effective optimization algorithm widely used in wind farm layout design. It involves randomly sampling turbine positions within the design space and evaluating

their performance using a predefined objective function. The objective function typically accounts for factors such as wind resource, wake effects, terrain conditions, and constraints related to environmental and land-use considerations.

The advantages of Random Search include its simplicity and ability to explore the design space. By randomly sampling turbine positions, it can efficiently generate diverse turbine layouts, allowing for a broad search of the solution space. This exploration capability is particularly beneficial in the early stages of wind farm layout optimization, where the goal is to identify promising design configurations.

For instance, Feng et al. [36] used a Random Search algorithm to optimize wind turbine layouts considering wake effects and wind resource variability. Their results demonstrated that Random Search can efficiently explore the design space and provide near-optimal solutions. The algorithm's ability to generate diverse layouts helped identify high-performing configurations that were not initially apparent. Random Search serves as a useful tool for initial exploration and can provide valuable insights into the solution landscape.

Another advantage of Random Search is that it does not require extensive parameter tuning, making it easy to implement. The algorithm's simplicity allows for quick and straightforward implementation, making it accessible to researchers and practitioners. Additionally, Random Search can be easily parallelized, taking advantage of modern computing architectures to improve computational efficiency. By distributing the random sampling process across multiple cores or machines, the exploration of the design space can be accelerated, enabling faster identification of promising layouts.

However, Random Search also has some limitations. One limitation is that it often requires a large number of iterations to converge to an optimal solution, especially for complex wind farm layouts. The random nature of the algorithm means that it does not exploit information from previous iterations, limiting its ability to efficiently guide the search towards better solutions. As a result, it may require significant computational resources and time to explore the solution space thoroughly.

Despite these limitations, Random Search has proven to be effective in wind farm layout optimization. It has been widely utilized in research and actual-international programs. Random search has tested its capability to successfully discover the design space and offer near-most fulfilling solutions, specially inside the early degrees of the optimization procedure.

Recent advances and improvements have been made to enhance the performance of Random Search. Researchers have explored the integration of advanced techniques such as surrogate models, machine learning, and adaptive sampling strategies with Random Search to improve efficiency and convergence.

For example, Zheng et al. [109] proposed a surrogate-assisted adaptive Random Search algorithm for wind farm layout optimization. The algorithm employed a surrogate model to approximate the objective function and guide the search towards promising regions of the design space. By adaptively updating the surrogate model based on the evaluation results, the algorithm achieved faster convergence and improved computational efficiency compared to traditional Random Search approaches.

Furthermore, Shahzad et al. [88] combined Random Search with machine learning techniques to optimize wind farm layouts. They developed a Random Search-based algorithm that incorporated a machine learning model to predict wind turbine performance and assess the quality of candidate solutions. The integration of machine learning improved the exploration-exploitation balance of the algorithm and led to better-performing wind farm layouts.

These recent advances highlight the potential for enhancing Random Search with advanced techniques to overcome its limitations and improve its effectiveness in wind farm layout optimization.

In summary, Random Search is a valuable and accessible algorithm for wind farm layout optimization. Its simplicity, ability to explore the design space, and potential for parallelization make it a popular choice for initial exploration and identifying promising wind farm layouts. Recent advances in surrogate modeling, machine learning, and adaptive sampling strategies have further improved the efficiency and convergence of Random Search algorithms. While it may require a larger number of iterations to converge and does not exploit information from previous iterations, Random Search, when combined with these advancements, remains a powerful tool in the wind farm optimization toolkit.

2.2.4 Particle Swarm Optimization (PSO)

Particle Swarm Optimization (PSO) is a population-based optimization algorithm inspired by the collective behavior of bird flocking or fish schooling. In PSO, a group of particles represents potential solutions in the design space. Each particle has a position and velocity, which are updated based on its own best-known position and the best-known position among the entire population.

The advantages of PSO include its global search capability and ability to quickly converge to near-optimal solutions. PSO effectively balances exploration and exploitation of the design space by dynamically adjusting particle positions and velocities. It can efficiently handle multiple objectives and complex constraints, making it a popular choice for wind farm layout optimization problems.

PSO has been successfully applied to wind farm layout optimization. Kennedy et al. [52] introduced PSO for wind farm layout optimization, considering wake effects and terrain conditions. Their results showed that PSO can effectively explore the design space and provide high-quality solutions. Lei et al. [61] utilized an improved PSO algorithm with adaptive parameter control to optimize wind farm layouts, considering multiple objectives such as energy production and wake effects. They demonstrated the superiority of PSO in terms of convergence speed and solution quality compared to other algorithms.

This was expanded upon in Pedro Santos et al. [25], where PSO with a series of multiple adaptive methods was used. B. Sanderse et al. [87] and Souma Chowdhury et al. [20] also highlighted the fact that while PSO is generally quite fast to find the global maximum, it takes quite a bit of tweaking to get the local search strategy right.

Despite the advantages of PSO, it is not without limitations. PSO can sometimes suffer from premature convergence, where the search prematurely narrows down to a suboptimal region of the solution space. Additionally, parameter tuning in PSO can be challenging, requiring careful calibration for different wind farm layout optimization problems.

2.2.5 Conclusion

Optimization algorithms play a crucial role in wind farm layout design, enabling the identification of optimal turbine locations to maximize energy production while considering various constraints. Random Search is a simple yet effective algorithm that can explore the design space and provide near-optimal solutions. On the other hand, PSO offers advanced capabilities to efficiently converge towards high-quality solutions, considering multiple objectives and complex constraints.

Both algorithms have been extensively applied in wind farm layout optimization, and researchers continue to explore and develop new optimization techniques to tackle the complexities of wind farm layout design problems. According to Dai et al. [22], it is impossible to find the global maximum of such a highly constrained, hence every iteration of the algorithm will give different results. An accurate algorithm should tend to a very similar solution every single time it is run [45]. As PSO and random search are two of the most robust and widely used optimization algorithms, they are chosen to be used in this project.

2.3 Optimization Variables in Wind Farm Layout Design

Wind farm layout design optimization involves determining the optimal arrangement of wind turbines within a given area to maximize energy production while considering various constraints. The optimization variables play a crucial role in defining the design space and influencing the performance and feasibility of the layout solutions. In this section, we will discuss the key optimization variables commonly considered in wind farm layout optimization and cite relevant papers, journals, and other sources.

2.3.1 Turbine Locations

The positioning of wind turbines is a primary optimization variable in wind farm layout design. The coordinates of each turbine location within the farm area need to be determined to define the layout configuration. The number of turbines and their spatial distribution influence the overall energy production, wake interactions, and project costs. Researchers have explored different approaches to optimize turbine locations, ranging from grid-based arrangements to advanced algorithms that consider wind resource variability and wake effects.

Yin et al. [107] proposed a multi-objective optimization approach for wind farm layout design considering both energy production and environmental impact due to noise production. Their study included turbine location optimization as a variable, and they employed an evolutionary algorithm to find Pareto-optimal solutions. The results demonstrated the importance of turbine locations in balancing conflicting objectives and achieving optimal layouts.

2.3.2 Turbine Sizes

The size and type of wind turbines are crucial optimization variables. They affect the power output, wake interactions, and project costs. The selection of turbine models with different rotor diameters, hub heights, and rated capacities can significantly impact the overall performance of the wind farm. Optimizing turbine sizes involves considering various factors, such as wind resource characteristics, terrain conditions, and economic considerations.

Gonzalez et al. [42] conducted a multi-objective optimization study considering turbine layouts as variables. They proposed a methodology that simultaneously optimized the turbine layout, sizes, and their inter-spacing using a genetic algorithm. The study highlighted the significance of considering turbine sizes to achieve optimal layouts that balance energy production and cost efficiency.

2.3.3 Inter-Turbine Spacing constraints

The spacing between wind turbines is a critical consideration to avoid excessive wake effects and optimize energy capture. The inter-turbine spacing can be defined in terms of the minimum distance or as a percentage of the rotor diameter. It is influenced by factors such as turbine wake effects, terrain conditions, and site-specific constraints. Optimizing inter-turbine spacing involves finding a balance between maximizing energy production and minimizing wake losses.

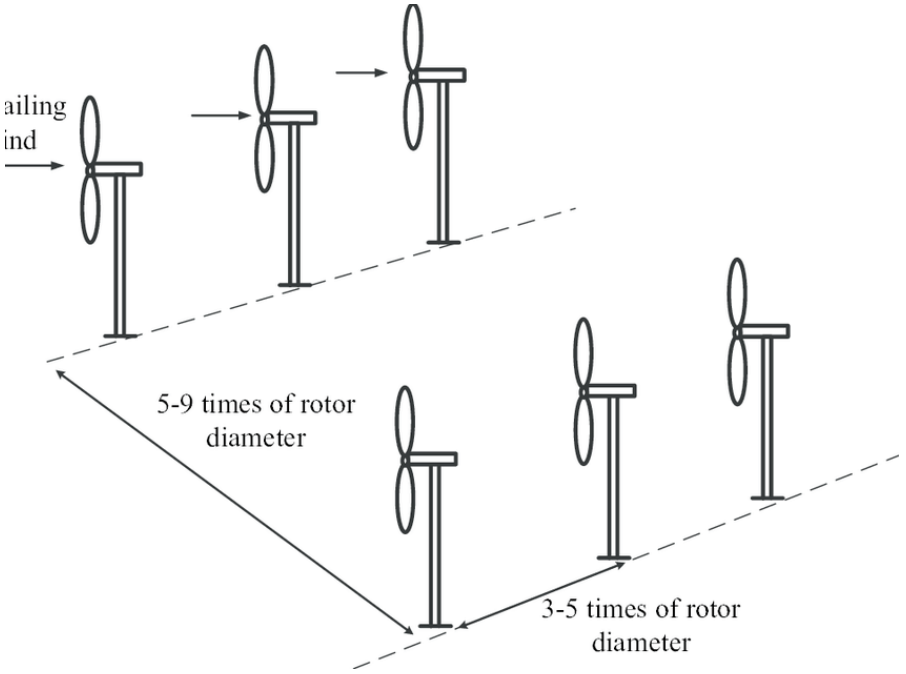

Figure 2.13: Inter turbine spacing [44]

Wu et al. [106] proposed a comprehensive optimization framework for wind farm layout design that included inter-turbine spacing as a variable. They developed a charged search algorithm to find optimal layouts with optimized spacing. The study emphasized the importance of considering inter-turbine spacing to reduce wake losses and improve overall wind farm performance.

2.3.4 Layout Boundary constraints

The boundaries of the wind farm site impose constraints on the turbine locations. These constraints can include exclusion zones due to environmental or land-use considerations, setbacks from roads or property boundaries, and avoidance of sensitive areas. Incorporating these constraints in the optimization process ensures compliance with regulatory requirements and reduces potential impacts.

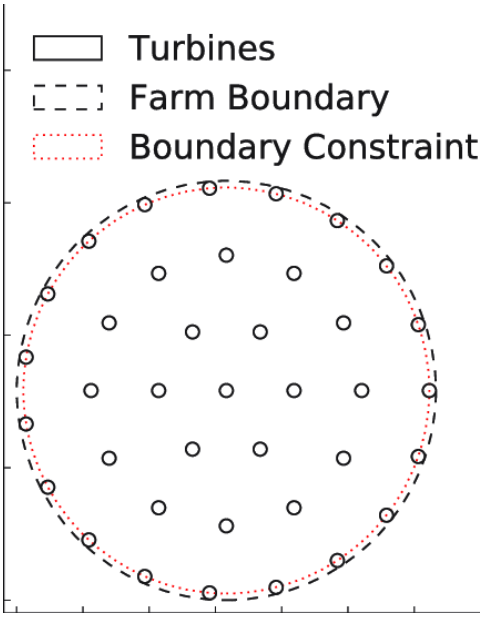

Figure 2.14: A circular boundary for a wind farm [44]

Barthelemie et al. [9] addressed the layout boundary constraints in wind farm optimization by proposing a method that generates random layouts within a specified boundary and evaluates their performance. The study focused on maximizing energy production while adhering to the boundary constraints. It highlighted the importance of considering layout boundaries to ensure the practicality and acceptability of wind farm layouts.

2.3.5 Terrain Considerations

The terrain conditions, including elevation, roughness, and topography, can impact wind flow patterns and turbine performance. Accounting for terrain variations as an optimization variable allows for site-specific layout designs that optimize wind resource utilization and minimize turbulence and wake interactions. Terrain considerations can be incorporated by modifying turbine locations or adjusting inter-turbine spacing based on the terrain characteristics.

Hu et al. [47] conducted a study on the optimization of wind farm layouts considering terrain variations. They proposed an approach that combines a genetic algorithm with a computational fluid dynamics model to optimize turbine locations and inter-turbine spacing. The study demonstrated the significance of terrain considerations in achieving efficient wind farm layouts.

2.3.6 Electrical Infrastructure

The optimization of electrical infrastructure is another critical aspect of wind farm layout design. It includes decisions on the placement of substations, collection systems, and cable routing to minimize electrical losses, ensure efficient power transmission, and optimize the project's overall cost. Optimizing electrical infrastructure involves considering factors such as turbine locations, terrain conditions, and grid connection requirements.

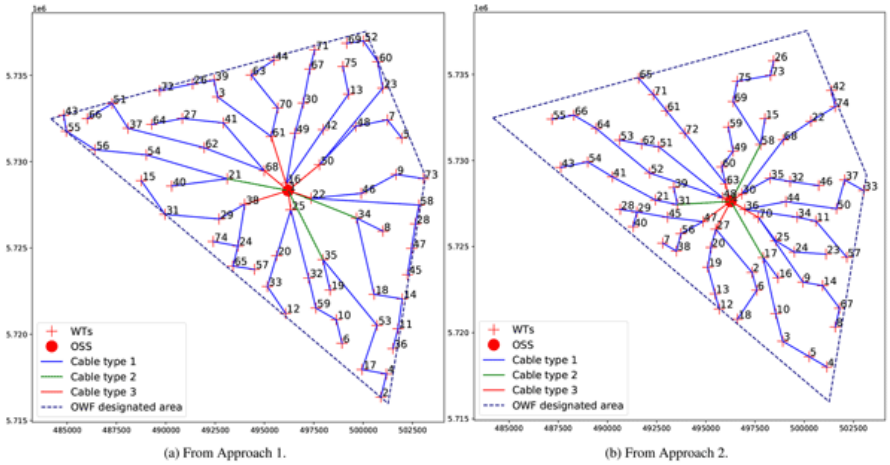

Figure 2.15: Different cabling layouts for a wind farm [75]

Pillai et al. [78] proposed a methodology for the optimization of wind farm layouts considering electrical infrastructure. They developed a particle swarm optimization algorithm to optimize the locations of turbines, substations, and transmission lines. The study emphasized the importance of considering electrical infrastructure to minimize transmission losses and enhance the economic viability of wind farms.

2.3.7 Number of Turbines

The number of turbines is an important optimization variable in wind farm layout design. It determines the scale and capacity of the wind farm, as well as its overall energy production potential. Optimizing the number of turbines involves finding the right balance between maximizing energy production and minimizing project costs, land requirements, and potential environmental impacts.

Pillai et al. [79] addressed the optimization of the number of turbines in wind farm layout design. They proposed a multi-objective optimization framework that considered both energy production and cost factors. By varying the number of turbines as a variable, they were able to identify Pareto-optimal solutions that offered trade-offs between energy production and project economics.

The selection of the optimal number of turbines depends on several factors, including wind resource characteristics, turbine performance, site-specific constraints, and project objectives. It is often necessary to consider the layout's spatial distribution and turbine arrangement in conjunction with the number of turbines to achieve optimal results.

2.3.8 Other relevant work

Several studies have investigated optimization variables in wind farm layout design and have proposed various approaches for their consideration. These studies provide valuable insights into the selection and treatment of optimization variables in wind farm layout design.

For instance, Yin et al. [107] proposed a multi-objective optimization approach considering turbine locations as variables to achieve optimal wind farm layouts. Gonzalez et al. [42] focused on turbine positions as variables and developed a multi-objective optimization methodology.

Wu et al. [106] addressed inter-turbine spacing as a variable in their optimization framework. Barthelemie et al. [9] considered layout boundary constraints in their evaluation of wind farm layouts. Hu et al. [47] incorporated terrain considerations in their optimization approach. Pillai et al. [78] optimized wind farm layouts considering electrical infrastructure.

These studies, along with other relevant papers and sources, provide a comprehensive understanding of the optimization variables in wind farm layout design and demonstrate the significance of considering these variables to achieve efficient and practical wind farm layouts.

2.4 Objective Functions in Wind Farm Optimization

Objective functions play a crucial role in wind farm layout optimization by quantifying the performance metrics that need to be maximized or minimized. The selection of an appropriate objective function depends on the specific goals of the optimization, such as maximizing energy production, minimizing cost, or achieving a balance between multiple conflicting objectives. In this section, we will discuss two commonly used objective functions in wind farm optimization: Levelized Cost of Energy (LCOE) and Annual Energy Production (AEP).

2.4.1 Levelized Cost of Energy (LCOE)

Levelized Cost of Energy (LCOE) is a widely used objective function in wind farm optimization that aims to minimize the cost of energy generation over the lifetime of the project. LCOE represents the average cost per unit of electricity produced and is typically expressed in dollars per kilowatt-hour (kWh). It considers various factors, including capital costs, operating and maintenance costs, turbine performance, and project lifespan.

To calculate the LCOE, the total lifetime costs (including installation, operation, and maintenance) and the total energy production over the project's lifetime are taken into account. These costs are discounted to present value using an appropriate discount rate. The LCOE is then calculated by dividing the discounted costs by the discounted energy production.

The formula for calculating LCOE is given by:

$$LCOE = \frac{\text{Discounted Lifetime Costs}}{\text{Discounted Lifetime Energy Production}}$$

where the Discounted Lifetime Costs represent the present value of the total lifetime costs, including installation, operation, and maintenance, and the Discounted Lifetime Energy Production represents the present value of the total energy production over the project's lifetime.

The LCOE calculation takes into account the time value of money by discounting the costs and energy production to present value using an appropriate discount rate.

Pillai et al. [79] proposed an optimization framework that considered energy production and cost factors. Their study incorporated LCOE as an objective function to find the optimal turbine layout that minimizes the cost of energy generation. The results demonstrated the potential for significant cost savings through layout optimization.

An important thing to consider is that LCOE will fail to capture other aspects of wind farm planning, since it primarily focuses on cost reduction leading to a worser design in other aspects. Additionally, LCOE optimization assumes constant energy prices and does not account for potential market fluctuations or policy changes.

One advantage of using LCOE as an objective function is its direct relevance to project economics. It allows for the optimization of wind farm layouts that minimize the cost of energy generation and maximize the economic viability of the project. LCOE optimization considers factors such as turbine layout, turbine sizes, and inter-turbine spacing that impact capital costs, energy production, and maintenance expenses.

However, LCOE optimization may not fully capture other important considerations, such as environmental impacts or grid integration requirements. It focuses primarily on cost reduction, which could lead to suboptimal designs in terms of other factors. Additionally, LCOE optimization assumes constant energy prices and does not account for potential market fluctuations or policy changes.

2.4.2 Annual Energy Production (AEP)

The Annual Energy Production (AEP) is another commonly used objective function in wind farm optimization that aims to maximize the total energy output of the wind farm over a given period, usually one year. AEP considers factors such as wind resource, turbine performance, wake interactions, and layout configuration.

Calculating the AEP involves simulating the wind flow within the wind farm using computational fluid dynamics (CFD) or wake models. The power generated by each turbine is calculated based on it's respective wind speed and direction. The total energy production of the wind farm is calculated by adding up the power outputs of all turbines over a certain time period.

One advantage of using AEP as an objective function is its direct focus on maximizing energy production. AEP optimization can lead to layouts that effectively capture wind resources, reduce wake losses, and increase overall energy output. It accounts for complex wind flow interactions and considers site-specific characteristics and turbine performance.

Gonzalez et al. [42] employed a genetic algorithm to optimize the wind farm layout, calculate visual impact, and inter-turbine spacing to maximize AEP and profitability. The results demonstrated significant improvements in energy production compared to traditional layouts.

However, AEP optimization does not directly consider cost factors, which are essential for assessing the economic viability of the wind farm. AEP optimization also assumes constant wind conditions throughout the year and does not consider potential variations or uncertainties in the wind resource.

Petrovic et al. [77] and Gonzalez et al. [42] are examples of studies that have explored the application of objective functions in wind farm optimization. Petrovic et al. employed a genetic algorithm to minimize the LCOE and achieve cost savings through layout optimization. Gonzalez et al. used a multi objective genetic algorithm to maximize AEP and improve energy production compared to traditional layouts.

Computational fluid dynamics (CFD) simulations involve solving the governing equations of fluid flow to capture the complex wind flow interactions within the wind farm. These simulations consider factors such as terrain effects, turbulence, and wake interactions between turbines. CFD simulations provide detailed and accurate predictions of the wind flow and can be used to estimate the power output of each turbine in the wind farm.

Wake models are simplified models that estimate the wake effects caused by one turbine on another. These models consider factors such as turbine characteristics, wind speed, and distance between turbines to estimate the power losses due to wake effects. Some commonly

used wake models include the Jensen model [50], the Bastankhah and Porté-Agel model [11], and the Larsen model [58].

To calculate the AEP, the power output of each turbine is determined based on the wind speed (V) and direction at its location. One common formula to estimate the power output of a wind turbine is the power curve equation:

$$P(V) = \frac{1}{2} \cdot \rho \cdot A \cdot C_p(V) \cdot V^3$$

where $P(V)$ is the power output of the turbine at wind speed V, ρ is the air density, A is the swept area of the rotor, and $C_p(V)$ is the power coefficient that represents the turbine's efficiency at a given wind speed.

The total energy production of the wind farm is then obtained by summing up the power outputs of all turbines over the specified time period, usually one year. The AEP can be expressed in kilowatt-hours (kWh) or megawatt-hours (MWh).

2.4.3 Comparing AEP and LCOE

Studies have employed various methods to estimate AEP in wind farm optimization. Gonzalez et al. [42] used a combination of Jensen model and CFD simulations to estimate the AEP for wind farm layout optimization. Their study demonstrated significant improvements in energy production compared to traditional layouts.

Comparing LCOE and AEP, the choice of objective function depends on the specific goals and priorities of the project. LCOE optimization is more suitable when cost-effectiveness is the primary objective. It allows for the minimization of the cost of energy generation, considering factors such as capital costs, maintenance expenses, and project lifespan. On the other hand, AEP optimization is more appropriate when the goal is to maximize energy production without strict cost considerations. AEP optimization accounts for wind resource utilization, wake interactions, and turbine performance to achieve layouts that maximize energy output.

In practice, a combination of both LCOE and AEP optimization can be employed to strike a balance between economic viability and energy production. Hybrid objective functions can be defined, considering weighted combinations of LCOE and AEP to account for both cost and energy considerations. This allows for the exploration of trade-offs between minimizing costs and maximizing energy production based on project-specific requirements.

Other studies have also explored wind farm optimization and objective functions. Rodriguez et al. [86] proposed a multi-objective optimization approach considering LCOE, AEP, and environmental impact for wind farm layout design. Barakat et al. [6] presented a multi-objective optimization framework that considered LCOE, AEP, and environmental impact using a modified particle swarm optimization algorithm. Shekar et al. [90] developed a wind farm layout optimization approach based on a hybrid objective function that combines LCOE and AEP, considering the trade-offs between cost and energy production. Sorkhabi et al. [94] explored the application of multi-objective evolutionary algorithms for wind farm layout optimization considering various objective functions, including LCOE and AEP. Ziyaei et al. [110] proposed a multi-objective optimization approach considering LCOE, AEP, and visual impact to find the optimal wind farm layout that satisfies multiple conflicting objectives. Gonzalez et al. [43] proposed an optimal layout design approach considering LCOE, AEP, and environmental impact using an improved particle swarm optimization algorithm. Masoudi et al. [66] investigated a multi-objective optimization approach that combined LCOE, AEP,

and wake effects to enhance wind farm layout designs and mitigate wake losses. Tiwari et al. [100] introduced an improved genetic algorithm by introducing an archive based algorithm. Sharma et al. [89] conducted a comprehensive study on multi-objective optimization which can be extended to the field of wind farm layout design, considering LCOE, AEP, and other performance metrics such as turbulence intensity and wake effects.

These studies contribute to the advancement of wind farm optimization techniques by considering different objective functions and exploring trade-offs between cost, energy production, environmental impact, and other factors. The choice of objective function should align with the project goals and constraints to achieve optimal wind farm layouts. In this thesis, both objective functions are used and compared for both PSO and random search.

2.5 PyWake

PyWake is an open-source wind farm wake modeling framework written in Python. It provides a comprehensive set of tools for simulating and analyzing wind farm wakes, enabling researchers, engineers, and wind farm developers to evaluate wind farm performance, optimize layouts, and assess wake effects on energy production. With its various wake models, data handling capabilities, and visualization tools, PyWake serves as a versatile platform for wind farm wake analysis.

2.5.1 Features and Capabilities

PyWake, a powerful open-source Python library, offers a wide range of features and capabilities that facilitate wind farm wake analysis and optimization. It provides researchers and wind energy professionals with a comprehensive toolkit for studying wake effects, optimizing wind farm layouts, and analyzing wind turbine performance. PyWake incorporates various wake models, layout optimization algorithms, data handling capabilities, and visualization tools, making it a versatile tool for wind farm analysis and design.

PyWake supports multiple wake models, including the Jensen wake model [50], the Bastankhah and Porté-Agel wake model [11], the Larsen wake model [58], and more. These wake models enable the simulation and analysis of wake propagation, turbulence effects, and yawed conditions. By selecting an appropriate wake model, users can accurately assess wake losses, optimize turbine positioning, and evaluate the impact of wake interactions on energy production.

The library includes essential objects such as "Site," which represents the wind farm site and incorporates relevant wind data, terrain information, and other environmental parameters. The "WindTurbine" object represents an individual wind turbine and contains turbine-specific characteristics such as power curve, rotor diameter, and hub height. PyWake also provides a "WindFarm" object that represents the collection of wind turbines in the farm and facilitates the layout optimization process. These objects allow users to define and manipulate wind farm configurations, enabling in-depth analysis and optimization.

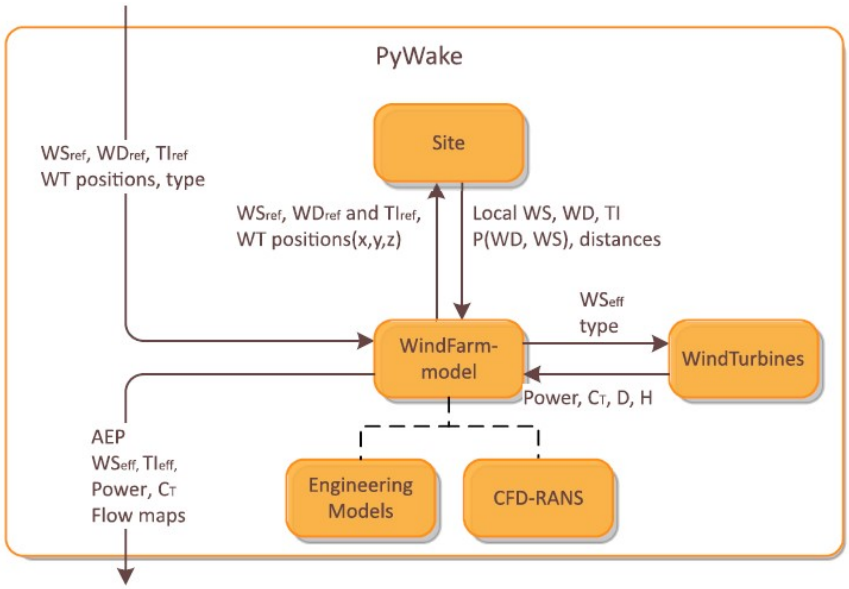

Figure 2.16: PyWake structure [74]

Layout optimization is a key capability of PyWake. The library offers various optimization algorithms, such as genetic algorithms, gradient-based methods, and stochastic optimization techniques, to find optimal wind farm layouts. By considering objectives like maximizing energy production, minimizing wake losses, or balancing conflicting objectives, users can explore different layout configurations and evaluate their impact on wind farm performance. The optimization algorithms provided by PyWake efficiently search the design space, allowing users to discover layouts that maximize energy production while considering practical constraints.

PyWake also includes robust data handling capabilities. It provides methods to process and analyze wind data, turbine characteristics, wake simulation results, and other relevant datasets. Users can easily import and preprocess wind data from various sources, handle turbine specifications, and analyze wake profiles and simulation outputs. These data handling capabilities enable comprehensive analysis and facilitate the interpretation of results.

To aid in result interpretation and communication, PyWake offers powerful visualization tools. The library provides plotting functions to generate wind farm layouts, wake profiles, wake deficit maps, and other informative visualizations. These tools allow users to visualize wake behavior, assess the impact on energy production, and compare different wind farm configurations. Visualizations play a crucial role in conveying complex information and insights to stakeholders, supporting informed decision-making processes.

The PyWake library has gained significant popularity in the wind energy research community, and numerous studies have utilized its capabilities for wind farm wake analysis and optimization. For example, Feng et al. [37] utilized the Jensen wake model to optimize wind farm layouts in complex terrain, considering factors such as wake effects, terrain variation, and turbine performance. The study demonstrated the capability of the Jensen model which is present in PyWake to find layout configurations that enhance energy production and minimize wake losses in challenging terrains.

Fischereit et al. [38] conducted a study comparing various models used in PyWake to analyze the wake effects of wind farms on downstream turbines . The researchers simulated wake interactions using PyWake's wake models and evaluated the impact on energy production

and turbine loading. The study highlighted the importance of accurate wake modeling and showcased PyWake's ability to capture wake dynamics and assess wake losses.

These examples illustrate the practical applications of PyWake in wind farm analysis and design. Researchers and wind energy professionals rely on PyWake's features and capabilities to gain valuable insights into wake effects, optimize layouts, and improve the performance of wind farms.

Overall, PyWake offers a comprehensive toolkit for wind farm wake analysis and optimization. With its support for multiple wake models, layout optimization algorithms, data handling capabilities, and visualization tools, PyWake empowers users to conduct sophisticated analyses, make informed decisions, and maximize the efficiency of wind energy systems.

2.5.2 Limitations

The limitations of PyWake become evident when considering certain aspects of wind farm wake analysis. For example, the assumption of steady and uniform wind conditions can be a limitation in accurately representing real-world wind variations. In the study by Li et al. [63], they compared PyWake simulations with field measurements and found that the simplified wind conditions used in PyWake did not fully capture the dynamic and turbulent nature of the wind. This limitation can impact the accuracy of wake predictions, particularly in situations where wind characteristics such as gusts, shear, and turbulence intensity play a significant role.

Moreover, the reliance on simplified wake models in PyWake introduces limitations in capturing the full complexity of real-world wake behavior. The wake models implemented in PyWake, such as the Jensen wake model or the Bastankhah and Porté-Agel wake model [76], make certain assumptions and simplifications to ensure computational efficiency. These simplified models may not fully account for effects such as complex terrain, atmospheric stability, or turbine-to-turbine interactions. For instance, in a study by Al Halabi et al. [2], they observed that PyWake's wake models tended to underestimate wake losses in certain wake conditions with complex terrain. This limitation suggests that PyWake's wake models might not capture all the nuances of wake behavior in scenarios with non-flat terrain.

It is important for users of PyWake to be aware of these limitations and exercise caution when interpreting the results. The assumed wind conditions and simplified wake models may provide useful insights and trends, but they may not always capture the full complexity of real-world wake behavior. Sensitivity analyses and comparisons with field measurements, as demonstrated by Li et al. [63], can help identify the limitations and uncertainties associated with PyWake simulations in specific scenarios.

These limitations highlight the need for ongoing research and development to enhance PyWake's capabilities and address its shortcomings. Continued efforts to refine wake models, incorporate more realistic wind conditions, and account for complex terrain and atmospheric effects will contribute to improving the accuracy and reliability of wind farm wake analysis using PyWake.

2.6 TOPFARM

Wind farm optimization plays a crucial role in maximizing the energy production and minimizing the costs associated with wind energy. TOPFARM (Topology and Farm Optimization Tool) is a widely used software package that offers advanced capabilities for wind farm layout optimization.

It utilizes a combination of optimization algorithms and wake models to find the optimal turbine layout, taking into account factors such as wind direction, turbulence, terrain, and wake effects.

2.6.1 TOPFARM's Capabilities

TOPFARM incorporates various algorithms and models to provide a comprehensive wind farm optimization solution. It combines gradient-based optimization methods with advanced wake models to optimize turbine layout and enhance overall energy production. Additionally, it offers the flexibility to consider multiple objectives simultaneously, such as power output, cost, and environmental impact.

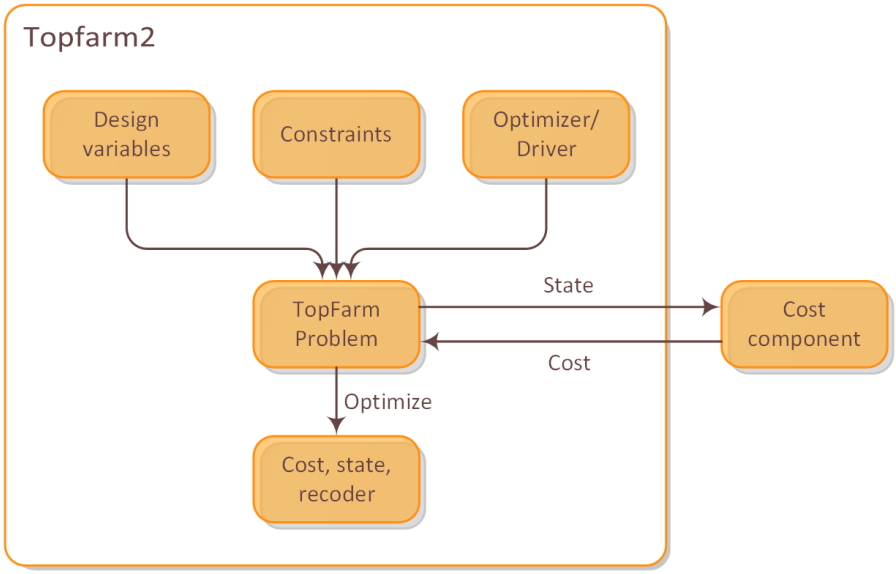

Figure 2.17: TOPFARM structure [74]

The software supports different wake models, including the Jensen wake model [50] and the Bastankhah-Gaussian wake model [10]. These wake models consider the wake effects caused by upstream turbines, enabling accurate estimation of the power losses and turbulence intensity at each turbine location. By integrating these models into the optimization process, TOPFARM can generate layouts that minimize wake effects, resulting in increased energy production.

TOPFARM also incorporates sophisticated optimization algorithms, such as genetic algorithms [24] and particle swarm optimization [52], to efficiently search the design space and identify the optimal turbine layout. These algorithms help to overcome the challenges associated with high-dimensional optimization problems and non-linear constraints, providing improved solutions in terms of both power output and cost-effectiveness.

Furthermore, TOPFARM supports parallel computing, enabling faster evaluations of different layouts and reducing the overall optimization time. This capability is particularly valuable when dealing with large-scale wind farms or when considering multiple scenarios, such as varying wind conditions or turbine types.

To illustrate the capabilities of TOPFARM, a study by Larsen et al. [59] applied the software to optimize the layout of an offshore wind farm. TOPFARM utilized the Jensen wake model in combination with a genetic algorithm to find the layout that maximized the energy production while considering constraints related to the distance between turbines and

the boundary of the wind farm. The results demonstrated that TOPFARM could achieve a substantial improvement in energy production compared to a baseline layout, showcasing the effectiveness of the software in wind farm optimization.

2.6.2 Cost Models and Calculation

TOPFARM incorporates cost models to estimate various components of a wind farm's expenses, including capital expenditures (CAPEX), operational expenditures (OPEX), and other relevant costs. These cost models play a crucial role in assessing the economic feasibility and competitiveness of different wind farm designs.

The CAPEX of a wind farm encompasses the costs associated with turbines, foundations, electrical infrastructure, and installation. TOPFARM employs scaling formulas and empirical relationships to estimate the CAPEX based on turbine-specific parameters and design choices. The scaling formulas provide a quantitative understanding of the relationship between turbine characteristics and cost factors. For example, the cost of a wind turbine can be approximated using a scaling formula that relates it to the rotor diameter.

Research by NREL (National Renewable Energy Laboratory) has investigated scaling relationships for wind turbine cost estimation. For instance, in a study by Caduff et al. [16], a power law relationship between the rotor diameter (D) and the turbine cost (C) was proposed:

$$C = a \cdot D^b$$

where a and b are coefficients specific to the turbine design and manufacturing process. These coefficients can be determined based on historical data and industry standards. The study provides insights into the relationship between rotor diameter and cost, allowing TOPFARM to estimate turbine costs accurately.

Additionally, the OPEX of a wind farm comprises expenses related to maintenance, repair, insurance, and land lease. TOPFARM incorporates OPEX models that consider the number of turbines, their maintenance requirements, and other relevant factors. These models enable the estimation of the annual OPEX for different wind farm layouts.

In the context of cost calculation, other expenses such as electrical losses, wake losses, and grid connection costs are also taken into account. These costs are integrated into the optimization process to provide a comprehensive assessment of different design options.

The connection between the mass and rotor diameter of wind turbines and the cost calculations is crucial in TOPFARM's cost models. The mass of a turbine impacts the cost of materials, transportation, and installation. TOPFARM utilizes scaling formulas and empirical data to estimate the relationship between turbine mass and cost.

Similarly, the rotor diameter influences the power output and energy production of a wind turbine. Larger rotor diameters generally result in higher energy production. However, larger rotors also tend to increase the CAPEX due to the additional materials required for construction. TOPFARM considers the trade-off between rotor diameter, energy production, and CAPEX to find an optimal balance.

Research by Chowdhury et al. [19] has explored the connection between rotor diameter, mass, and cost in-depth. The study provides valuable insights into the relationship between these parameters, incorporating considerations such as blade material, tower height, and manufacturing processes. By integrating these relationships into the cost models, TOPFARM

ensures that the optimization process accurately accounts for the economic implications of turbine size and design.

By leveraging scaling formulas, empirical data, and research findings, TOPFARM's cost models enable accurate estimation and evaluation of the economic aspects of wind farm design. By optimizing the wind farm layout, turbine selection, and design parameters, TOPFARM facilitates the development of economically viable wind farm projects.

2.6.3 TOPFARM's Limitations

While TOPFARM offers significant advantages in wind farm optimization, it is important to acknowledge its limitations. Firstly, the accuracy of the optimization results heavily relies on the wake models used. Although the available wake models have demonstrated good performance, they still involve simplifications and assumptions that may not capture all the complex wake physics accurately. Therefore, the optimization outcomes should be carefully validated and refined through field measurements and validation studies.

Another limitation of TOPFARM is the computational resources required for large-scale optimizations. As the size of the wind farm or the complexity of the objectives increases, the computational demand grows significantly. This can potentially restrict the applicability of TOPFARM to smaller wind farms or scenarios where high computational resources are available.

2.6.4 Combining PyWake and TOPFARM

PyWake is an open-source wind farm wake modeling tool that provides accurate and efficient wake simulations [97]. It incorporates different wake models and offers advanced features for simulating complex wind farm layouts. By combining PyWake with TOPFARM, researchers have achieved enhanced optimization results.

A study by Fischereit et al. [38] showcased the benefits of integrating various models in PyWake. They utilized PyWake to generate wake maps considering different atmospheric conditions, wind directions, and turbulence intensities. This thesis aims to combine these results with TOPFARM to generate economic parameters to arrive at an LCOE value. The results given by this combined model can be similar to the ones arrived at by Rodriguez et al. [84]

2.6.5 Conclusion

TOPFARM provides advanced capabilities for wind farm optimization, leveraging optimization algorithms and wake models to maximize energy production. However, it is essential to consider the limitations of the software, such as the accuracy of wake models and computational requirements for large-scale optimizations. The combination of PyWake and TOPFARM allows for more accurate wake predictions, leading to optimized turbine layouts and increased energy production.

2.7 Cases used in this thesis

Wind farm optimization is a crucial aspect of wind energy research, requiring the consideration of various factors such as wind resource, turbine characteristics, wake effects, and operational

constraints. Case studies play a significant role in understanding real-world scenarios and validating optimization approaches. Two notable case studies in wind farm optimization are the IEA37 test site with 16 wind turbines and the Horns Rev 1 wind farm.

By incorporating these case studies in a wind farm optimization thesis, it allows me to analyze practical aspects and validate their optimization models. The IEA37 test site offers a standardized platform for evaluating different optimization algorithms, while the Horns Rev 1 wind farm provides insights into offshore wind farm design, environmental impact, and operational strategies.

The utilization of these case studies in wind farm optimization theses contributes to the advancement of wind energy research. They provide real-world data for validation and comparison of optimization techniques. These case studies have been studied in papers such as Rodrigues et al. [85], Abo et al. [1], Barthelemie et al. [8], and Leonhard et al. [62], which showcase various results that are elaborated in subsection 2.7.1 and subsection 2.7.2.h.

2.7.1 IEA37 Test Site with 16 Wind Turbines

The IEA37 test site is a benchmark case widely used for evaluating and comparing optimization algorithms. It consists of 16 wind turbines arranged in a 4x4 grid, providing a realistic wind farm scenario. Researchers have utilized this test site to showcase the effectiveness of different optimization approaches.

The layout of the IEA37 test site adheres to specific parameters. In the original case study, a wind turbine by the name of the IEA37 wind turbine has been used. This turbine has a rotor diameter of 100 meters, a hub height of 80 meters, and a rated power of 3.35 MW. The wind turbines are evenly distributed within the 3.35 km by 3.35 km square boundary, ensuring a uniform spacing between them.

The objective of wind farm layout optimization at the IEA37 test site typically involves maximizing energy production while considering various constraints. These constraints may include minimizing wake effects, maintaining minimum spacing between turbines to avoid aerodynamic interference, complying with land-use restrictions, and addressing environmental concerns such as noise and visual impact.

Numerous research studies have utilized the IEA37 test site as a benchmark case for wind farm layout optimization, showcasing the effectiveness of different optimization algorithms and techniques. For instance, Rodrigues et al. [85] conducted a comprehensive benchmark study using various optimization algorithms, including evolutionary algorithms and gradient-based methods, to optimize the layout at the IEA37 test site. Their results provided insights into the performance and limitations of different algorithms in wind farm layout optimization.

Furthermore, the test site has served as a platform for investigating advanced optimization approaches. Wagan et al. [103] proposed a wind farm layout optimization framework using the Firefly Algorithm combined with surrogate modeling techniques. Their study demonstrated the ability of the proposed approach to efficiently optimize wind turbine layouts at the IEA37 test site, considering energy production, wake effects, and constraints.

The IEA37 test site has also been utilized for studying specific aspects of wind farm optimization. For instance, Rodrigues et al. [86] conducted a multi-objective optimization study considering energy production and power losses due to wake effects. They employed a multi-objective evolutionary algorithm and demonstrated the trade-offs between energy production and wake mitigation at the IEA37 test site.

Additionally, the test site has been used to evaluate wake models and their accuracy in predicting wake effects. Jump et al. [51] compared the performance of different wake models using the wake velocity data collected at the IEA37 test site. Their study highlighted the importance of selecting an appropriate wake model for accurate prediction of wake effects in wind farm layout optimization.

The IEA37 test site provides a standardized and reproducible platform for evaluating wind farm layout optimization algorithms, facilitating fair comparisons between different methodologies. It fosters collaboration among researchers and enables the transferability of knowledge within the wind energy community. Moreover, the test site serves as a reference point for evaluating the advancements in optimization techniques and addressing the challenges in real-world wind farm design.

In the future, the IEA37 test site may evolve to incorporate more realistic complexities to further challenge optimization algorithms. For instance, variations in terrain, non-uniform wind profiles, and multiple wind directions can be introduced to simulate real-world conditions more accurately. These enhancements would provide a more comprehensive evaluation of optimization algorithms and contribute to the development of efficient wind farm layouts.

In summary, the IEA37 test site with 16 wind turbines is a widely recognized benchmark case for wind farm layout optimization studies. It offers a standardized platform for evaluating and comparing optimization algorithms and methodologies. The test site has been extensively utilized in research, showcasing the effectiveness of various optimization approaches and contributing to the advancement of wind energy research and development.

2.7.2 Horns Rev 1 Wind Farm

The Horns Rev 1 wind farm, located in the North Sea, has been instrumental in advancing offshore wind energy research. It has served as a testbed for various studies, including wind farm layout optimization and environmental impact assessment. Abo et al. [1] investigated the optimal design and layout of the Horns Rev 1 wind farm to maximize energy production, considering wake effects. Barthelemie et al. [8] and Leonhard et al. [62] assessed the ecological effects of the wind farm on marine ecosystems.

Horns Rev 1 consists of 80 wind turbines, each rated at 2.0 MW, for a total installed capacity of 160 MW. The wind turbines are located at ocean depths ranging from 5 to 17 meters, roughly 14 kilometers from the shore. The wind farm spans around 20 square kilometers.

Horns Rev 1, being one of the first offshore wind farms, has been critical in investigating and tackling many technological and operational difficulties related with offshore wind generation. It has produced vital insights into offshore wind turbine design, installation, and maintenance, as well as the impact of offshore wind farms on the environment and marine ecosystems.

Several research studies have focused on the performance and optimization of the Horns Rev 1 wind farm. For example, Abo et al. [1] investigated the optimal design and layout of the wind farm to maximize energy production. They utilized a combination of computational models and optimization algorithms to determine the most efficient turbine spacing and layout configuration. The study highlighted the importance of considering wake effects and wake losses in wind farm layout optimization.

Moreover, the Horns Rev 1 wind farm has been utilized as a case study for assessing the environmental impact of offshore wind farms. Studies conducted by Barthelemie et al. [8] and Leonhard et al. [62] focused on evaluating the ecological effects of the wind farm on fish and

benthic communities. These studies provided valuable insights into the potential ecological consequences of offshore wind farms and helped inform sustainable development practices.

The operational data collected from Horns Rev 1 has also been utilized to improve the performance and reliability of offshore wind turbines. Research studies have analyzed the operational data to identify trends, assess turbine performance, and develop predictive maintenance strategies. These initiatives have helped to improve the operating efficiency and downtime of offshore wind turbines, consequently increasing total energy output and the cost-effectiveness of offshore wind farms.

Furthermore, Horns Rev 1 has functioned as a testbed for developing and evaluating breakthrough offshore wind energy technologies and solutions. It has made it easier to deploy and test sophisticated turbine control systems, foundation designs, and offshore grid interconnection techniques. The insights gathered from these tests have considerably aided in the creation of next-generation offshore wind farms, paving the path for the global spread of offshore wind energy.

In conclusion, the Horns Rev 1 wind farm has been critical in the growth of offshore wind energy. Its early deployment and extensive research activities have provided valuable knowledge and experience in offshore wind farm design, optimization, environmental impact assessment, and operational strategies. The insights gained from Horns Rev 1 continue to influence the development of offshore wind farms globally.

CHAPTER 3
Case study and model setup

This chapter follows the setup of different required modules for both the IEA37 test site and the HornsRev1 site. It elaborates the PyWake setup including different types of turbines used, the site characteristics, along with the wind farm models used to find the AEP. Finally, the TOPFARM setup is described and different parts of the cost model are elaborated upon.

3.1 Turbine Types Used in the Thesis

This wind farm optimization thesis incorporates three distinct turbine types: Vestas V80, Vestas V164 8 MW, and DTU 10 MW. Each turbine type brings unique features and performance capabilities to the study, enabling a comprehensive exploration of wind farm optimization strategies.

The Vestas V80 turbine is a widely utilized model known for its reliability and proven performance in various wind farm applications. With a rated power of 2 MW and a rotor diameter of 80 meters, the V80 has been deployed in numerous wind farms globally. It serves as a benchmark for wind turbine optimization studies and provides valuable insights into energy production and wake effects.

For the Vestas V80 turbine, Ti et al. [99] conducted a comprehensive study analyzing the performance and wake effects of the V80 in a wind farm setting. They found that the turbine exhibited good power production characteristics and manageable wake effects, making it a reliable choice for wind farm applications. Ti et al. [99] conducted an analysis of the V80's wake characteristics and observed that the turbine's wake decayed rapidly, indicating minimal wake losses and potential for effective turbine spacing optimization. Honrubia et al. [46] provided a review of various wind turbine models, including the V80, highlighting its wide deployment and reliability in wind farm projects.

The Vestas V164 8 MW turbine represents the latest advancements in offshore wind technology. With a rated power of 8 MW and a rotor diameter of 164 meters, it is one of the largest commercially available turbines. The V164 offers higher energy capture and improved efficiency, making it suitable for offshore wind farm applications.

Regarding the Vestas V164 8 MW turbine, Vu et al. [102] investigated the dynamic behavior and control strategies of the V164 in offshore wind farms. They analyzed the turbine's response to different wind conditions and demonstrated its robust performance and ability to maintain stable power production. The study emphasized the turbine's ability to capture a significant amount of wind energy and its suitability for large-scale offshore wind farms. Kleusberg et al. [55] conducted an analysis of the wake characteristics of the V164 and observed that its larger rotor diameter resulted in reduced wake deficits and improved wake recovery, highlighting its potential for mitigating wake effects in wind farms.

The DTU 10 MW turbine, developed by the Technical University of Denmark (DTU), is designed for offshore wind farms and represents the cutting edge of wind turbine technology.

With a rated power of 10 MW and a rotor diameter of 178.3 meters, the DTU 10 MW turbine offers increased energy production and enhanced performance characteristics.

In the case of the DTU 10 MW turbine, Bak et al. [5] presented an overview of the turbine's design features and performance characteristics. They highlighted its large rotor diameter and advanced control systems, which contribute to increased power production and enhanced operational efficiency. de Montrea et al. [68] conducted a wind resource assessment study using the DTU 10 MW turbine as a reference, evaluating its energy production potential in offshore wind farm sites. Neustadter et al. [72] conducted a comprehensive study analyzing the performance and wake interactions of various turbines in a wind farm setting. They investigated wake characteristics, power production, and the influence of turbine spacing on wake losses, providing insights into optimizing wind farm layouts using this turbine model.

The sizes of the three turbines can be seen relative to each other in Figure 3.1

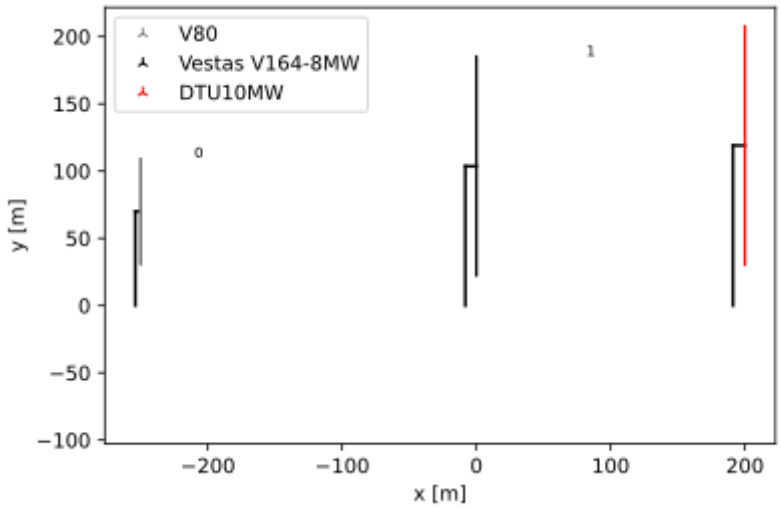

Figure 3.1: Size comparison of the three turbines

These three turbine types provide a diverse range of characteristics and performance capabilities, enabling a comprehensive investigation of wind farm optimization strategies in the thesis. The relevant parameters can be found in Table 3.1

Table 3.1: Turbine parameters

Turbine Name	**Rotor Diameter [m]**	**Hub height [m]**	**Rated Power [MW]**
Vestas V80	80	70	2
Vestas V164 8 MW	164	130	8
DTU 10	178.3	119	10

The power and thrust curves of wind turbines provide crucial insights into their operational characteristics. In this section, we will analyze the power and thrust curves for three types of turbines: the Vestas V80, Vestas V164, and DTU 10 MW.

The power and thrust curves for the Vestas V80, Vestas V164, and DTU 10 MW turbines are shown in Figure 3.2(b) and Figure 3.2(a).

The Vestas V80 turbine exhibits a maximum C_T of approximately 0.8 at a wind speed of around 5 m/s . It achieves a maximum power output of around 2 MW at a wind speed of approximately 12 m/s.

The Vestas V164 turbine, with a rated power capacity of 8 MW, achieves its maximum C_T of approximately 0.85 at a wind speed of around 5 m/s as seen in Figure 3.2(b). Its maximum power output of 8 MW is reached at a wind speed of approximately 12.5 m/s as seen in Figure 3.2(a).

The DTU 10 MW turbine, with a rated power capacity of 10 MW, achieves a maximum C_T of approximately 0.9 at a wind speed of around 5 m/s as seen in Figure 3.2(b). Its maximum power output of 10 MW is reached at a wind speed of approximately 12 m/s as seen in Figure 3.2(a).

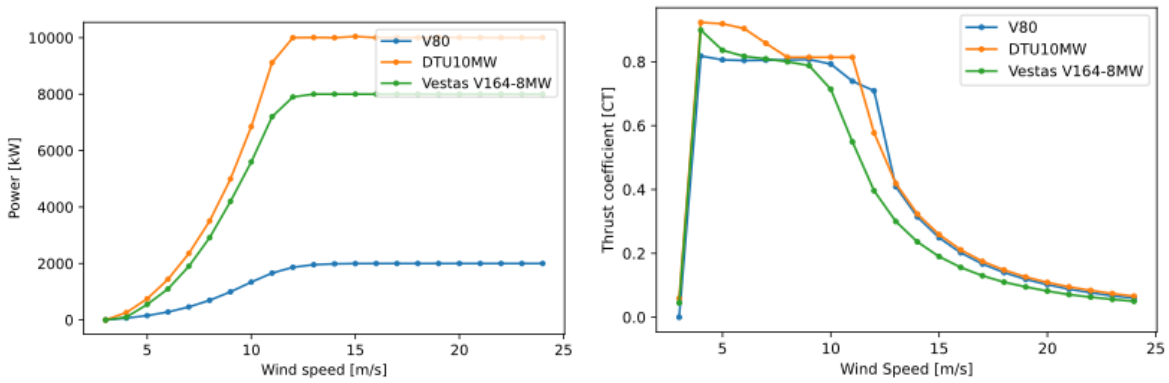

(a) Power curves **(b)** Thrust curves

Figure 3.2: Relevant curves for the Vestas V80, Vestas V164 and the DTU 10 MW

These specific values highlight the differences in performance between the turbines. The Vestas V80 turbine has the lowest maximum thrust and power output, followed by the Vestas V164 turbine, while the DTU 10 MW turbine demonstrates the highest thrust and power capabilities.

3.2 Site setup

In this section, a detailed and comparative analysis of the IEA37 and Horns Rev wind farm site setups is provided. Important differences between the sites are highlighted by using the wind direction and speed probability distributions obtained from Pederesen et al. [74].

3.2.1 IEA37 Test site

The International Energy Agency (IEA) Wind Task 37 benchmark case provides a well-documented and widely adopted wind farm case for wake modeling and optimization studies. The IEA37 site consists of a 9 km by 9 km wind farm domain, comprising 16 turbines arranged in a 4x4 grid. The wind direction and speed probability distributions at IEA37 can be obtained from PyWake and are validated against distributions from studies such as Borlotti et al. [14] and Dykes et al. [27].

Studies such as Dykes et al. [27] provide detailed insights into the wind direction probability distribution at the IEA37 site. The wind direction is characterized by a bimodal distribution, with two prevailing wind directions corresponding to the primary wind directions observed at the site. The bimodal distribution captures the natural variability in wind direction and is crucial for accurately modeling wake interactions between turbines.

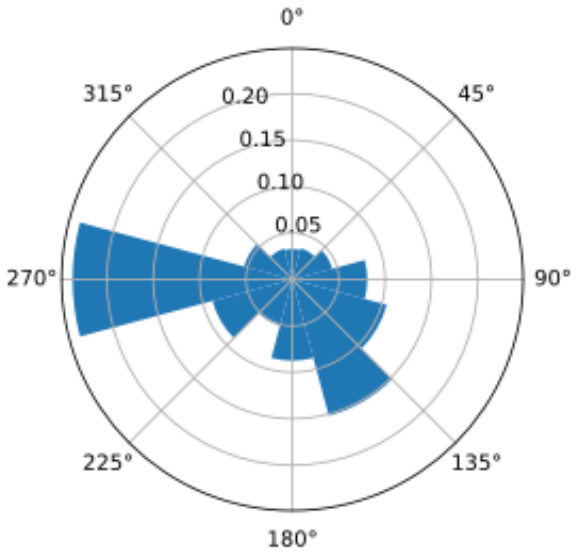

Figure 3.3: Wind direction distribution for the IEA site

Furthermore, the wind speed probability distribution at IEA37 can be obtained from PyWake and validated against studies such as Borlotti et al. [14]. The wind speeds at the site are of a very simple nature with a single probability value for all wind speeds. A constant probability for all wind speeds implies that there is no preference or bias towards certain wind speeds. This type of wind speed distribution is relatively rare in practice, but allows for easier computations.

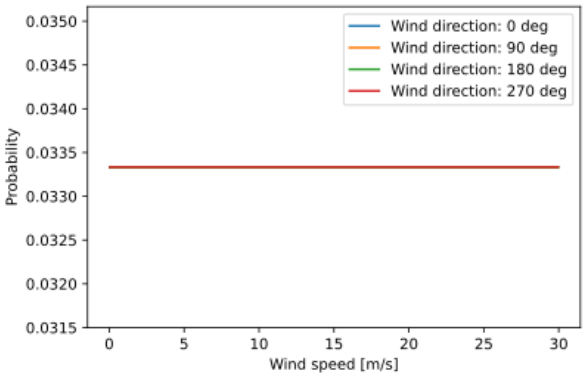

Figure 3.4: Wind speed distribution for the IEA site

3.2.2 Horns Rev

Horns Rev is an operational offshore wind farm located in the North Sea. It represents a real-world wind farm scenario with complex atmospheric conditions and wake interactions. The site consists of 80 wind turbines, each with a hub height of 70 m and a rotor diameter of 80 m [40]. Studies such as Wu et al. [105] and Gaumond et al. [40] provide valuable information about the wind characteristics at Horns Rev.

Wu et al. [105] conducted a LES simulation of the HornsRev 1 site which included the use of wind characteristics at Horns Rev using long-term measurements. The wind direction at Horns Rev exhibits a multi-modal distribution due to the complex atmospheric conditions and the influence of offshore terrain. This multi-modal distribution can significantly impact the wake behavior and power production in the wind farm.

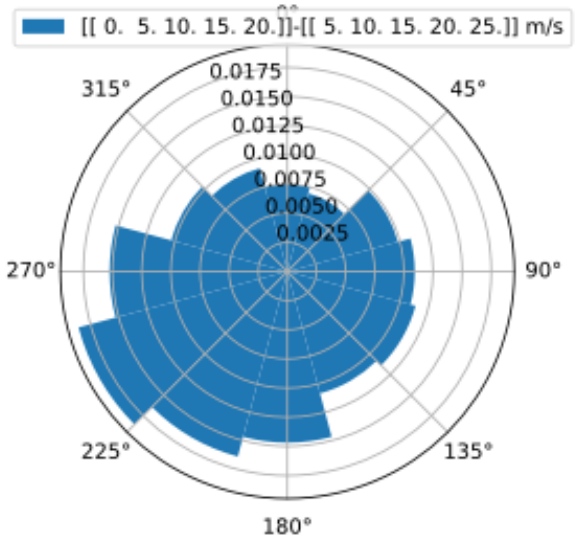

Figure 3.5: Wind direction distribution for the Horns Rev 1 site

Moreover, the wind speed probability distribution at Horns Rev is crucial for accurate wind farm modeling. Studies by Gaumond et al. [40] highlight the presence of specific wind speed regimes, including a predominant low wind speed regime and intermittent high wind speed events. Understanding these wind speed regimes and their associated probability distributions is vital for assessing turbine performance and optimizing energy production at Horns Rev.

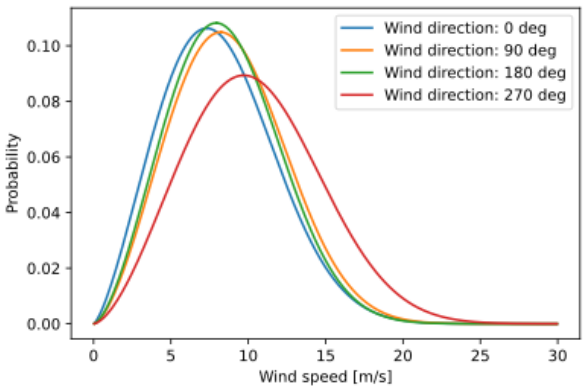

Figure 3.6: Wind speed distribution for the Horns Rev 1 site

3.2.3 Wind Shear Modeling

Accurate modeling of wind turbine performance is essential for optimizing energy production in wind farms. Wind shear, which accounts for the vertical variation of wind speed, plays a crucial role in accurately predicting the power output of wind turbines. In this section, we discuss the application of wind shear modeling at the site using PyWake.

To account for the vertical variation of wind speed, we incorporate the `PowerShear` method available in PyWake. The `PowerShear` method considers the vertical profile of wind speed using a shear exponent, which determines the rate of change of wind speed with height. For both the sites, we set the reference hub height, h_{ref}, to 80 m, which is a typical height for wind turbine installations. The shear exponent, α, is set to 0.1, representing a moderate increase in wind speed with height. By incorporating the wind shear model, PyWake considers the vertical variation of wind speed and its impact on the power output of each wind turbine.

$$V(z) = V_{\text{ref}} \left(\frac{z}{h_{\text{ref}}} \right)^{\alpha}$$

Wind shear modeling is crucial for accurate performance assessment and power prediction of wind turbines. Vertical variation in wind speed affects the energy extraction capability of turbines and can lead to variations in power production across different heights within the rotor swept area. By accounting for wind shear, we can better estimate the expected power output of each turbine and optimize the overall energy production of the wind farm.

Moreover, wind shear modeling allows for the consideration of different wind profiles and atmospheric conditions at the site. The shear exponent captures the site-specific characteristics related to turbulence, terrain, and wind flow patterns. By utilizing the `PowerShear` method in PyWake, we can enhance the accuracy of our simulations and provide more reliable estimates of power production.

In summary, the incorporation of wind shear modeling using the `PowerShear` method in PyWake enables me to account for the vertical variation of wind speed and improve the accuracy of power predictions. This modeling approach supports better assessment of turbine performance and aids in the optimization of energy production at the site.

3.3 AEP modelling using PyWake

The next step involves setting up the models required to accurately model the AEP for each site depending on it's wind speed and direction distributions. Accurately estimating the Annual Energy Production (AEP) of a wind farm is crucial for evaluating its economic viability and optimizing its performance. In this section, the AEP modeling approach implemented in PyWake, which combines various models to simulate wake effects and blockage within the wind farm is discussed. The key models employed in the AEP calculation are the wake deficit model, superposition model, and blockage deficit model.

3.3.1 Wake Deficit Model

The wake deficit model calculates the reduction in wind speed caused by the wake of upstream turbines. In PyWake, the wake deficit is modeled using the No-Jensen Deficit (NOJDeficit) model [50].

The wake deficit at a given location x and height z within the wind farm is given by:

$$\frac{u_w}{u_0} = 1 - \frac{2a}{(1 + 2\alpha x/D_r)^2} \tag{3.1}$$

where u_0 is the undisturbed wind speed, and a is the axial induction factor, whereas D_r is known as the downstream rotor diameter. The downstream rotor diameter D_r relates to the rotor diameter D_0 as

$$D_r = D_0\sqrt{\frac{1-a}{1-2a}} \tag{3.2}$$

The wake decay constant α is given by

$$\alpha = \frac{0.5}{\ln(z/z_0)} \tag{3.3}$$

while the axial induction factor is defined by

$$a = \frac{1-\sqrt{1-C_T}}{2} \tag{3.4}$$

where C_T is the thrust coefficient of the upstream turbine.

3.3.2 Superposition Model

The superposition model combines the individual wake deficits from multiple turbines to calculate the total wake effect on each downstream turbine. In this thesis, the `LinearSum` model is used for superposition.

The total wake deficit at a given location x and height z within the wind farm, accounting for the contribution from all upstream turbines, is calculated by summing the individual wake deficits:

$$\Delta U_{\text{total}}(x,z) = \sum_{i=1}^{N} \Delta U_i(x,z), \tag{3.5}$$

where $\Delta U_i(x, z)$ is the wake deficit from the i-th upstream turbine, and N is the total number of upstream turbines.

The `LinearSum` superposition model is commonly employed in various wake modeling frameworks [7], striking a balance between accuracy and computational efficiency.

3.3.3 Blockage Deficit Model

The blockage deficit model accounts for the reduction in wind speed caused by the presence of neighboring turbines. In PyWake, the `SelfSimilarityDeficit` model is used for blockage modeling [7].

The blockage deficit at a given location x and height z within the wind farm is given by:

$$\Delta U_{\text{block}}(x, z) = \frac{A_{\text{rotor}}}{A_{\text{wind farm}}} \cdot \Delta U_{\text{total}}(x, z), \tag{3.6}$$

where A_{rotor} is the rotor area of an individual turbine, and $A_{\text{wind farm}}$ is the total area of the wind farm.

The `SelfSimilarityDeficit` blockage deficit model [7] provides a practical approach for accounting for the blockage effect in large wind farms.

In conclusion, PyWake integrates various models, including the wake deficit model, superposition model, and blockage deficit model, to accurately estimate the Annual Energy Production (AEP) of a wind farm. By considering wake interactions and blockage effects, PyWake provides a more precise assessment of AEP. The power output of each turbine is calculated using the formula:

$$P_{\text{turbine}}(i) = C_p(\lambda_i, \beta_i) \cdot U_{\text{eff}}(i)^3, \tag{3.7}$$

$C_p(\lambda_i, \beta_i)$ is the power coefficient, and $U_{\text{eff}}(i)$ is the effective wind speed at the location of the i'th turbine, considering wake effects and blockage. The AEP is then calculated by summing the power outputs of all turbines weighted by their operating hours:

$$\text{AEP} = \sum_{i=1}^{n} \left(P_i \times \sum_{j=1}^{m} H_{ij} \right) \tag{3.8}$$

where $H(i)$ is estimated as the total number of hours a turbine operates at a specific wind speed. It can derived from the pdf for each site and tells us the probability of wind turbine i operating in that particular wind speed bin.

3.4 Cost modelling using TOPFARM

This section focuses on the cost modelling aspect of wind farm analysis using the TOPFARM framework. Estimating the expenses of wind farm installations accurately is critical for evaluating the economic feasibility and maximizing the financial performance of wind energy projects. TOPFARM is a flexible platform that incorporates multiple cost elements into a complete cost model, such as turbine costs, installation charges, operating and maintenance costs, and other financial aspects. By leveraging the capabilities of TOPFARM, users can systematically evaluate and optimize wind farm designs based on their economic implications. This section explores the methodologies and tools offered by TOPFARM for cost modelling,

highlighting its ability to facilitate detailed cost analysis, enhance decision-making processes, and contribute to the overall economic viability of wind farm projects.

3.4.1 The Ecoeval library

In the cost modelling process of wind farm analysis, TOPFARM incorporates the EcoEval library and certain parameters to accurately calculate the costs associated with wind farm installations. These parameters include:

- **Distance from Shore**: The distance of the wind farm from the shore, which influences installation and grid connection costs. In this thesis, the distance is assumed to be a constant at 30 kilometers.
- **Energy Price**: The price at which the generated wind energy is sold, affecting the revenue and overall economic viability of the wind farm, and is assumed to be 0.1 Euros/kWh.
- **Project Duration**: The estimated duration of the wind farm project, impacting operational and maintenance costs over the project's lifespan. The project duration is assumed to be 20 years.
- **Water Depth**: The depth of the water where the wind farm is situated, influencing the costs of foundation design and installation. The water depth is also assumed to be a constant at 15 meters.

The values used for the distance from shore and water depth in this thesis were derived from relevant literature [28]. According to Diaz et al. [28], offshore wind structures in Denmark are typically installed at an average distance of 25 kilometers from the shore and at an average water depth of 10 meters. It is important to note that these values can vary significantly from site to site and even within the wind farm itself, depending on specific conditions. However, the focus of this thesis is not on capturing the effects of these variations on calculated costs, and therefore, they have been neglected in the development of the cost model and subsequent analysis.

Another significant limitation of the cost model is that the scaling factors utilized to calculate costs are derived from the value of the Euro in 2017. Consequently, the calculated costs may be lower compared to the costs estimated for the current value and present time.

3.4.2 DEVEX (DEVelopment EXpenditure)

Table 3.2 provides a breakdown of the costs associated with the development and exploration (DEVEX) phase of a wind energy project, all denominated in euros. These costs represent additional expenses beyond the primary components of the turbine system and are crucial for comprehensive financial evaluation. The `Factor` is a calculated value used in subsequent cost calculations. The `Environmental Survey` cost is determined by multiplying the factor by the distance from the shore and a constant value of €1,000,000, covering the expenses of conducting an environmental survey. The `Sea Bed Survey` cost is calculated by multiplying a fixed factor of €150,000 by the number of turbines, accounting for the survey of the sea bed. The `Met Mast` cost includes the installation and maintenance of a meteorological mast to collect wind data and is determined by multiplying the factor by the distance from the shore and €1,000,000. Lastly, the `Development Services` cost is based on a factor of €70,000 multiplied by the sum of the

rated power of all turbines, covering expenses related to project development and management services.

Table 3.2: DEVEX costs incurred

Cost Component	Cost Calculation
Factor	$\frac{2.0\times10^3}{39} \times 0.3 \times \frac{1}{80}$
Environmental Survey	Factor $\times 10^6 \times$ Distance from shore
Sea Bed Survey	$1.5 \times 10^5 \times$ Number of turbines
Met Mast	Factor $\times 10^6 \times$ Distance from shore
Development Services	$0.7 \times 10^5 \times \sum$ Rated Power

3.4.3 OPEX (OPerational EXpenditure)

Table 3.3 presents an overview of the operational expenditure (OPEX) costs associated with a wind energy project, expressed in euros. These expenses contribute to the turbine system's long-term operation and maintenance. The `Onshore Personnel` cost is calculated by multiplying a factor of €5,500 by the total rated power of all turbines, while accounting for onshore staff expenditures. The `Buildings, Harbor Fees, etc.` cost is a fixed value of €3,000,000, encompassing infrastructure costs and harbor utilization expenses. The `Mobilization, Rental Time` cost is calculated by multiplying a factor of €96,000 by the number of turbines, considering the expenses associated with mobilizing equipment and the rental duration. The `Jackup Personnel` cost is determined by multiplying a factor of €8,500 by the number of turbines, covering the personnel involved in jackup operations. The `Offshore Service Personnel` cost is calculated by multiplying a factor of €12,000 by the sum of the rated power of all turbines, accounting for the expenses associated with offshore service personnel. The `Service, Failed Components` cost considers maintenance and replacement of components and is calculated by multiplying a factor of €2,100 by the sum of the rated power of all turbines. Lastly, the `Ships, Offshore Operations` cost takes into account the expenses associated with offshore vessel usage and operation and is calculated by multiplying a factor of €4,600 by the number of turbines and the distance from the shore.

Table 3.3: OPEX costs incurred

Cost Component	Cost Calculation
Onshore Personnel	$5.5 \times 10^3 \times \sum$ Rated Power
Buildings, Harbor Fees, etc.	3.0×10^6
Mobilization, Rental Time	$9.6 \times 10^4 \times$ Number of Turbines
Jackup Personnel	$8.5 \times 10^3 \times$ Number of Turbines
Offshore Service Personnel	$1.2 \times 10^4 \times \sum$ Rated Power
Service, Failed Components	$2.1 \times 10^3 \times \sum$ Rated Power
Ships, Offshore Operations	$4.6 \times 10^3 \times$ Number of Turbines $\times$ Distance from Shore

3.4.4 CAPEX (CAPital EXpenditure)

CAPEX, short for Capital Expenditure, encompasses the upfront costs associated with the development, construction, and installation of a wind turbine. It is divided into several key components, namely blades, tower, foundation, nacelle, hub, and drivetrain. The blades

are responsible for capturing wind energy, while the tower provides structural support. The foundation ensures stability and anchors the turbine to the ground. The nacelle houses vital components such as the generator and control systems. The hub connects the blades to the drivetrain, which includes the main shaft, bearings, gearbox, and coupling.

3.4.4.1 Blades

Table 3.4 presents the calculations for blade mass and costs incurred in a wind energy project. The `Blade Mass` is determined using the formula $0.3 \times \text{rotor diameter}^{2.5}$. This formula takes into account the rotor diameter and calculates the mass of the blades. The `Blade Cost` is then calculated by multiplying the `Blade Mass` by a factor of 12.0 to account for the manufacturing and material costs. The result is a comprehensive estimate of the costs associated with the blades in the wind turbine system.

Table 3.4: Blade costs incurred

Calculation	**Formula**
Blades Mass	$0.3 \times \text{rotor diameter}^{2.5}$
Blades Cost	$12.0 \times (3 \times \text{Blades Mass})$

3.4.4.2 Hub

Table 3.5 provides an overview of the calculations for various components contributing to the hub mass in a wind energy project. The `Structure mass` is determined using the formula $6.0 \times 10^3 + 0.1 \times \text{rotor diameter}^{2.5}$. This equation considers a base mass of €6,000 and adds a component proportional to the rotor diameter, reflecting the size-dependent contribution to the structure mass. The `Pitch bearings mass` is calculated as $5.0 \times 10^2 + 0.07 \times \text{rotor diameter}^{2.5}$. It incorporates a fixed component of €500 and an additional term based on the rotor diameter, accounting for the mass of the pitch bearings. Similarly, the `Pitch system mass` is determined using $5.0 \times 10^2 + 0.03 \times \text{rotor diameter}^{2.5}$. It includes a fixed term of €500 and a size-dependent factor related to the rotor diameter, considering the mass of the pitch system components. Lastly, the `Secondary mass` is calculated as $7.0 \times 10^2 + 15.0 \times \text{rotor diameter}^{1.0}$. This formula combines a fixed term of €700 and a term proportional to the rotor diameter, reflecting the contribution of additional secondary components to the overall hub mass.

Table 3.5: Hub mass components

Calculation	**Formula**
Structure mass	$6.0 \times 10^3 + 0.1 \times \text{rotor diameter}^{2.5}$
Pitch bearings mass	$5.0 \times 10^2 + 0.07 \times \text{rotor diameter}^{2.5}$
Pitch system mass	$5.0 \times 10^2 + 0.03 \times \text{rotor diameter}^{2.5}$
Secondary mass	$7.0 \times 10^2 + 15.0 \times \text{rotor diameter}^{1.0}$

Table 3.6 provides an overview of the cost calculations for various components contributing to the hub cost in a wind energy project. The Structure cost is determined by multiplying the structure mass by a factor of 2.5. This formula, $2.5 \times$ structure mass, accounts for the cost associated with the materials, manufacturing, and assembly of the hub structure. The `Pitch bearings cost` is calculated by multiplying the pitch bearings mass by a factor of 8.0. Using

the formula 8.0 × pitch bearings mass, this cost component considers the expenses related to the pitch bearing components, including procurement, installation, and maintenance. Similarly, the `Pitch system cost` is determined by multiplying the pitch system mass by a factor of 8.0. The formula 8.0 × pitch system mass represents the cost associated with the pitch system components, including the control mechanisms, hydraulic systems, and related infrastructure. Lastly, the `Secondary cost` is calculated by multiplying the secondary mass by a factor of 8.0. Using the formula 8.0 × secondary mass, this cost component considers the expenses related to the additional secondary components integrated into the hub, such as sensors, electrical wiring, and auxiliary systems.

Table 3.6: Hub cost components

Calculation	**Formula**
Structure cost	2.5 × structure mass
Pitch bearings cost	8.0 × pitch bearings mass
Pitch system cost	8.0 × pitch system mass
Secondary cost	8.0 × secondary mass

3.4.4.3 Nacelle

Table 3.7 presents the various components contributing to the overall mass of the nacelle in a wind turbine system. Each component is calculated based on specific formulas. The `Nacelle Mass (Cooling)` component is determined by a formula that includes the rated power of the turbine, reflecting the mass contribution of the cooling system responsible for maintaining optimal operating temperatures within the nacelle. The `Nacelle Mass (Converter)` is calculated using a formula involving the rated power, representing the mass of the power converter, which converts the variable-speed electricity generated by the turbine to the required grid frequency. Similarly, the `Nacelle Mass (Controller)` is calculated based on the rated power and reflects the mass of the control system responsible for monitoring and regulating various turbine operations. The `Nacelle Mass (Yaw)` is determined by a formula incorporating the rotor diameter, representing the mass of the yaw system that enables the turbine to rotate and align with the wind direction. The `Nacelle Mass (Canopy)` component considers the rated power and reflects the mass of the protective canopy that shelters the internal components. Finally, the `Nacelle Mass (Secondary)` is calculated using the rated power and represents the mass of additional auxiliary components and supporting structures within the nacelle.

Table 3.7: Nacelle mass components

Calculation	**Formula**
Nacelle Mass (Cooling)	$0.0 + 500.0 \times \text{Rated Power}^{1.0}$
Nacelle Mass (Converter)	$0.0 + 1.0e3 \times \text{Rated Power}^{1.0}$
Nacelle Mass (Controller)	$200.0 + 100.0 \times \text{Rated Power}^{1.0}$
Nacelle Mass (Yaw)	$0.0 + 0.1 \times \text{Rotor Diameter}^{2.5}$
Nacelle Mass (Canopy)	$1.0e3 + 1.5e3 \times \text{Rated Power}^{1.0}$
Nacelle Mass (Secondary)	$1.0e3 + 1.0e3 \times \text{Rated Power}^{1.0}$

Table 3.8 provides a breakdown of the cost components associated with the nacelle in a wind turbine system. Each component's cost is calculated based on specific formulas and

corresponds to the respective mass components. The `Nacelle Cost (Cooling)` is determined by multiplying a factor of €8.0 by the nacelle mass attributed to the cooling system, representing the cost of implementing and maintaining the cooling infrastructure within the nacelle. The `Nacelle Cost (Converter)` is calculated by multiplying a factor of €30.0 by the nacelle mass associated with the power converter, representing the cost of the converter and its integration into the system. Similarly, the `Nacelle Cost (Controller)` is obtained by multiplying a factor of €50.0 by the nacelle mass attributed to the control system, reflecting the cost of the control components and their implementation. The `Nacelle Cost (Yaw)` is calculated by multiplying a factor of €6.0 by the nacelle mass linked to the yaw system, representing the cost of the yaw mechanism and its associated components. The `Nacelle Cost (Canopy)` considers the nacelle mass associated with the protective canopy and is obtained by multiplying a factor of €10.0, representing the cost of the canopy structure and its installation. Finally, the `Nacelle Cost (Secondary)` reflects the cost of additional auxiliary components and supporting structures within the nacelle and is calculated by multiplying a factor of €10.0 by the corresponding nacelle mass.

Table 3.8: Nacelle cost components

Calculation	**Formula**
Nacelle Cost (Cooling)	8.0 × Nacelle Mass (Cooling)
Nacelle Cost (Converter)	30.0 × Nacelle Mass (Converter)
Nacelle Cost (Controller)	50.0 × Nacelle Mass (Controller)
Nacelle Cost (Yaw)	6.0 × Nacelle Mass (Yaw)
Nacelle Cost (Canopy)	10.0 × Nacelle Mass (Canopy)
Nacelle Cost (Secondary)	10.0 × Nacelle Mass (Secondary)

3.4.4.4 Tower

Table 3.9 outlines the various components contributing to the mass of the tower in a wind turbine system. Each component's mass is calculated using specific formulas based on relevant parameters. The `Tower Mass (Structure)` is determined by a formula that incorporates the rotor area and hub height, resulting in the mass of the tower structure necessary to support the turbine system. The `Tower Mass (Internal)` considers the internal components of the tower and is determined by a formula that takes into account the hub height, reflecting the mass associated with the internal systems and equipment. The `Tower Mass (Cabling)` is calculated based on the rated power of the turbine and the hub height, accounting for the mass of the cabling required for electrical connections. The `Tower Mass (Secondary)` represents the mass of additional auxiliary components within the tower and is determined by a formula that considers the rated power of the turbine. Finally, the `Tower Mass (Transformer)` reflects the mass associated with the transformer within the tower and is calculated based on the rated power of the turbine.

Table 3.9: Tower mass components

Calculation	Formula
Tower Mass (Structure)	$0.0 + 0.25 \times (\sqrt{\text{Rotor Area}} \times \text{Hub Height})^{1.0}$
Tower Mass (Internal)	$1.0e3 + 100.0 \times \text{Hub Height}^{1.0}$
Tower Mass (Cabling)	$0.0 + 25.0 \times (\sqrt{\text{Rated Power}} \times \text{Hub Height})^{1.0}$
Tower Mass (Secondary)	$1.0e3 + 500.0 \times \text{Rated Power}^{1.0}$
Tower Mass (Transformer)	$0.0 + 2.5e3 \times \text{Rated Power}^{1}$

Table 3.10 provides a breakdown of the various cost components associated with the tower in a wind turbine system. These cost components are calculated based on the corresponding tower mass components using specific formulas. The `Tower Cost (Structure)` is determined by multiplying the mass of the tower structure by a factor of 1.5, representing the cost associated with the structural materials and construction of the tower. The `Tower Cost (Internal)` reflects the cost of the internal components and systems within the tower and is obtained by multiplying the corresponding tower mass by a factor of 8.0. Similarly, the `Tower Cost (Cabling)` represents the cost of the cabling required for electrical connections and is calculated by multiplying the tower mass by a factor of 8.0. The `Tower Cost (Secondary)` accounts for the cost of additional auxiliary components within the tower and is obtained by multiplying the corresponding tower mass by a factor of 10.0. Lastly, the `Tower Cost (Transformer)` reflects the cost associated with the transformer within the tower and is determined by multiplying the tower mass by a factor of 8.0.

Table 3.10: Tower cost components

Calculation	Formula
Tower Cost (Structure)	$1.5 \times$ Tower Mass (Structure)
Tower Cost (Internal)	$8.0 \times$ Tower Mass (Internal)
Tower Cost (Cabling)	$8.0 \times$ Tower Mass (Cabling)
Tower Cost (Secondary)	$10.0 \times$ Tower Mass (Secondary)
Tower Cost (Transformer)	$8.0 \times$ Tower Mass (Transformer)

3.4.4.5 Ancilliary turbine costs

Table 3.11 outlines the cost components associated with ancillary turbine costs in a wind energy project. These costs are calculated using specific formulas based on relevant parameters. Under the `Direct Production` category, the `Direct Labor` cost is determined by multiplying a factor of 0.03 by the Bill of Material Cost, representing the labor expenses directly associated with production. The `Production Overhead` cost is calculated by multiplying the Bill of Material Cost by 0.1, accounting for additional overhead expenses related to production activities.

The `SGA Costs` category includes the `SGA Overhead`, the `RD`, and the `SGA` costs. The `SGA Overhead` indicates the overhead cost of selling, general, and administrative expenditures and is determined by multiplying the Direct Production Cost by a factor of 0.05. The `RD` cost represents research and development expenditures and is calculated by multiplying the Direct Production Cost by a factor of 0.03. The `SGA` cost, representing additional selling, general, and administrative expenses, is calculated by multiplying a factor of 0.05 by the Direct Production Cost.

The `Project Costs` category includes various cost components related to the overall project. The `Total Production Cost` is the sum of the Direct Production Cost and the SGA Cost. The `Transportation` cost considers the expenses associated with transporting turbine components and is calculated based on the total mass of the turbine components. The `Harbor Storage and Assembly` cost reflects the expenses related to storage and assembly in the harbor area and is determined by multiplying a factor of $25,000$ by the Rated Power and adding $150,000$. The `Installation and Commissioning` cost accounts for the installation and commissioning activities and is calculated by multiplying a factor of $50,000$ by the Rated Power and adding $100,000$. The `Warranty and Accruals` cost represents the estimated warranty expenses and is determined by multiplying a factor of 0.03 by the Total Production Cost. Lastly, the `Financing` cost reflects the financing expenses of the project and is calculated by multiplying a factor of 0.02 by the Total Production Cost.

Table 3.11: Ancilliary turbine costs

Cost Component	**Cost Calculation**
Direct Production	
Direct Labor	$0.03 \times$ Bill of Material Cost
Production Overhead	$0.1 \times$ Bill of Material Cost
SGA Costs	
SGA Overhead	$0.05 \times$ Direct Production Cost
RD	$0.03 \times$ Direct Production Cost
SGA	$0.05 \times$ Direct Production Cost
Project Costs	
Total Production Cost	Direct Production Cost + SGA Cost
Transportation	$0.2 \times (\sum$ Turbine Component Mass$) + 10,000$
Harbor Storage and Assembly	$25,000 \times$ Rated Power $+ 150,000$
Installation and Commissioning	$50,000 \times$ Rated Power $+ 100,000$
Warranty and Accruals	$0.03 \times$ Total Production Cost
Financing	$0.02 \times$ Total Production Cost

3.4.4.6 Foundation costs

The mass calculation for the foundation, including both the monopile and the transition piece (TP), is represented in Table 3.12. The `Foundation Mass` is determined by the following formula: $(6.5 \times 10^4 + 4.5 \times 10^3 \times$ Water Depth $+ 40.0 \times$ Water Depth$^2) \times$ Rated Power. This formula considers the water depth as a parameter and takes into account the rated power of the wind turbine. By incorporating these factors, the calculation estimates the total mass of the foundation required to support the wind turbine structure.

Table 3.12: Foundation mass

Component	**Formula**
Foundation Mass	$(6.5 \times 10^4 + 4.5 \times 10^3 \times$ Water Depth $+40.0 \times$ Water Depth$^2) \times$ Rated Power

The cost calculation for the foundation, encompassing both the monopile and the transition piece (TP), is presented in Table 3.13. The `Foundation Cost` is determined by multiplying

the `Foundation Mass` by a factor of 1.5. This calculation estimates the total cost associated with the foundation, taking into account factors such as material expenses, construction, and installation costs. The foundation is a critical component of a wind turbine system, providing structural support and stability.

Table 3.13: Foundation cost

Component	**Formula**
Foundation Cost	$1.5 \times$ Foundation Mass

3.4.4.7 Ancilliary foundation costs

The breakdown of ancillary costs associated with the foundation of a wind turbine is provided in Table 3.14. These costs include direct production expenses, SGA (selling, general, and administrative) costs, and various project-related expenses.

Under the "Direct Production" category, the `Direct Labor` cost is calculated as 0.03 times the `Bill of Material Cost`, representing the labor expenses directly involved in the production process. The `Production Overhead` is determined as 0.1 times the `Bill of Material Cost`, accounting for indirect production expenses.

The `SGA Costs` section includes costs related to selling, general, and administrative activities. The `SGA Overhead` is calculated as 0.05 times the `Direct Production Cost`, representing the overhead expenses associated with the production process. The `RD` (Research and Development) cost is determined as 0.03 times the `Direct Production Cost`, considering expenses allocated to research and development activities. The `SGA` cost is calculated as 0.05 times the `Direct Production Cost`, covering general administrative costs.

The `Project Costs` category includes various expenses related to the overall project. The `Total Production Cost` is obtained by adding the `Direct Production Cost` and the `SGA Cost`. The `Transportation` cost is determined as 0.2 times the sum of the mass of all turbine components plus 10,000, accounting for transportation expenses. The `Harbor Storage and Assembly` cost is calculated as 25,000 times the `Rated Power` plus 150,000, representing the expenses associated with storage and assembly in the harbor. The `Installation and Commissioning` cost is determined as 50,000 times the `Rated Power` plus 100,000, covering the costs of installation and commissioning activities. The `Warranty and Accruals` cost is calculated as 0.03 times the `Total Production Cost`, considering warranty expenses and accruals. Finally, the `Financing` cost is determined as 0.02 times the `Total Production Cost`, accounting for financing expenses.

Table 3.14: Ancilliary foundation costs

Cost Component	**Cost Calculation**
Direct Production	
Direct Labor	$0.03 \times$ Bill of Material Cost
Production Overhead	$0.1 \times$ Bill of Material Cost
SGA Costs	
SGA Overhead	$0.05 \times$ Direct Production Cost
RD	$0.03 \times$ Direct Production Cost
SGA	$0.05 \times$ Direct Production Cost
Project Costs	
Total Production Cost	Direct Production Cost + SGA Cost
Transportation	$0.2 \times (\sum$ Turbine Component Mass$) + 10,000$
Harbor Storage and Assembly	$25,000 \times$ Rated Power $+ 150,000$
Installation and Commissioning	$50,000 \times$ Rated Power $+ 100,000$
Warranty and Accruals	$0.03 \times$ Total Production Cost
Financing	$0.02 \times$ Total Production Cost

3.4.4.8 Drivetrain costs

Table 3.15 presents the mass calculations for various components of the wind turbine drivetrain. The drivetrain is responsible for converting the rotational energy of the rotor into electrical energy. The mass of each component is calculated based on specific formulas using parameters such as rotor diameter, rated torque, and rated RPM.

The `Bedplate` mass is determined as 0.0 plus 2.4 times the square of the rotor diameter. It represents the supporting structure that holds and connects the major components of the drivetrain.

The `Main Shaft` mass is calculated as 0.0 plus 0.02 times the rotor diameter raised to the power of 2.8. It refers to the central shaft that transmits the rotational energy from the rotor to the gearbox.

The `Main Bearings` mass is determined as 0.0 plus 0.02 times the rotor diameter raised to the power of 2.5. It represents the bearings that support and allow the rotation of the main shaft.

The `Bearing Housing` mass is calculated as 0.0 plus 0.03 times the rotor diameter raised to the power of 2.5. It refers to the housing that encloses and protects the main bearings.

The `Gearbox` mass is determined as 0.0 plus 15.0 times the rated torque. It represents the gearbox component responsible for increasing the rotational speed of the generator.

The `Coupling and Brake` mass includes two components. The first component is 500.0, representing the mass of the coupling and brake components. The second component is 50.0 times the quantity of the rated torque multiplied by the rated RPM divided by 1.5 raised to the power of 1.0. It accounts for additional mass related to the torque and speed requirements.

The `Generator` mass includes two components as well. The first component is 1.0×10^3, representing the base mass of the generator. The second component is 400.0 times the quantity of the rated torque multiplied by the rated RPM divided by 1.5 raised to the power of 1.0. It represents the additional mass associated with the torque and speed requirements.

Table 3.15: Drivetrain mass

Component	**Mass Calculation**
Bedplate	$0.0 + 2.4 \times \text{Rotor Diameter}^{2.0}$
Main Shaft	$0.0 + 0.02 \times \text{Rotor Diameter}^{2.8}$
Main Bearings	$0.0 + 0.02 \times \text{Rotor Diameter}^{2.5}$
Bearing Housing	$0.0 + 0.03 \times \text{Rotor Diameter}^{2.5}$
Gearbox	$0.0 + 15.0 \times \text{Rated Torque}^{1.0}$
Coupling and Brake	$500.0 + 50.0 \times \left(\frac{\text{Rated Torque} \times \text{Rated RPM}}{1.5}\right)^{1.0}$
Generator	$1.0 \times 10^3 + 400.0 \times \left(\frac{\text{Rated Torque} \times \text{Rated RPM}}{1.5}\right)^{1.0}$

Table 3.16 presents the cost calculations for various components of the wind turbine drivetrain. The drivetrain is responsible for converting the rotational energy of the rotor into electrical energy. The cost of each component is calculated based on the respective mass and a cost factor.

The `Bedplate` cost is calculated as 2.5 times the mass of the bedplate component. It represents the cost associated with the supporting structure that holds and connects the major components of the drivetrain.

The `Main Shaft` cost is determined as 5.0 times the mass of the main shaft component. It accounts for the cost of the central shaft that transmits the rotational energy from the rotor to the gearbox.

The `Main Bearings` cost is calculated as 15.0 times the mass of the main bearings component. It represents the cost of the bearings that support and allow the rotation of the main shaft.

The `Bearing Housing` cost is determined as 2.5 times the mass of the bearing housing component. It accounts for the cost of the housing that encloses and protects the main bearings.

The `Gearbox` cost is calculated as 8.0 times the mass of the gearbox component. It represents the cost associated with the gearbox that increases the rotational speed of the generator.

The `Coupling and Brake` cost is calculated as 8.0 times the mass of the coupling and brake components. It accounts for the cost of the components that provide coupling and braking functions within the drivetrain.

The `Generator` cost is calculated as 8.0 times the mass of the generator component. It represents the cost associated with the generator that converts the mechanical energy into electrical energy.

Table 3.16: Drivetrain cost

Component	**Cost Calculation**
Bedplate	$2.5 \times$ Bedplate Mass
Main Shaft	$5.0 \times$ Main Shaft Mass
Main Bearings	$15.0 \times$ Main Bearings Mass
Bearing Housing	$2.5 \times$ Bearing Housing Mass
Gearbox	$8.0 \times$ Gearbox Mass
Coupling and Brake	$8.0 \times$ Coupling and Brake Mass
Generator	$8.0 \times$ Generator Mass

The total CAPEX can be calculated by summing the costs:

$$\text{CAPEX} = (\text{Turbine costs}) + (\text{Foundation costs}) + (\text{Drivetrain costs}) \tag{3.9}$$

3.4.5 BOP (Balance Of Plant)

Table 3.17 provides a breakdown of the costs associated with the Balance of Plant (BOP) for a wind energy project. The BOP includes various components and infrastructure necessary for the operation and connection of the wind turbines to the electrical grid.

The `BOP Substation` cost is calculated as 6.0×10^6 plus 1.0×10^4 times the sum of the `Rated Power` raised to the power of 1.5. This cost accounts for the construction and equipment of the substation required for transforming and transmitting the generated power.

The `BOP Array of Cables` cost is determined as 3.5×10^3 times the sum of the `Rotor Diameter` of all turbines. This cost covers the installation and connection of cables within the wind farm, ensuring the transfer of electricity between the turbines and the substation.

The `BOP Cables Export` cost is calculated as 1.4×10^6 times the distance from shore. This cost represents the expenses associated with the export cables that transmit the generated power from the offshore wind farm to the onshore grid connection point.

The `BOP Onshore Electrical` cost includes two components. The first component is 5.0×10^4 times the sum of the `Rated Power`, covering the electrical infrastructure required for connecting the wind farm to the onshore electrical grid. The second component is 50.0 times the sum of the `Rated Power` squared, representing additional costs related to the onshore electrical system.

Table 3.17: BOP costs

Cost Component	**Cost Calculation**
BOP Substation	$(6.0 \times 10^6) + (1.0 \times 10^4) \times (\sum \text{Rated Power})^{1.5}$
BOP Array of Cables	$3.5 \times 10^3 \times (\sum \text{Rotor Diameter})$
BOP Cables Export	$1.4 \times 10^6 \times \text{Distance from shore}$
BOP Onshore Electrical	$5.0 \times 10^4 \times (\sum \text{Rated Power}) + 50.0 \times (\sum \text{Rated Power})^2$

3.4.6 ABEX (Annual Base EXpenditure)

In this section, we will discuss the ABEX (Annual Base Expenditure) associated with the wind turbine project. The ABEX represents the ongoing operational expenses and maintenance costs after the project's completion.

The ABEX is calculated by multiplying a factor of 0.03 with the CAPEX (Capital Expenditure) of the project:

$$\text{ABEX} = 0.03 \times \text{CAPEX} \tag{3.10}$$

The ABEX represents the annual expenditure required to maintain and operate the wind turbine project. It includes costs such as routine maintenance, repairs, inspections, and other operational expenses necessary to keep the turbines operating efficiently and safely.

3.5 Calculating LCOE

The main objective function is to reduce the LCOE of the layout design in question. The Levelized Cost of Energy is defined as the total cost of energy per unit of energy production. Therefore, it is quite necessary to calculate the LCOE accurately to represent the overall cost of the wind farm. A very simplified and reduced formula taken from [30] for the LCOE can be given by

$$\mathrm{LCOE} = \frac{\sum_{t=1}^{n} \frac{\mathrm{I}_t + \mathrm{M}_t + \mathrm{A}_t + \mathrm{BOP}_t + \mathrm{D}_t}{(1+\mathrm{r})}}{\sum_{t=1}^{n} \frac{Et}{(1+\mathrm{r})^t}} \tag{3.11}$$

where
$\mathrm{I_t}$ = Investment expenditures in year t (including financing)
$\mathrm{D_t}$ = Development expenditures in year t
$\mathrm{BOP_t}$ = Balance of plant expenditures in year t
$\mathrm{A_t}$ = Annual base expenditure in year t
$\mathrm{M_t}$ = Operations and maintenance expenditures in year t
$\mathrm{E_t}$ = Electricity generation in year t
r = Discount rate
n = Life of the system

To reduce the complexity of the problem and due to data management and availability constraints, the main contributors to the wind farm costs are considered to be the capital expenditure i.e. I_t (CAPEX), operations and maintenance expenditures i.e. M_t (OPEX), the Balance of Plant expenditures i.e. BOP_t,and the development expenditure D_t (DEVEX) and the annual base expenditure A_t (ABEX).

CHAPTER 4
Optimization algorithms

In this section, the optimization algorithms that are used are detailed. As mentioned in subsection 2.2.2, two prominent techniques are employed, namely Random Search and Particle Swarm Optimization (PSO). These algorithms offer distinct approaches to tackling optimization problems and have gained widespread recognition in various domains.

Optimization algorithms typically consist of three main components when applied to problems such as optimizing wind farm layouts for maximizing energy production and minimizing costs. These components are:

1. Objective Function: The objective function represents the goal of the optimization problem. The Levelized Cost of Energy (LCOE) and Annual Energy Production (AEP) are the two primary objective functions considered in this thesis. The first seeks to reduce the cost of energy generation, while the latter seeks to increase the wind farm's overall energy production. Both functions will be examined independently, and the findings will be compared.
2. Design or Optimization Variables: These variables are the parameters that can be adjusted or optimized to find the optimal solution. For this thesis, the design variables typically include the geographical location of the wind farm, hub height, turbine type, and the total number of turbines. These variables directly influence the energy production, cost, and feasibility of the wind farm layout.
3. Constraints: Constraints define the limitations or restrictions that must be considered during the optimization process. In the context of this thesis, constraints include boundaries for the wind farm area, minimum spacing requirements between turbines to avoid wake effects, maximum and minimum turbine capacity, and restrictions on the maximum and minimum number of turbines. These constraints ensure that the optimized layout satisfies practical considerations, such as safety, land availability, and regulatory requirements.

By considering both the Levelized Cost of Energy and the Annual Energy Production as objective functions, and including the appropriate design variables and constraints, the optimization algorithm can effectively search for wind farm layouts that are optimized for cost-efficiency or energy production, allowing us to analyze various trends and postulate the effects of changing designs.

4.1 Design Variables and Constraints

The optimization algorithms for wind farm layout design involve altering the site design by manipulating various design variables. These variables, along with the associated constraints, play a crucial role in finding an optimal layout. The four main ways in which the algorithms can modify the wind farm's design are:

4.1.1 Change the Geographical Location of a Random Turbine

One design variable is the geographical location of a turbine. The algorithms can modify the position of a turbine by adjusting two main variables: step size and angle. These variables control the movement of the turbine in a 2-dimensional space.

When changing the geographical location, two constraints need to be considered: the minimum spacing requirement and the boundary constraint. The minimum spacing requirement ensures that turbines are positioned a certain distance apart to mitigate wake effects and optimize power production. It is typically defined as a multiple of the rotor diameter, such as:

$$\text{Minimum spacing} = 5 \times \text{Rotor Diameter}$$

where

$$\text{Rotor Diameter DTU 10 MW} = 178.3 \text{ m}$$

$$\text{Rotor Diameter Vestas V164 8MW} = 164 \text{ m}$$

$$\text{Rotor Diameter Vestas V80} = 80 \text{ m}$$

The determination of turbine spacing in the wind farm optimization process involves calculating the distances between the turbine under evaluation and every other turbine in the farm. The minimum spacing is then defined as the rotor diameter of the turbine with the larger rotor diameter among the two turbines being evaluated. This dynamic approach ensures that the minimum spacing requirement adjusts based on the specific type of turbine being considered. By taking into account the varying rotor diameters, the optimization process accommodates the specific requirements and characteristics of each turbine type, allowing for an effective and customized layout design.

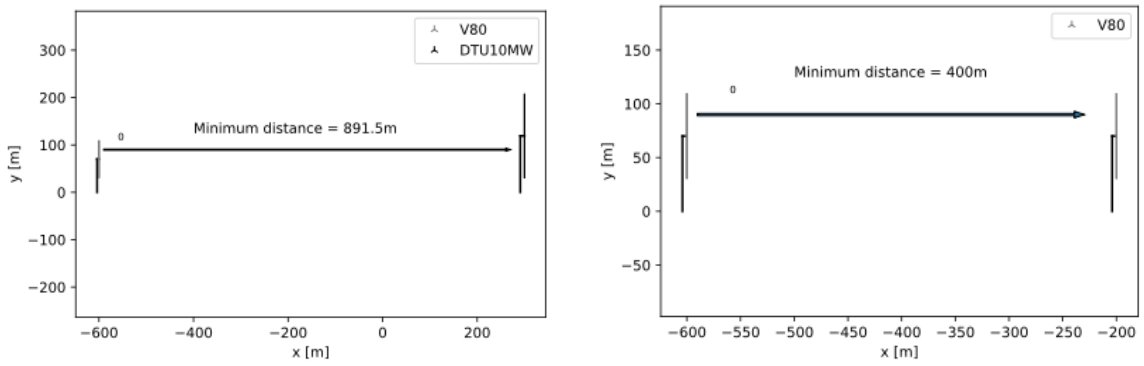

(a) Different turbine types **(b)** Same type of turbine

Figure 4.1: Dynamic minimum distance calculation

Additionally, the boundary constraint ensures that turbines remain within the designated wind farm area. The algorithms must ensure that any changes in the geographical location respect this boundary constraint to avoid placing turbines outside the defined wind farm site.

4.1.2 Change the Hub Height of the Turbine

Another design variable is the hub height of the turbine. The hub height represents the height at which the turbine is installed. The algorithms can adjust the hub height as part of the optimization process.

Predefined hub heights can be chosen based on established guidelines or empirical data. For example, guidelines such as those provided in Feng et al. [34] offer recommendations for suitable hub heights based on wind resource characteristics and turbine performance. Selecting a higher or lower hub height affects the wind resource available at different heights and can influence the optimal turbine placement. Reduced wake effects will also be evident if two turbines with different hub heights are placed next to each other leading to lower wake interaction (as both wakes will be at different heights), thus leading to a lower wake loss.

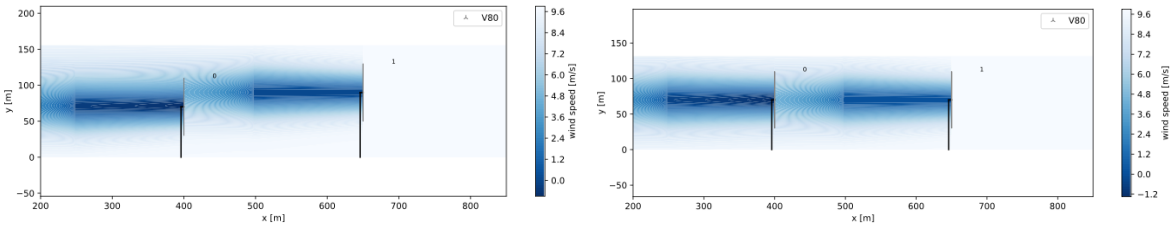

(a) Different hub heights **(b)** Same hub heights

Figure 4.2: Effect of hub height on wake interaction and mixing

Each turbine has a range of hub height values in steps of 5. These are given below
Vestas V80:

$$\text{Minimum hub height} = 70 \text{ m}$$
$$\text{Maximum hub height} = 90 \text{ m}$$

Vestas V164:

$$\text{Minimum hub height} = 100 \text{ m}$$
$$\text{Maximum hub height} = 130 \text{ m}$$

DTU 10 MW:

$$\text{Minimum hub height} = 110 \text{ m}$$
$$\text{Maximum hub height} = 140 \text{ m}$$

4.1.3 Change the Type of Turbine

The type of turbine used in the wind farm layout is another design variable. Different turbine models have distinct characteristics, including rotor diameter and power rating, which directly impact the layout's performance.

For example, in the optimization process, you can consider turbine models such as the V80 2MW, DTU 10 MW, and Vestas V164 8 MW. When changing the turbine type, the minimum spacing criteria should be adjusted based on the rotor diameter of the new turbine. Dai et

al. [22] provides guidelines for determining appropriate minimum spacing based on turbine characteristics.

Constraints on the maximum and minimum turbine capacities are crucial during the optimization process. These constraints ensure that the selected turbine types fall within the feasible range of the wind farm. The maximum and minimum capacities can be defined based on the initial capacity of the site's chosen, such as:

IEA Test Site:

$$\text{Minimum capacity} = 40 \text{ MW}$$
$$\text{Maximum capacity} = 80 \text{ MW}$$

Horns Rev 1 Site:

$$\text{Minimum capacity} = 160 \text{ MW}$$
$$\text{Maximum capacity} = 320 \text{ MW}$$

4.1.4 Add/Remove Turbines from the Site

The optimization algorithms may allow for adding or removing turbines from the wind farm layout. When initializing a layout, the minimum and maximum number of turbines allowed for the site are defined.The constraints on the number of turbines for each site can be specified as follows:

IEA Test Site:

$$\text{Maximum turbines} = 12$$
$$\text{Minimum turbines} = 20$$

Horns Rev 1 Site:

$$\text{Maximum turbines} = 60$$
$$\text{Minimum turbines} = 100$$

These constraints ensure that the wind farm layout remains within the defined limits for the number of turbines.

By considering and manipulating these design variables and constraints, the optimization algorithms aim to find an optimal wind farm layout that maximizes or minimizes the desired objective functions which can either be the Annual Energy Production (AEP) or the Levelized cost of Energy (LCOE).

4.2 Random Search Algorithm

The random search algorithm is a simple yet effective approach for wind farm layout optimization [36]. It has been widely used in various optimization problems and has shown promising results in wind farm layout design.

The random search algorithm seeks to arrive at an ideal wind farm architecture that maximizes or reduces the chosen objective functions, such as Annual Energy Production (AEP) and Levelized Cost of Energy (LCOE) [98]. The AEP is the total energy generated by the

wind farm in a year, whereas the LCOE is the cost of generating each unit of energy during the wind farm's lifetime.

The random search algorithm explores the design space by randomly selecting actions to modify the layout. These actions include moving a random turbine, changing the hub height of a turbine, changing the type of a turbine, or adding/removing a random turbine [36]. The choice of action is determined by generating a random number a between 1 and 4 that corresponds to each possible action. This new layout is stored as D_{new}. To ensure feasibility, the algorithm applies constraints on the design variables, which are specified in section 4.1 To ensure feasibility, the algorithm applies constraints on the design variables given in section 4.1.

Once a layout is generated, the algorithm calculates the objective function value, either the AEP or the LCOE. If the objective function is the AEP, the algorithm aims to maximize the AEP value by exploring different wind farm layouts. If a newly generated layout has a higher AEP than the previous layout, it is stored as the current "best" layout [22] as $D = D_{new}$. On the other hand, if the objective function is the LCOE, the algorithm seeks to minimize the LCOE value. If a newly generated layout has a lower LCOE than the previous layout, it is considered an improvement and stored as the current "best" layout [22] as $D = D_{new}$

The random search algorithm continues to iteratively explore the design space by generating new layouts and evaluating their objective function values. The process repeats until a convergence criterion is met. In this thesis, the convergence criterion is defined as the maximum number of iterations, which is set to 5000 [36]. This criterion ensures that the algorithm terminates after a predefined number of iterations.

Although the random search algorithm provides a straightforward and intuitive optimization approach, it may require running the algorithm multiple times to obtain the most optimal layout due to its inherent randomness [36]. However, by incorporating suitable convergence criteria and leveraging computational resources, this algorithm effectively explores the design space and contributes to the development of efficient wind farm layouts [98].

A flowchart illustrating the random search algorithm used in this thesis is shown in Figure 4.3. It is important to note that the flowchart depicted in Figure 4.3 represents the LCOE as the objective function.

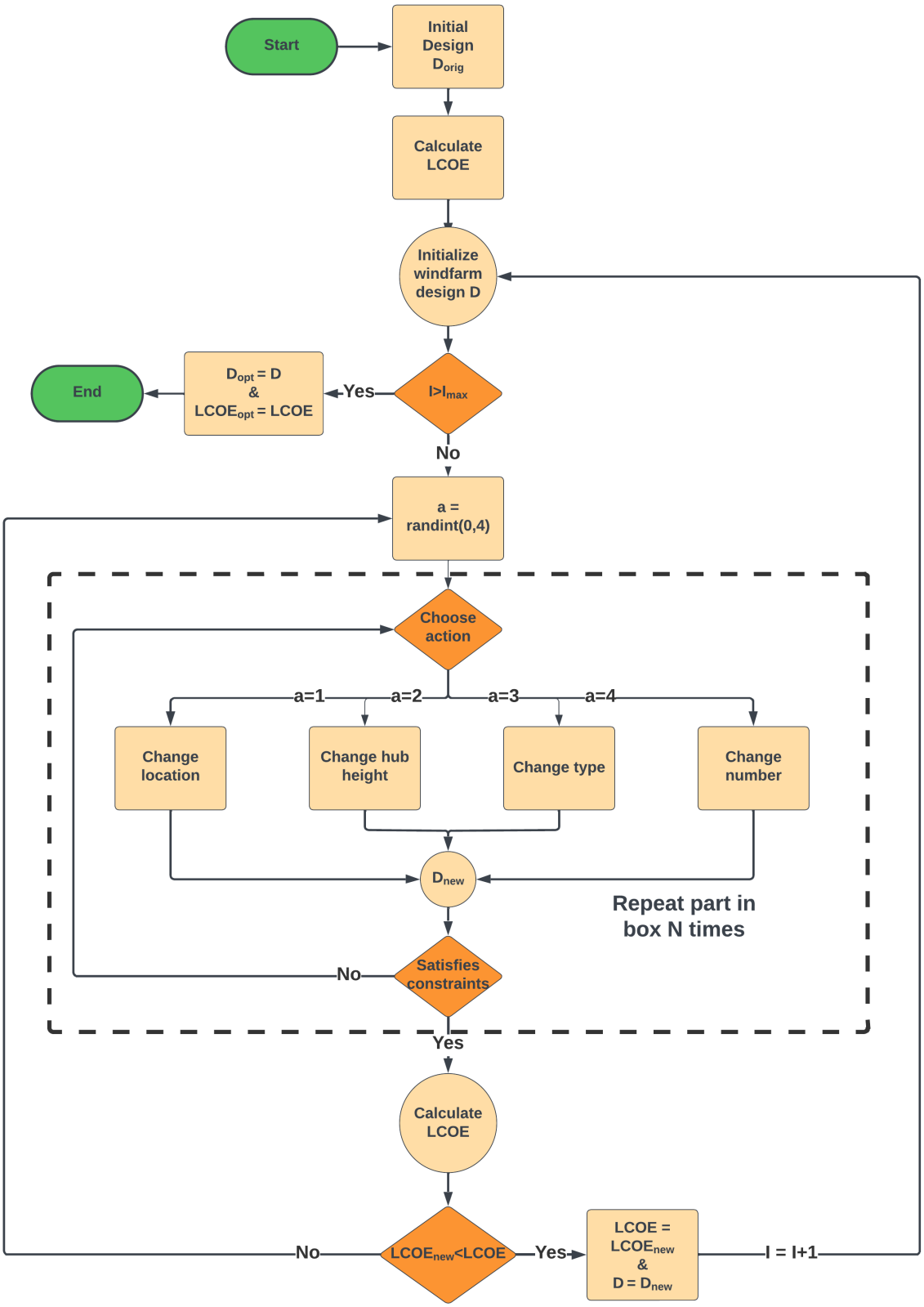

Figure 4.3: Flowchart of the Random Search Algorithm

4.3 Particle Swarm Optimization

Particle Swarm Optimization (PSO) is a population-based optimization technique proposed by Kennedy and Eberhart [52]. It aims to find the optimal solution by iteratively moving particles within a search space. PSO combines individual and global knowledge to guide the particles' movements, making it suitable for solving complex optimization problems [53].

In PSO, a population of particles represents potential solutions. Each particle's position in the search space corresponds to a candidate solution. Let p_{p_i} denote the current position of particle i at iteration t. For wind farm layout optimization, p_{p_i} includes multiple dimensions such as x-coordinates, y-coordinates, turbine types, and a number of turbines variable that allows the algorithm to manipulate the size of other arrays as needed.

To commence the optimization process, an initial population of particles is generated in Particle Swarm Optimization (PSO). The particles' positions are initialized randomly within the feasible region of the search space, taking into account the problem constraints. Notably, one of the particles is initialized with the initial layout provided in PyWake [74]. This initial layout serves as a valuable starting point, leveraging existing knowledge to improve the convergence speed and overall effectiveness of the optimization process.

By ensuring that the initial population satisfies the problem constraints, the optimization algorithm can explore the search space more efficiently. This initialization strategy enhances the likelihood of discovering promising solutions early on, facilitating faster convergence towards optimal or near-optimal solutions [13]. Incorporating the initial layout from PyWake within the initial population provides a practical foundation for the PSO algorithm, leveraging domain-specific insights and pre-existing knowledge to expedite the optimization process. The PSO algorithm updates the velocities and positions of particles based on their historical best position (p_{b_i}) and the swarm's best position (g_b). The velocity update equation is given by:

$$\begin{aligned} c_v &= c_w \cdot r_1 \cdot (p_{b_i} - p_{p_i}) \\ s_v &= s_w \cdot r_2 \cdot (g_b - p_{p_i}) \\ v_i &= w \cdot v_i + c_v + s_v \end{aligned} \tag{4.1}$$

In these equations, c_v represents the cognitive velocity, while s_v represents the social velocity. The cognitive weight is represented by(c_w), while the social weight is represented by (s_w). The particle's best position and its current position are represented by (p_{b_i}) and (p_{p_i}) respectively. (r_1) and (r_2) represent two random values that introduce stochasticity into the algorithm. The updated velocity (v_i) is obtained by combining the inertia weight (w), the current velocity, cognitive component (c_v), and social component (s_v) [64, 29]. The particle positions are then updated according to Equation 4.2

$$\mathbf{p}_{p_i} = \mathbf{p}_{p_i} + \mathbf{v}_i \tag{4.2}$$

The inertia weight (w) balances exploration and exploitation. Lower values promote local exploration, while higher values encourage global exploration. In this thesis, linearly decreasing values of w from $\omega_{start} = 0.8$ to $\omega_{end} = 0.4$ are used. The cognitive weight (c_w) represents the particle's self-confidence or self-awareness. It controls the influence of the particle's own best position on its velocity update. A higher c_w value increases the particle's focus on its individual best position, promoting exploitation of local solutions [29].The social weight (s_w) represents the particle's social influence or awareness of its neighbors. It determines the impact of the global best position on the particle's velocity update. A higher s_w value enhances the particle's

exploration of the search space by considering the best position found by other particles in the swarm [29].The random values (r_1 and r_2) are uniformly distributed random numbers between 0 and 1. They introduce randomness to the velocity update equation, allowing particles to explore different directions in the search space. The random values help in balancing the exploration and exploitation tendencies of the algorithm [29].

Determining an appropriate swarm size is essential in PSO. While smaller swarm sizes may hinder exploration capabilities, larger swarms increase the number of function evaluations required for convergence. For wind farm layout optimization, a swarm size within the range of 50 to 300 has been suggested as a reasonable choice [13]. In this thesis a swarm size of 100 is employed.

To handle constraints in the optimization process, Particle Swarm Optimization (PSO) commonly employs a penalty function approach. The penalty function transforms the constrained optimization problem into an unconstrained one, ensuring feasibility by penalizing infeasible solutions. In this thesis, the penalty function primarily focuses on constraints related to the installed capacity and turbine spacing [26, 67, 73].In this thesis, two types of penalty functions were employed based on the objective function: an exponential function when the Levelized Cost of Energy (LCOE) was the objective, and a logarithmic function when the Annual Energy Production (AEP) was the objective. It is worth noting that the definition and formulation of penalty functions can vary across different optimization codes and problem domains. For this thesis, the penalty function was specifically tailored and fine-tuned to achieve optimal performance within the implemented code.

The following code snippet showcases the penalty function used to penalize excess capacity in the PSO algorithm (Listing 4.1):

```
1 penalty_factor = 150
2 if total_capacity[i, iteration] > max_capacity:
3     excess_capacity = total_capacity[i, iteration] -
        max_capacity
4     penalty[i, iteration] = np.log(excess_capacity+1) *
        penalty_factor
5
6 if total_capacity[i, iteration] < min_capacity:
7     remaining_capacity = min_capacity - total_capacity[i,
        iteration]
8     penalty[i, iteration] = np.log(remaining_capacity+1) *
        penalty_factor
```

Listing 4.1: Penalty function for capacity

In this thesis, the Particle Swarm Optimization (PSO) algorithm was equipped with two termination conditions to ensure effective convergence. The first condition involved setting a maximum number of iterations, specifically limiting the algorithm to 1000 iterations. This constraint prevented the PSO algorithm from running indefinitely, enabling timely convergence within a reasonable computational timeframe.The second termination condition was based on a convergence counter, which evaluated the stability of the global best Levelized Cost of Energy (LCOE) or Annual Energy Production (AEP) across successive generations. The convergence counter assessed the standard deviation of the LCOE/AEP values among the global best solutions. If the difference between these values remained below the threshold of 10^{-6} for

more than 10 consecutive generations, it signified that the algorithm had reached a state of convergence.

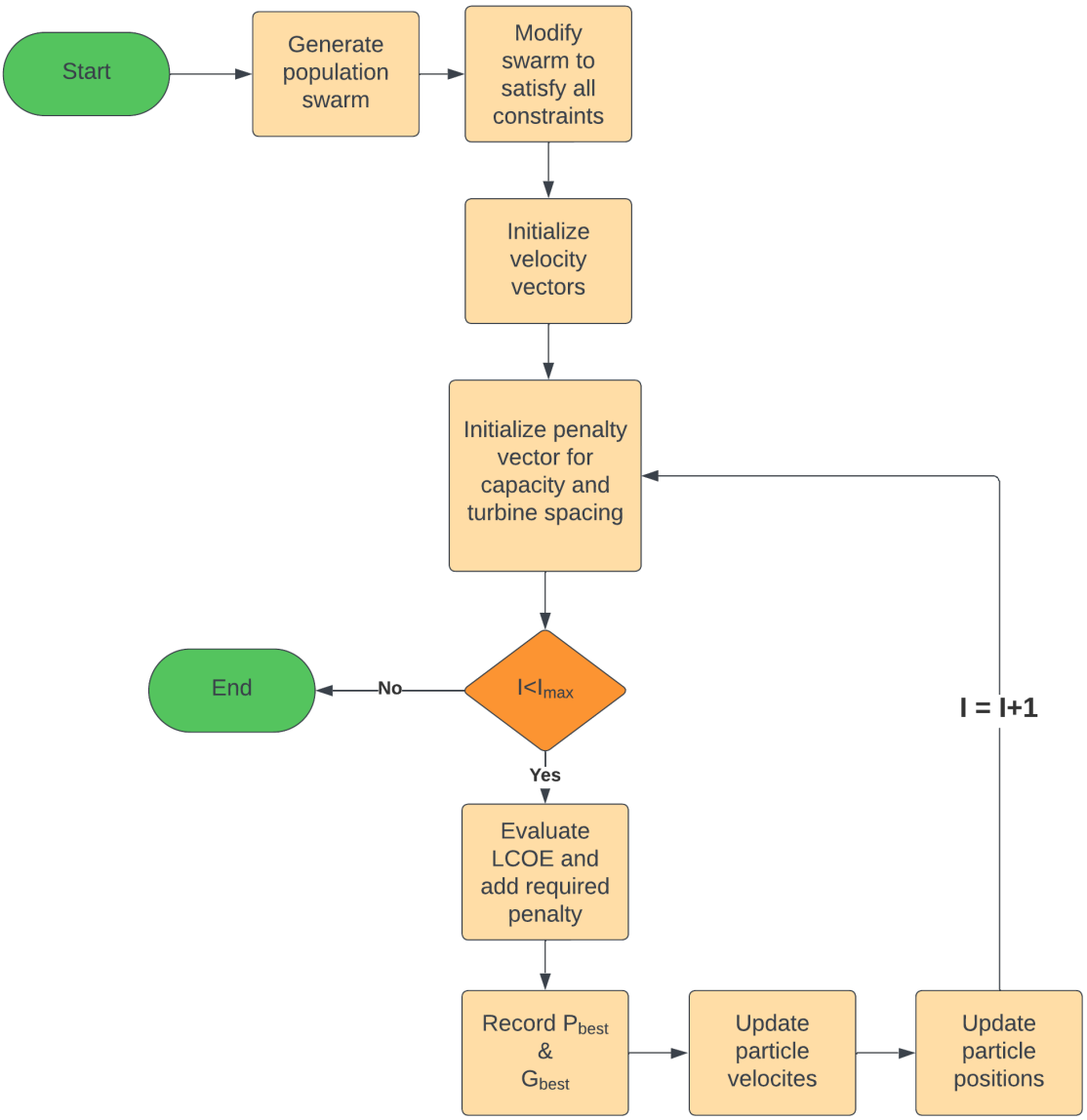

Figure 4.4: Flowchart of the Particle Swarm Optimization algorithm

By employing these termination conditions, the thesis ensured the convergence of the PSO algorithm while taking into account both a maximum iteration limit and a precise measure of stability based on the LCOE/AEP values. These termination conditions contributed to the effective optimization of the problem while reducing unnecessary computational costs.

CHAPTER 5

Results

In this section, the results of both simulations for both cases will be presented. Each section is followed by a comprehensive analysis of the results highlighting important findings and answering the research questions and fulfilling objectives formulated in section 1.5.

The main purpose of this section is to present empirical results given by the optimization algorithms. It is important to remember that each algorithm has a relative degree of randomness to it, which can be attributed to the nature of the random search algorithm and the randomly generated layouts to fulfill population sizes for Particle Swarm Optimization respectively.

Each section details various trends and it's implications for the algorithms. These trends are very important in identifying various advantages, limitations and key parameters that affect the performance and application of each of these algorithms.

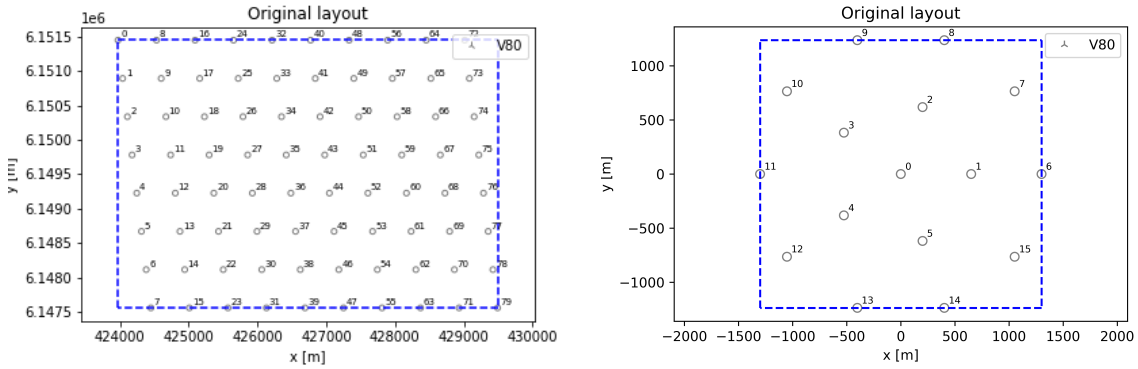

(a) Horns Rev 1 **(b)** IEA37

Figure 5.1: Original layouts

The original parameters for each layout are given in Table 5.1.

Table 5.1: Original parameters for both sites

Site	Number of wind turbines	Original LCOE [Euro/kWh]	Original AEP [GWh]
HornsRev	80	0.0660	680
IEA	16	0.092	160

5.1 Random Search

This section presents the results obtained from the application of the random search algorithm to optimize two objective functions, namely Annual Energy Production (AEP) and Levelized

Cost of Energy (LCOE). The algorithm's performance is evaluated for two case studies: the IEA test case and the Horns Rev 1 wind farm. To enhance precision and examine the impact of wind direction sectorization, three different sector sizes were considered: 1°, 1.5°, and 3°. The results reported below are exclusively for the finest wind direction sector resolution, i.e., 1° sectors.

The selection of multiple wind direction sector sizes is motivated by the need to account for the intricacies of wind flow patterns and their influence on wind energy applications. A comprehensive understanding of wind direction variability is crucial in optimizing wind turbine configurations. Previous studies have highlighted the importance of accurately capturing these variations. Furthermore, Dai et al. [22] suggest that an appropriate number of sectors can improve the precision of wind resource assessments and enhance the efficiency of wind farm layouts. By considering these factors, the investigation of varying sector sizes enables a comprehensive assessment of the algorithm's performance across different wind direction resolution levels.

The results presented below are obtained through a rigorous evaluation process. To ensure reliability and account for inherent randomness of the algorithm, each scenario was simulated 10 times. This approach provides a more robust assessment of the algorithm's performance and reduces the influence of random initialization. The reported values correspond to the best-performing configurations obtained from these ten simulation runs.

5.1.1 AEP

Table 5.2 presents the results of the Random Search algorithm for the optimization of the AEP objective function. The table includes the site name, the number of wind direction sectors, the optimized LCOE in Euro/kWh, the optimized AEP in GWh, the total capacity in MW, the number of V80 turbines, the number of V164 turbines, the number of DTU10 MW turbines, and the run time in seconds.

Table 5.2: Random Search AEP results

Site	No. of wind direction sectors	Optimized LCOE [Euro/kWh]	Optimized AEP [GWh]	Total Capacity [MW]	No. of V80 turbines	No. of V164 turbines	No. of DTU10 MW turbines	Run Time [s]
HornsRev	120	0.0483	1437.152	320	77	12	7	19501
	240	0.0481	1439.253	320	78	13	6	41842
	360	0.0478	1440.101	320	82	12	6	65489
IEA	120	0.0462	452.673	80	14	4	2	568
	240	0.0459	455.480	78	15	1	4	728
	360	0.0457	462.269	78	15	1	4	966

Analyzing the table, several trends can be observed. Firstly, for the HornsRev site, as the number of wind direction sectors increases from 120 to 360, there is a slight decrease in the optimized LCOE from 0.0483 Euro/kWh to 0.0478 Euro/kWh while the optimized AEP experiences a small increase from 1437.152 GWh to 1440.101 GWh. This suggests that increasing the number of wind direction sectors can lead to improved AEP values while maintaining a relatively consistent LCOE.

To visualize the impact of the Random Search algorithm on layout optimization, Figure 5.2(a) and Figure 5.2(b) display the initial and optimized layouts of the HornsRev wind farm, respectively. Something interesting to note is that Figure 5.2(b)) has the highest number of turbines possible i.e. 100.

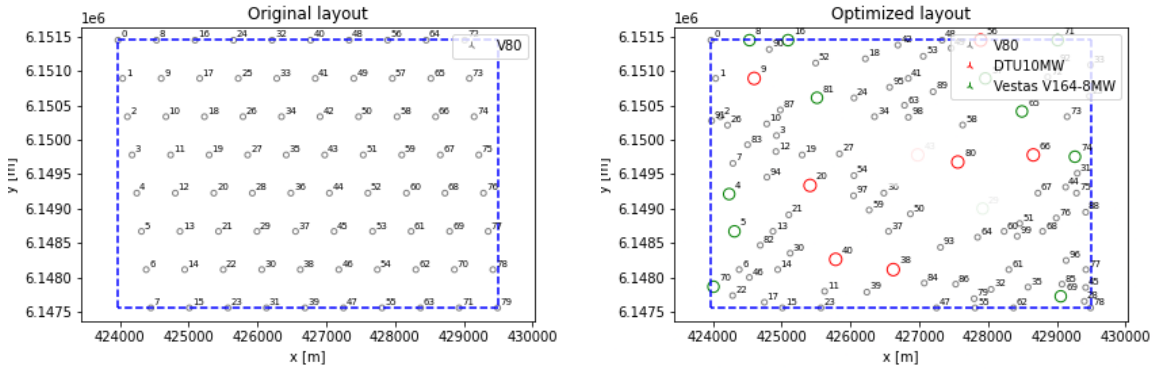

(a) Initial layout **(b)** Optimized layout

Figure 5.2: IEA37 layouts

Additionally, Figures Figure 5.3(a) and Figure 5.3(b) showcase the convergence histories of the LCOE and AEP, respectively, providing valuable insights into the algorithm's progress over iterations and its ability to approach optimal solutions. Notably, it is worth mentioning that around the 1000th iteration mark, the LCOE experiences a slight increase. This can be attributed to the algorithm's inclusion of an additional turbine, resulting in an improved AEP but also an overall increase in cost. This observation highlights the trade-off between maximizing energy production and minimizing expenses during the optimization process.

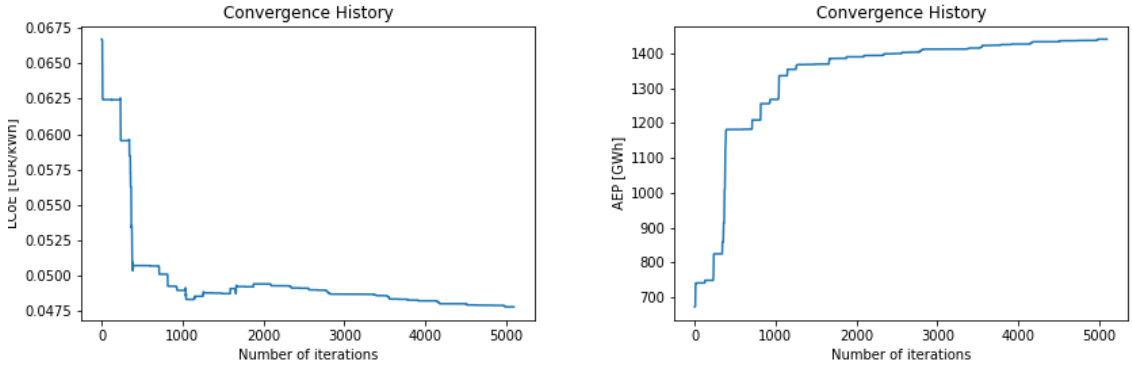

(a) LCOE **(b)** AEP

Figure 5.3: Convergence histories

Similar trends can be observed for the IEA test case as well. The results presented in Table 5.2 for the IEA site show that as the number of wind direction sectors increases from 120 to 360, there is a slight decrease in the optimized LCOE from 0.0462 Euro/kWh to 0.0457 Euro/kWh. Conversely, the optimized AEP exhibits a gradual increase from 452.673 GWh to 462.269 GWh.

The layouts depicted in Figure 5.4 provide visual representations of the initial and optimized wind farm configurations for the IEA case. In Figure 5.4(a), the initial layout shows the turbines distributed in a relatively uniform manner across the site. However, after the optimization process, as shown in Figure 5.4(b), a more optimized arrangement emerges, with the turbines positioned strategically, with the larger turbines being position towards the edges of the boundaries. In similarity to Figure 5.2(b), Figure 5.4(b) tends to move towards the highest number of turbines possible i.e. 20.

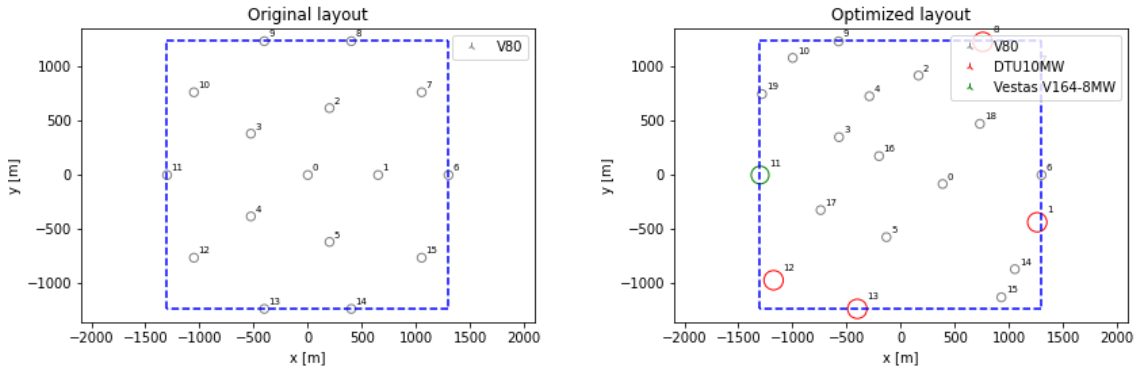

(a) Initial layout **(b)** Optimized layout

Figure 5.4: IEA37 layouts

The convergence histories depicted in Figure 5.5 provide insights into the optimization process for the IEA case, specifically regarding the LCOE and AEP objectives. Similar to the trends observed in the HornsRev case, the convergence histories for the IEA case show a progressive improvement in both LCOE and AEP values over the iterations. In Figure 5.5(a), the LCOE convergence history demonstrates a gradual decrease, indicating that the algorithm successfully explores and refines the wind farm layout to reduce the cost of energy production. Similarly, in Figure 5.5(b), the AEP convergence history shows a consistent increase over the iterations, indicating the algorithm's ability to find layouts that maximize energy production.

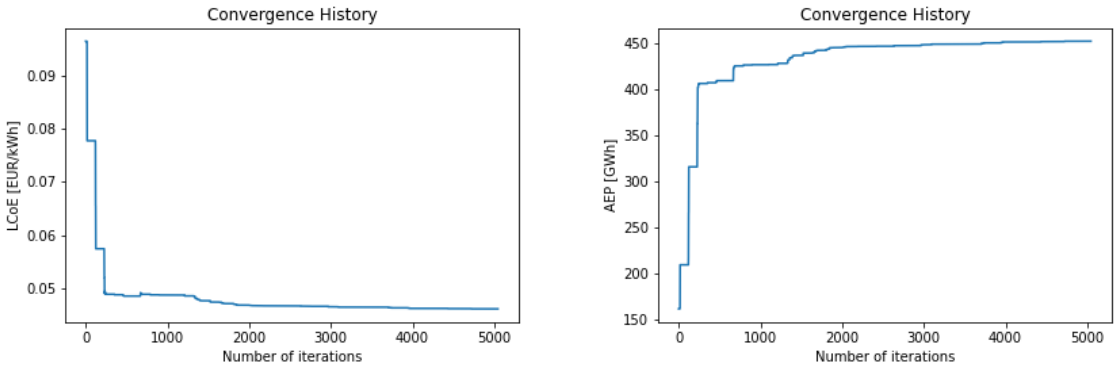

(a) LCOE **(b)** AEP

Figure 5.5: Convergence histories

An analysis of the hub heights in the optimized layout of the wind farm reveals a compelling

trend. It is evident that the hub heights consistently gravitate towards the largest feasible value for all turbines in the layout i.e. 90, 130, and 140 for the Vestas V80, Vestas V164 and DTU 10 MW respectively. This inclination can be attributed to the objective of harnessing the maximum available wind resources at higher altitudes, where wind speeds tend to be higher and more reliable. By setting the hub heights to their upper limits, the turbines are strategically positioned to capitalize on optimal wind conditions, thereby maximizing their energy production potential.

5.1.2 LCOE

The table shown in Table 5.3 presents the results of the random search algorithm applied to optimize the LCOE (Levelized Cost of Energy) for the Horns Rev wind farm and the IEA test site with varying numbers of wind direction sectors. The table includes information about the wind farm sites, the number of wind direction sectors, the optimized LCOE in Euro/kWh, the optimized AEP (Annual Energy Production) in GWh, the total capacity in MW, the number of turbines of different types (V80, V164, DTU10 MW), and the run time in seconds.

Table 5.3: Random Search LCOE Results

Site	No. of wind direction sectors	Optimized LCOE [Euro/kWh]	Optimized AEP [GWh]	Total Capacity [MW]	No. of V80 turbines	No. of V164 turbines	No. of DTU10 MW turbines	Run Time [s]
HornsRev	120	0.0381	1489.157	320	33	8	19	4494
	240	0.0377	1512.544	320	32	12	16	11479
	360	0.0376	1512.762	320	32	12	16	26613
IEA	120	0.0399	463.818	76	5	2	5	412
	240	0.0394	469.602	76	5	2	5	510
	360	0.0390	480.295	78	5	1	6	533

The analysis of the results presented in Table 5.3 reveals several noteworthy trends, providing valuable insights into the optimization process and the performance of wind farm layouts. Focusing on the HornsRev site, a systematic examination of the relationship between the number of wind direction sectors and the optimized LCOE and AEP values demonstrates intriguing patterns.As the number of wind direction sectors increases from 120 to 360, there is a discernible decrease in the optimized LCOE, with values decreasing from 0.0381 Euro/kWh to 0.0376 Euro/kWh. Comparing these results to the outcomes obtained in the previous analysis (Table 5.2), where the algorithm prioritized AEP as the objective function, provides valuable insights into the trade-off between energy production and cost efficiency. The lower LCOE values achieved through the LCOE-focused optimization indicate the algorithm's success in minimizing the overall cost of the wind farm. Furthermore, the higher optimized AEP values obtained in the LCOE-focused optimization, in comparison to the previous AEP-focused results, underscore the algorithm's effectiveness in improving the energy capture of wind farms. This suggests that by incorporating the LCOE objective into the optimization process, the algorithm can identify layout configurations that not only increase energy production but also achieve a more economically viable wind farm design. This same trend can be observed in the values for the IEA test site as well.

The examination of the HornsRev wind farm layouts, as depicted in Figure 5.6, provides valuable insights into the impact of turbine placement on the overall performance of the wind farm. The optimized layout, shown in Figure 5.6(b), exhibits a notable characteristic of having the minimum possible number of turbines with a total of 60. The design also has a higher number of larger turbines (16 DTU 10 MW turbines compared to 6 in Table 5.2) highlighting larger available spacing between the turbines leading to a lower wake loss.

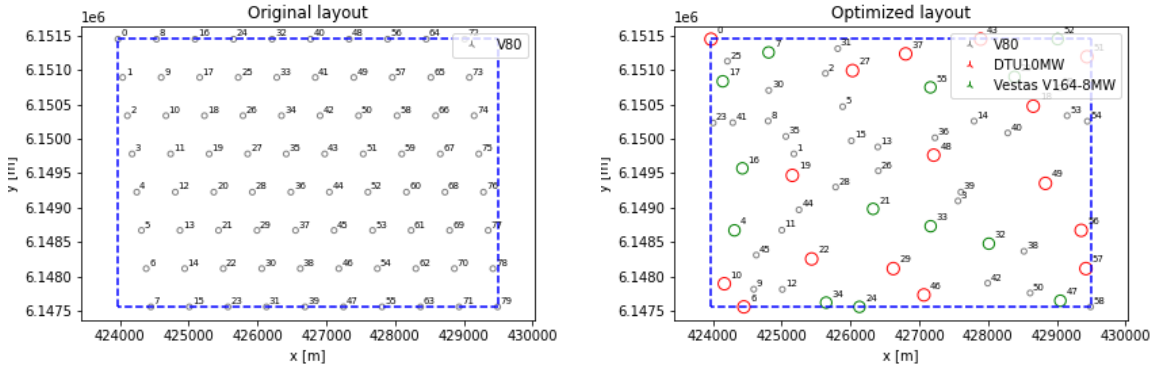

(a) Initial layout **(b)** Optimized layout

Figure 5.6: HornsRev layouts

The dissimilarity in the algorithm's performance when optimizing LCOE, as demonstrated in Figure 5.7, compared to its optimization for AEP, as shown in Figure 5.3, can be attributed to notable distinctions in their convergence characteristics. The convergence of LCOE, depicted in Figure 5.7(a), exhibits a gradual decline towards values proximate to its convergent state after approximately 2000 iterations. Conversely, the LCOE convergence in Figure 5.3(a) demonstrates a swifter attainment of values near its convergent state, occurring around the 800 iteration mark. This disparity can be elucidated by the algorithm's preference for the removal of turbines during LCOE optimization, in contrast to the inclination to add turbines in AEP optimization. The gradual and smoother convergence observed in LCOE optimization signifies the algorithm's effort to iteratively refine the wind farm layout by eliminating redundant turbines, resulting in improved cost-effectiveness and optimal utilization of available wind resources.

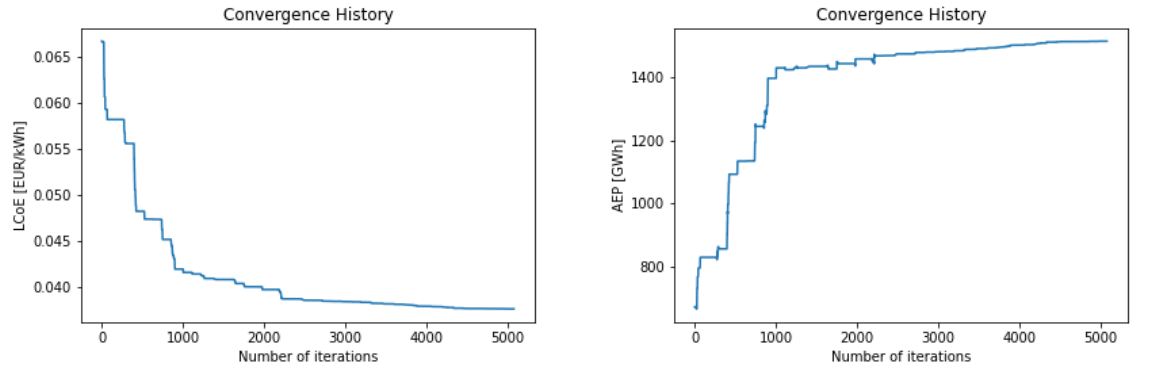

(a) LCOE **(b)** AEP

Figure 5.7: Convergence histories

Similar trends can be observed for the IEA test case as well. LCOE values presented in Table 5.3 gradually decrease from 0.0399 Euro/kwH to 0.0390 Euro/kWh. The layouts presented in Figure 5.8 display similar trends as well, where Figure 5.8(b) tends to the lowest possible number of turbines with 12 turbines compared to Figure 5.4(b). There is also an increase in the number of DTU 10 MW turbines present in Figure 5.8(b) (6 when optimizing LCOE in Table 5.3, compared to 4 when optimizing AEP in Table 5.2).

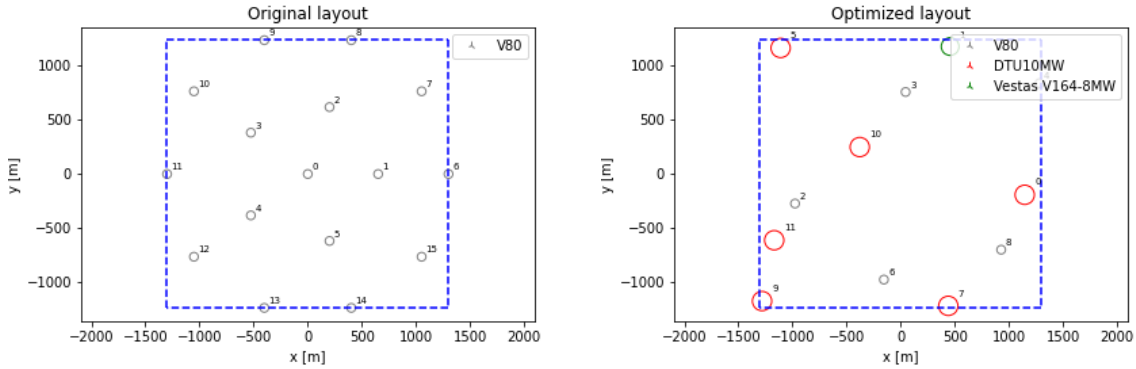

(a) Initial layout **(b)** Optimized layout

Figure 5.8: IEA37 layouts

Looking at the convergence histories in Figure 5.9, similar trends can be deduced. Compared to Figure 5.5, the algorithms tends to approach values close to convergence a lot slower, around 1600 iterations as seen in Figure 5.9(a) compared to 300 iterations in Figure 5.5(a). A noteworthy observation can be made in Figure 5.9(b), where around the 1500 iteration mark, a steep decrease in AEP can be observed whereas the LCOE in Figure 5.9(a) still continues to display a gradual decrease. This can be attributed to the removal of a turbine close to the boundary or a turbine which was experiencing minimal wake losses (i.e. generating a large chunk of the total AEP) resuling in the substantial observed decrease.

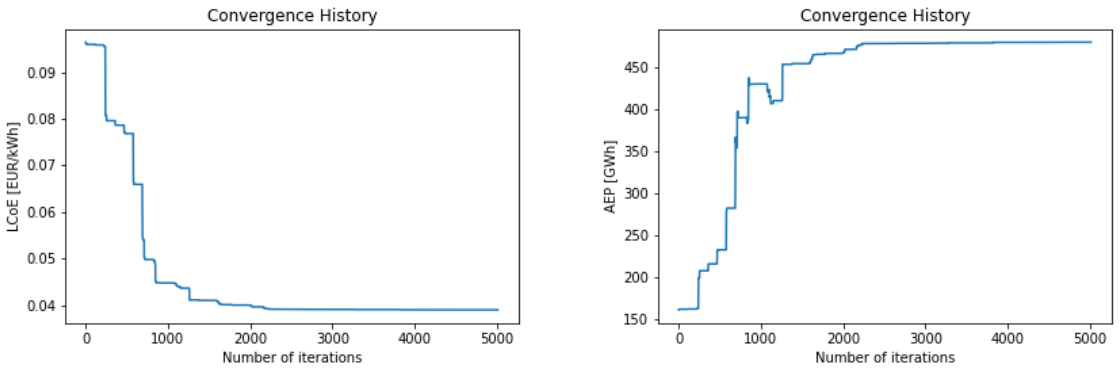

(a) LCOE **(b)** AEP

Figure 5.9: Convergence histories

Upon analyzing the hub height vectors across all scenarios presented in Table 5.3, a remarkable similarity emerges when compared with their counterparts in Table 5.2. Notably,

the hub height values for all turbines consistently gravitate towards the uppermost feasible limits. This trend holds significant implications for the observed higher AEP values in Table 5.3. By opting for layouts with a reduced number of turbines positioned at elevated hub heights, multiple advantages are realized. Firstly, the turbines situated at greater hub heights experience swifter wind speeds due to the power shear phenomenon. Additionally, the presence of a lower number of turbines within the vicinity contributes to diminished wake losses, thereby amplifying the overall energy production potential.

Another intriguing trend worth noting is the disparity in run times between the scenarios in Table 5.2 when optimizing for AEP and their counterparts in Table 5.3. The AEP optimization algorithm consistently exhibits nearly 50% longer run times compared to the LCOE optimization algorithm. This divergence can be attributed to the resulting layouts favored by each algorithm. The AEP-focused algorithm tends to generate layouts with a larger number of turbines, necessitating a higher computational burden. These additional turbines demand increased computations from wake deficit, blockage deficit, and superposition models. Furthermore, the feasibility validation process, involving the verification of minimum distance constraints outlined in subsection 4.1.1, is prolonged due to the larger number of turbines involved. In contrast, the LCOE optimization algorithm, which converges to layouts with fewer turbines, requires less computational effort and time for both wake-related calculations and feasibility assessments.

5.2 Particle Swarm Optimization

This section presents the outcomes obtained from the application of the Particle Swarm Optimization (PSO) algorithm to both Horns Rev 1 and the IEA case. In alignment with the random search algorithm, the PSO algorithm has been implemented utilizing three discrete wind direction sector sizes: 1°, 1.5°, and 3°. The subsequent graphs and design configurations presented herein specifically focus on the most refined resolution, namely the 1° wind direction sectors. To mitigate the influence of stochastic variations, the PSO algorithm has been executed 10 times for each scenario. This approach ensures a robust assessment of the algorithm's performance across multiple iterations, enhancing the reliability of the results.

5.2.1 AEP

Table 5.4 showcases key findings derived from the Particle Swarm Optimization (PSO) algorithm applied to the Horns Rev 1 and IEA cases. The table provides detailed information on various parameters such as the number of wind direction sectors, optimized LCOE (Levelized Cost of Energy), optimized AEP (Annual Energy Production), total capacity, turbine distribution, and run time.

Table 5.4: PSO AEP Results

Site	No. of wind direction sectors	Optimized LCOE [Euro/kWh]	Optimized AEP [GWh]	Total Capacity [MW]	No. of V80 turbines	No. of V164 turbines	No. of DTU10 MW turbines	Run Time [s]
HornsRev	120	0.0491	1265.630	310	75	7	11	83503
	240	0.0489	1285.823	314	77	5	12	95649
	360	0.0485	1328.242	320	76	6	12	110534
IEA	120	0.0486	430.266	70	15	5	0	14163
	240	0.0447	431.318	80	7	2	5	22536
	360	0.0456	446.606	80	12	2	4	29624

The analysis of the results presented in Table 5.4 provides valuable insights into the optimization process and performance of wind farm layouts. For the HornsRev site, the optimization was performed with 120, 240, and 360 wind direction sectors. The optimal LCOE (Levelized Cost of Energy) values decreased gradually as the number of sectors rose. The LCOE fell from 0.0491 Euro/kWh for 120 sectors to 0.0489 Euro/kWh for 240 sectors and then to 0.0485 Euro/kWh for 360 sectors.Simultaneously, as the number of wind direction sectors rose, so did the optimum AEP (Annual Energy Production). HornsRev's AEP values grew from 1265.630 GWh for 120 sectors to 1285.823 GWh for 240 sectors and 1328.242 GWh for 360 sectors. Regarding the IEA site, the optimization was conducted using the same range of wind direction sectors. The optimized LCOE values for IEA were 0.0486 Euro/kWh, 0.0447 Euro/kWh, and 0.0456 Euro/kWh for 120, 240, and 360 sectors, respectively. Similarly, the optimized AEP values increased from 430.266 GWh to 431.318 GWh and further to 446.606 GWh as the number of sectors increased.

Upon comparing the results presented in Table 5.4 with those of the Random Search algorithm (as shown in Table 5.2), a compelling trend emerges. The optimization outcomes achieved through the Particle Swarm Optimization (PSO) algorithm exhibit a similar pattern to the Random Search results, albeit with a noticeable distinction in performance. Specifically, the PSO algorithm yields an optimized AEP value of approximately 1330 GWh, whereas the Random Search algorithm excels by achieving a significantly higher AEP value of approximately 1490 GWh. This discrepancy suggests that the Random Search algorithm outperforms the PSO algorithm by approximately 20% in terms of AEP optimization.

The reason why PSO is outperformed can be found by looking at the total capacity of it's optimal layout in Table 5.4. While the design in Figure 5.2(b) consists of 100 turbines to maximize energy capture, the PSO algorithm converges at a maximum of 94 turbines. The discrepancy in the number of turbines employed by each algorithm plays a crucial role in the observed performance gap. The Random Search algorithm's ability to explore a larger turbine count range allows for a more extensive search space, potentially leading to layouts that offer higher energy production. Conversely, the PSO algorithm's convergence at a lower turbine count restricts its exploration capability, resulting in suboptimal layouts and lower energy capture.

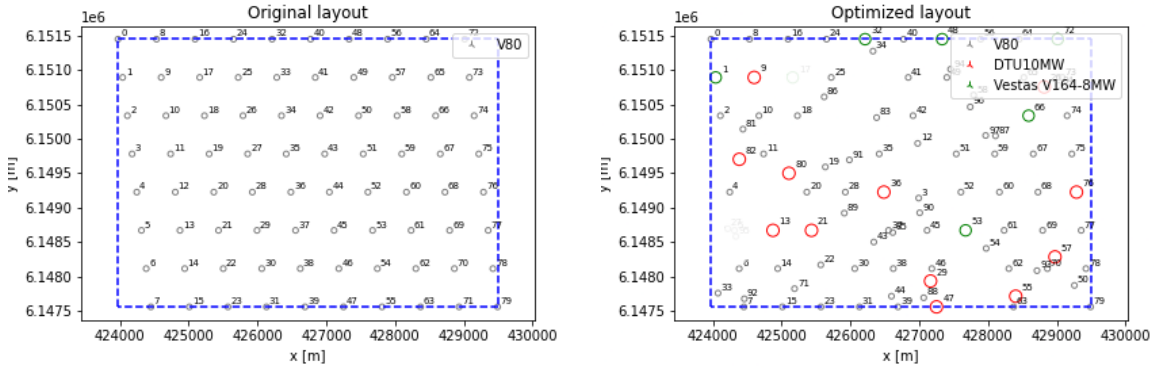

(a) Initial layout **(b)** Optimized layout

Figure 5.10: HornsRev layouts

An advantage of the Particle Swarm Optimization (PSO) algorithm over random search lies in its convergence speed, as demonstrated by the LCOE convergence history depicted in Figure 5.11(a). The graph exhibits a notable characteristic where the LCOE value experiences a rapid decline from its initial value and approaches proximity to the convergence value within the first 25 to 30 generations. A similar trend can be observed in the AEP convergence history illustrated in Figure 5.11(b).

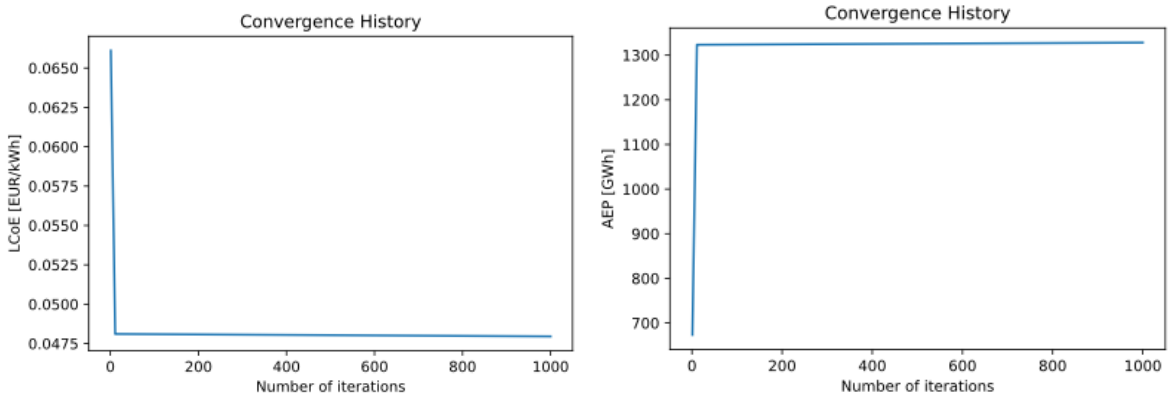

(a) LCOE **(b)** AEP

Figure 5.11: Convergence histories

Similar trends can also be observed in the IEA case. The PSO algorithm converges towards a smaller number of turbines, specifically 18 turbines, as indicated in Table 5.4, compared to the 20 turbines obtained through the Random Search algorithm, as shown in Table 5.2. A noteworthy observation emerges when examining the optimized layout depicted in Figure 5.12(b). It reveals striking similarities to the layout presented in Figure 5.4(b), where larger turbines are strategically positioned towards the boundaries to maximize the overall AEP.

This observation suggests that both PSO and Random Search algorithms recognize the potential benefits of placing larger turbines at the periphery of the wind farm. By harnessing the stronger and more consistent winds found in these outer regions, the algorithms aim to optimize the energy capture and enhance the overall AEP performance. This consistent pattern

in turbine positioning highlights the convergence of the algorithms towards efficient solutions that leverage the spatial characteristics of the wind resource to maximize energy production.

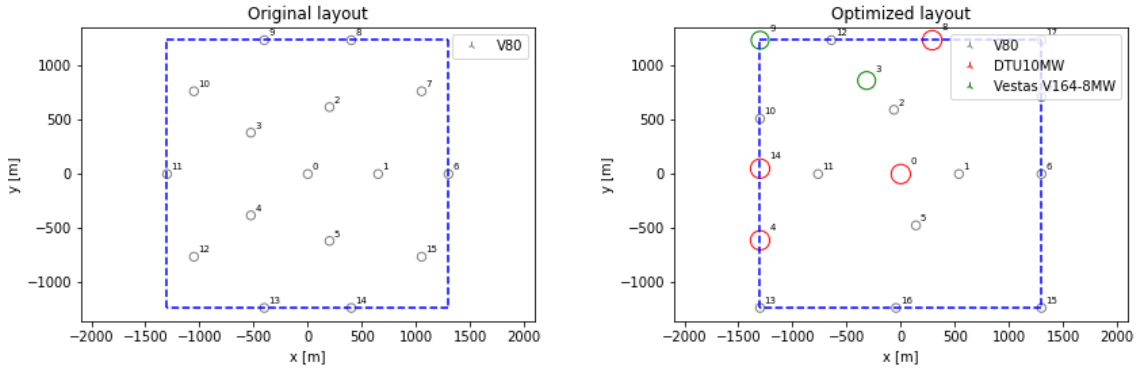

(a) Initial layout **(b)** Optimized layout

Figure 5.12: IEA37 layouts

The convergence histories of the IEA case, illustrated in Figure 5.13(a) and Figure 5.13(b), demonstrate predictable patterns. Notably, both the LCOE and AEP values exhibit a rapid decrease and increase respectively, approaching convergence levels within the initial 30 generations.

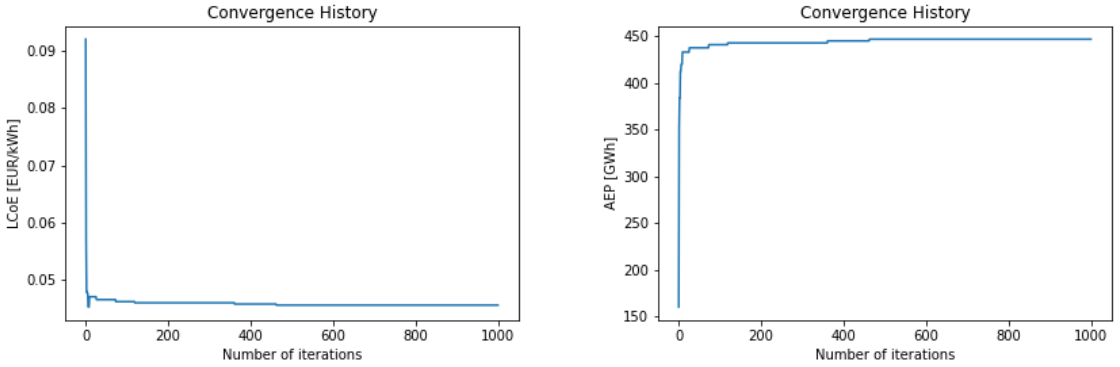

(a) LCOE **(b)** AEP

Figure 5.13: Convergence histories

Upon examining the hub heights for all scenarios listed in Table 5.4, a consistent trend similar to the random search algorithm is observed. The PSO algorithm strategically positions the turbines at the maximum achievable hub height for each turbine type. This deliberate placement results in an increase in the overall annual energy production (AEP) of the wind farm due to the exploitation of power shear effects. By capitalizing on higher hub heights, the PSO algorithm optimizes the wind farm layout to capture more energy and maximize AEP.

The observed high run times in the PSO simulations, ranging from 83,503 seconds to 110,534 seconds for the HornsRev site and from 14,163 seconds to 29,624 seconds for the IEA case, can be attributed to the nature of the PSO algorithm itself. PSO is a population-based algorithm that requires the evaluation of multiple designs within each iteration before proceeding to

the next generation. In the context of wind farm optimization, the PSO algorithm needs to calculate the Annual Energy Production (AEP) for the entire swarm, which consists of 100 different designs. This involves computing the AEP, penalties, costs, and velocity vectors for each design. Additionally, these designs must be randomly generated and subsequently modified to satisfy various constraints. The process of evaluating a large number of designs, performing calculations, and incorporating constraints can be computationally intensive, leading to the observed high run times. The PSO algorithm needs sufficient time to explore the solution space and converge towards an optimal layout.

5.2.2 LCOE

Finally, the table Table 5.5 presents the results obtained from the PSO optimization algorithm applied to wind farm layouts at the HornsRev and IEA sites. It provides valuable insights into the optimized Levelized Cost of Energy (LCOE), Annual Energy Production (AEP), total capacity, and turbine distribution for different configurations.

Table 5.5: PSO LCOE Results

Site	No. of wind direction sectors	Optimized LCOE [Euro/kWh]	Optimized AEP [GWh]	Total Capacity [MW]	No. of V80 turbines	No. of V164 turbines	No. of DTU10 MW turbines	Run Time [s]
HornsRev	120	0.0458	1302.925	310	46	11	13	74315
	240	0.0444	1317.523	310	50	10	13	81341
	360	0.0440	1331.913	306	53	10	12	94153
IEA	120	0.0449	420.633	80	9	4	3	12913
	240	0.0443	438.817	80	7	2	5	21162
	360	0.0436	449.214	76	6	3	4	27653

Analyzing the HornsRev site, we observe that as the number of wind direction sectors increases from 120 to 360, there is a consistent reduction in the optimized LCOE values. The LCOE decreases from 0.0458 Euro/kWh to 0.0440 Euro/kWh, indicating improved cost efficiency with more refined wind direction sectors. The corresponding optimized AEP values also show an increasing trend, rising from 1302.925 GWh to 1331.913 GWh, indicating higher energy generation potential.At the IEA site, a similar trend can be observed. Increasing the number of wind direction sectors from 120 to 360 results in a decrease in the optimized LCOE from 0.0449 Euro/kWh to 0.0436 Euro/kWh. This reduction in LCOE signifies improved cost-effectiveness of the wind farm layout. Furthermore, the optimized AEP values show an increasing trend, with values ranging from 420.633 GWh to 449.214 GWh, indicating enhanced energy production potential.

Both the PSO and random search algorithms exhibit a consistent trend towards reducing LCOE values and simultaneously increasing AEP values when optimizing for LCOE, as evident in Table 5.3 and Table 5.5 compared to Table 5.2 and Table 5.4, respectively.This can be attributed to their shared strategy of removing smaller turbines to reduce costs while simultaneously substituting them with larger turbines to optimize wake losses within the wind farm. By dynamically adjusting the turbine layout, these algorithms exploit the trade-off between cost reduction and increased energy production. The iterative optimization process of PSO effectively explores this trade-off, resulting in improved LCOE values and higher AEP values.

This approach aligns with the industry trend of deploying larger turbines to optimize wind farm performance, and the algorithms leverage this strategy to simultaneously optimize both economic and energy aspects. As a result, the PSO algorithm offers superior performance in terms of both cost efficiency and energy production compared to random search.

This trend is clearly reflected in the optimal layout achieved by the PSO algorithm, as depicted in Figure 5.14(b). The algorithm converges to a configuration consisting of 75 turbines, exhibiting resemblances to the layout shown in Figure 5.2(b) with turbines being pushed to the boundary and tending to the lowest possible number of turbines possible. Notably, smaller turbines are progressively replaced by larger ones, emphasizing the pursuit of maximizing the wind farm's total capacity.

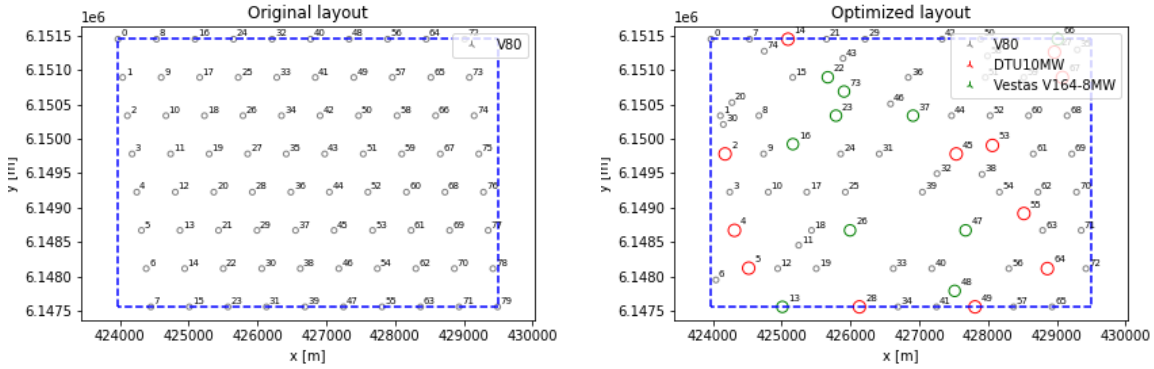

(a) Initial layout **(b)** Optimized layout

Figure 5.14: IEA37 layouts

Examining the convergence histories in Figure 5.11, similar trends emerge. The PSO algorithm demonstrates rapid progress, approaching convergence within approximately 35 generations. The resulting optimized LCOE and AEP graphs in Figure 5.15(a) and Figure 5.15(b) converge to 1331 GWh and 0.0440 Euro/kWh, respectively, showcasing the algorithm's effectiveness in optimizing the wind farm's economic and energy production performance.

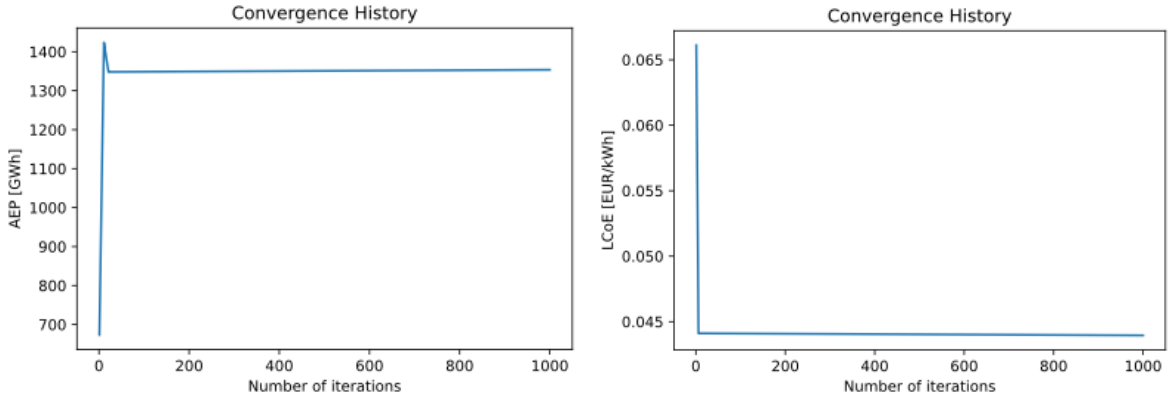

(a) AEP **(b)** LCOE

Figure 5.15: Convergence histories

Similar trends can also be observed for the IEA case. In this case, the PSO algorithm demonstrates a remarkable ability to approach the minimal number of turbines, converging at 13 turbines, as depicted in Figure 5.16(b). This aligns with the strategy of maximizing the wind farm's capacity by pushing turbines towards the boundaries, a pattern reminiscent of the previously discussed layouts.

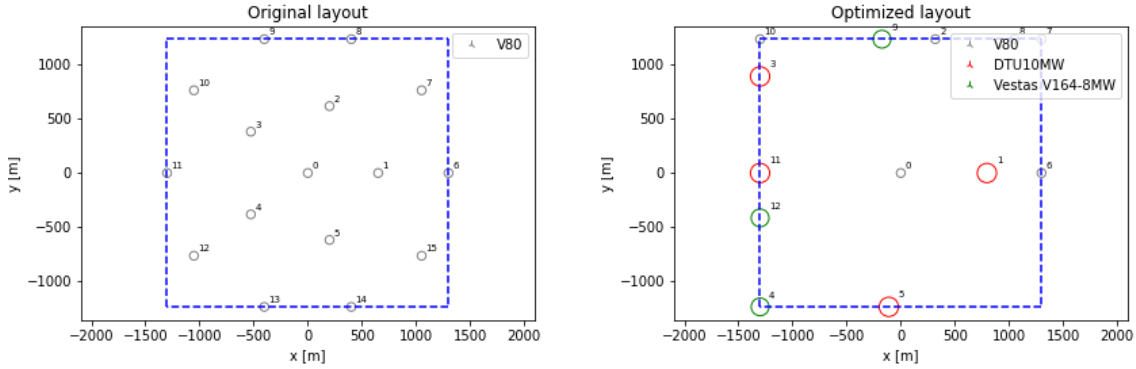

(a) Initial layout **(b)** Optimized layout

Figure 5.16: IEA37 layouts

The convergence histories of the PSO algorithm for the IEA case exhibit similar trends as before. Both the LCOE and AEP, as shown in Figure 5.17, converge to values close to convergence within approximately 40 generations. However, an interesting observation can be made from the convergence history depicted in Figure 5.17(a). It reveals an anomaly where the AEP converges to a lower value than it has previously achieved. This behavior can be attributed to a specific scenario where the algorithm removes a larger turbine, resulting in a decrease in AEP that cannot be fully compensated for by other adjustments. Despite this anomaly, the PSO algorithm consistently demonstrates its ability to optimize the wind farm layout in terms of both LCOE and AEP for the majority of the convergence process.

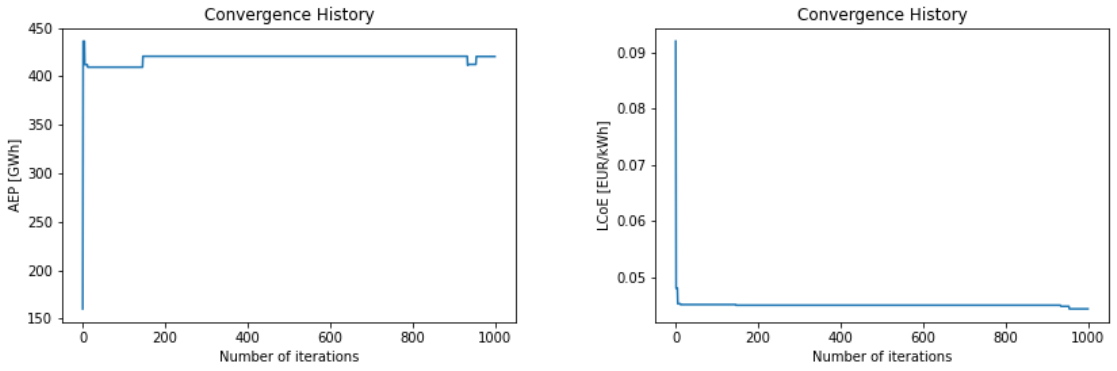

(a) AEP **(b)** LCOE

Figure 5.17: Convergence histories

The PSO algorithm, when optimizing for LCOE, exhibits a consistent trend in hub height selection, similar to its AEP optimization counterpart. The algorithm strategically positions all

turbines at their maximum achievable hub heights, thereby capitalizing on the improved wind resource available at higher elevations. This deliberate placement not only enhances the energy capture potential of each individual turbine but also contributes to a more favorable wind environment for the entire wind farm. The utilization of higher hub heights leads to increased wind speeds, reduced turbulence, and enhanced power production, resulting in improved energy yield and ultimately lower LCOE values.

An intriguing trend to note is the substantial difference in run time between optimizing for LCOE and AEP using the PSO algorithm. As demonstrated in Table 5.5 and Table 5.4, the optimization process for LCOE is significantly faster. This can be attributed to the fact that LCOE optimization tends to converge towards layouts with a reduced number of turbines, resulting in fewer computations required to calculate the AEP and overall costs of the wind farm design. The reduced computational complexity associated with fewer turbines leads to shorter run times, making the LCOE optimization process more efficient and time-effective. This trend in the PSO algorithm is also quite similar to it's random search counterpart.

5.3 Random Search v/s PSO Comparison

In this section, we analyze three key parameters for all scenarios discussed in section 5.1 and section 5.2. The parameters are Optimized AEP, Optimized LCOE and the run time for each scenario.

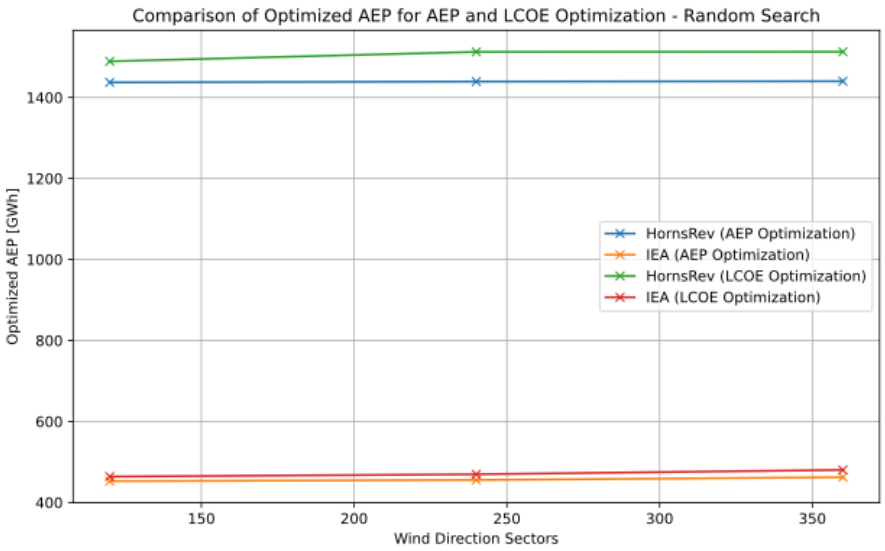

Figure 5.18: Random search - Optimized AEP values

Figure 5.18 shows the optimized AEP values for the Random Search algorithm when optimizing for both objective functions and both sites. The results demonstrate a consistent pattern that aligns with the trends identified in section 5.1, confirming our expectations. As anticipated, the HornsRev site, when optimized for LCOE, yields the highest AEP values among all scenarios. This outcome is in line with the findings presented in section 5.1. Similarly, the AEP-optimized HornsRev site closely follows this trend, delivering competitive AEP results. Furthermore, the IEA site exhibits a similar behavior, showcasing improved AEP values when optimized for LCOE compared to AEP optimization.

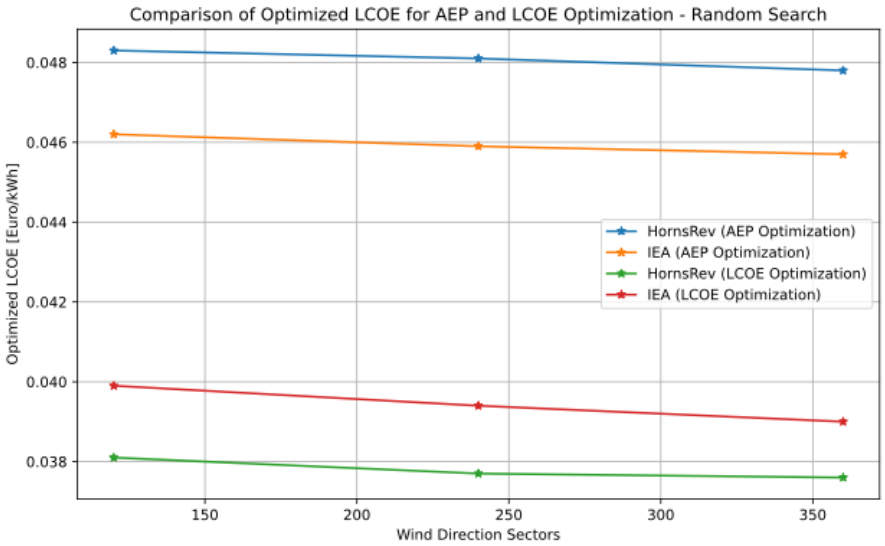

Figure 5.19: Random search - Optimized LCOE values

The LCOE values exhibit a consistent trend as illustrated in Figure 5.19, where the HornsRev site demonstrates the lowest LCOE values when optimized for LCOE. Similarly, the IEA site follows this trend, displaying lower LCOE values when optimized for LCOE as well. One intriguing observation is the disparity in LCOE values between the two sites when optimized for AEP and LCOE, respectively. Both sites exhibit a similar pattern, with significantly lower LCOE values when optimized for LCOE compared to AEP optimization. This difference in LCOE values is more pronounced than the difference observed in the optimized AEP values depicted in Figure 5.18. This divergence can be attributed to the removal of the right turbine, which results in a negligible loss in AEP but a significant reduction in LCOE. This suggests that the removal of specific turbines can lead to substantial cost savings, highlighting the importance of considering both AEP and LCOE optimization objectives in wind farm design.

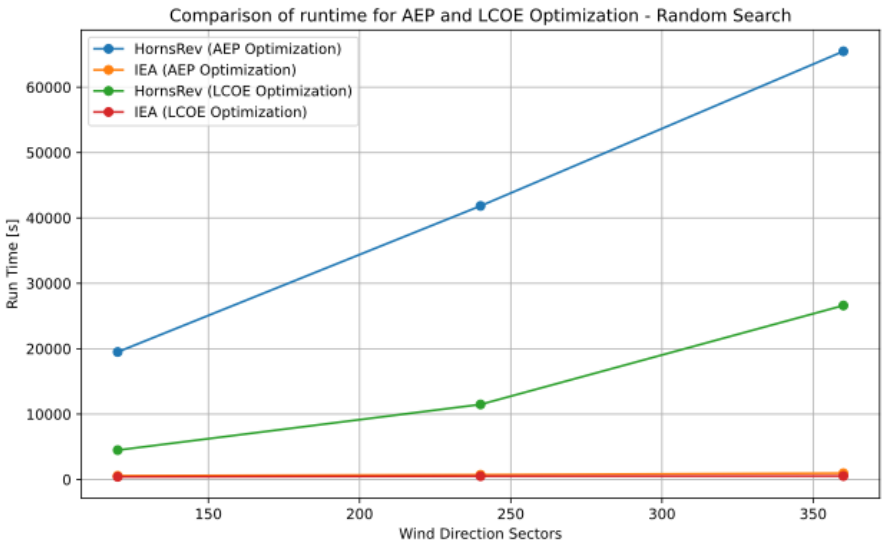

Figure 5.20: Random search runtime

The runtime values also exhibit a noticeable trend. In the case of the HornsRev site, there is an almost linear increase in runtime as the number of wind direction sectors increases. Similarly, when optimizing for LCOE at the HornsRev site, we observe a comparable trend of increasing runtime with an increasing number of wind direction sectors. Interestingly, the IEA site demonstrates distinct behavior. When optimized for AEP or LCOE, the runtime shows negligible differences. Furthermore, there is minimal variation in runtime as the number of wind direction sectors increases. This behavior can be attributed to the relatively simple wind speed distribution observed at the IEA site, as depicted in Figure 3.4 and Figure 3.3. The findings suggest that the runtime may vary based on factors such as the complexity of wind conditions and the number of wind direction sectors considered.

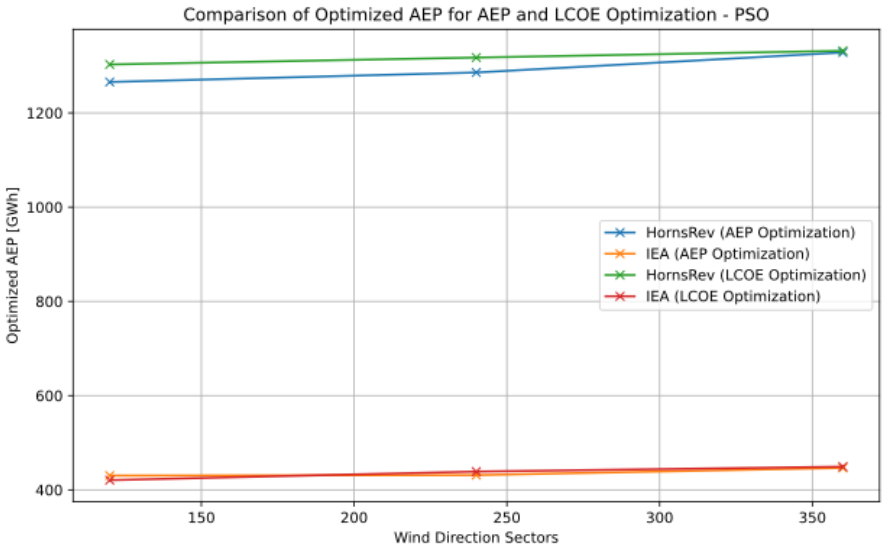

Figure 5.21: Particle Swarm Optimization - Optimized AEP values

The PSO algorithm exhibits similar trends to those observed in Figure 5.22. When optimizing for LCOE, the HornsRev site consistently yields the highest optimized AEP values, with the HornsRev site optimized for AEP closely following. Additionally, there is a slight increase in the optimized AEP values as the number of wind direction sectors increases. This trend holds true for the IEA site as well.

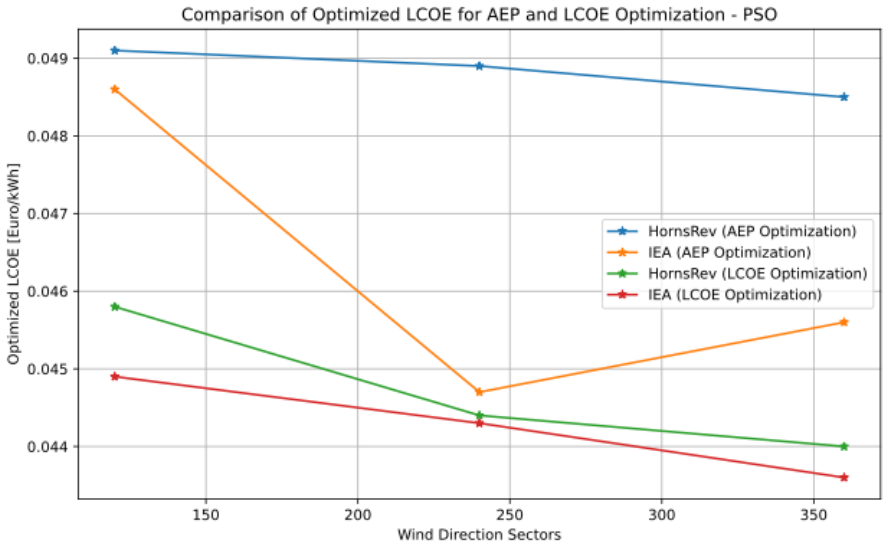

Figure 5.22: Particle Swarm Optimization - Optimized LCOE values

While most sites generally exhibit the expected trend of achieving the lowest LCOE values when optimized for LCOE, an interesting anomaly is observed in Figure 5.22 for the IEA site when optimized for AEP. At 240 wind direction sectors, the IEA site achieves the lowest optimized LCOE value, contrary to the trend observed for the other scenarios.This anomaly can be attributed to the inherent stochastic nature of optimization algorithms, such as the PSO algorithm used in this study. Optimization algorithms rely on randomization to explore the search space and find optimal solutions [52]. As a result, the algorithm may encounter variations in the optimization landscape, leading to occasional deviations from the expected trends.

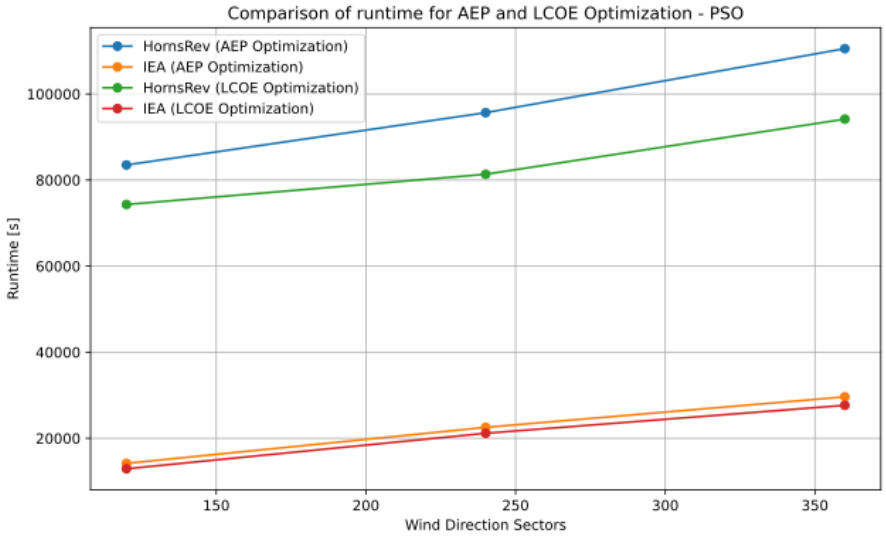

Figure 5.23: Particle Swarm Optimization runtime

The runtime values for the PSO algorithm exhibit a clear and predictable trend, as depicted in Figure 5.23. There is an almost linear increase in runtime as the number of wind direction

sectors increases. This trend is consistent across both the HornsRev and IEA sites. In contrast to the PSO algorithm, the runtime behavior for the IEA site shown in Figure 5.20 is relatively stable and displays a negligible increase as the number of wind direction sectors increases. This increase for PSO can be attributed to the nature of the algorithm requiring calculations of AEP and overall costs for the entire population. The discrepancy in runtime behavior between the PSO algorithm and the simpler IEA site emphasizes a disadvantage of the PSO algorithm. The PSO algorithm requires the calculation of AEP, overall costs, and penalties for the entire population, leading to increased computational time as the complexity of the problem increases.

CHAPTER 6

Conclusion

This thesis investigated the optimization of wind turbine layouts using two metaheuristic algorithms: Particle Swarm Optimization (PSO) and Random Search. The performance of these algorithms was evaluated based on two objective functions: Levelized Cost of Energy (LCOE) and Annual Energy Production (AEP). This chapter aims at summarizing the findings and outcomes of this study and thesis, and answer the research questions highlighted in section 1.5.

6.1 Algorithm Performance

In conclusion, the random search and PSO algorithms provide effective methods for deriving the optimal wind farm layout design by considering the defined variables and constraints. These algorithms work towards minimizing the LCOE and maximizing the AEP by exploring different turbine positions, types, hub heights, and the total number of turbines. Although random search explores the design space randomly, while PSO utilizes swarm intelligence, both algorithms aim to find the layout that strikes the best balance between power production and cost. The choice between random search and PSO depends on factors such as the complexity of the problem, available computational resources, and specific requirements. These algorithms offer valuable tools for optimizing wind farm layouts and can be adapted based on the specific needs of a project.

In the context of this thesis, both algorithms deliver a noticeable decrease in LCOE, with random search outperforming PSO by achieving an almost 40% reduction in LCOE (40%) compared to the approximately 30% decrease (30%) provided by PSO. These findings align with the observations of Feng et al. [35], who reported the superior convergence and solution quality of Random Search in wind farm layout optimization. The advantage of Random Search over PSO can be attributed to its better local search capabilities. While PSO excels at global exploration, it may struggle with local exploitation due to limited exploration of neighboring solutions. On the other hand, Random Search explores the search space extensively, allowing for the discovery of promising solutions locally [98, 48]. To enhance the performance of the PSO algorithm, improvements such as fine-tuning penalty functions and adjusting cognitive and social weights can be considered [80, 29]. These enhancements can promote better feasibility and balance between global exploration and local exploitation, enabling the algorithm to search more effectively in the search space.

6.2 Objective functions and models used

The AEP (Annual Energy Production) is calculated in this thesis by combining the NOJensen deficit model [50], the Linear Sum superposition model, and the Self Similarity blockage deficit model. These models consider factors such as wake effects and turbine spacing to estimate the power output of the wind farm. The LCOE is calculated using the Ecoeval library and

the DTU cost model implemented in TOPFARM [59]. The LCOE takes into account the costs associated with the entire life cycle of the wind farm project. This includes capital costs, operational costs, development costs, and annual expenditure costs. It's important to note that the cost calculations in this thesis are based on 2017 euro rates and may not accurately reflect the current costs in reality.

6.3 Design variables and trade-offs

The main design variable leading to a decrease in the LCOE and an increase in the AEP is the addition of a single larger turbine to replace several smaller ones. In these cases, the selection of an optimal hub height for wind turbines was found to be crucial in wind farm design optimization. Optimizing for higher hub heights can improve wind resource utilization and increase AEP. Both the random search and PSO algorithms in this study demonstrated a similar trend of pushing turbines towards the maximum possible hub height. This behavior aligns with previous research by Feng et al. [35] and Thomas et al. [98], which highlighted the positive impact of higher hub heights on AEP and wind farm performance. Although optimizing for larger hub heights increases costs due to taller towers and longer blades, the increase in AEP can potentially reduce the LCOE. The trade-off between increased costs and enhanced energy production underscores the importance of striking a balance in wind farm design optimization. This trade-off is consistent with the findings of Diaz et al. [28], who emphasized the significance of optimizing layouts to achieve a balance between AEP and construction costs.

It is important to note that in some cases, a higher number of wind turbines can lead to a lower LCOE as seen when optimizing either of the sites for AEP. This is because additional turbines can capture more wind energy and increase the overall power production, spreading the fixed costs over a larger energy output. However, there is a limit to the number of turbines that can be installed within the given constraints of the site, such as spacing requirements and available area. The LCOE objective function remains valid as it considers the trade-off between the cost of installing and maintaining turbines and the resulting energy production.

In the context of this thesis, it is also possible to have an optimal design that achieves the lowest LCOE while also having the highest AEP, as seen by optimal layouts obtained when either site is optimized for the LCOE instead of the AEP. The main design variables that impact AEP and LCOE differently is the total number of turbines and the types of turbines used. As seen in section 5.2 and section 5.1, smaller number of larger turbines perform much better than a larger number of smaller turbines. As noticed when optimizing for AEP, sometimes an increase in AEP can also cause a detrimental increase in the LCOE. This is mainly the result of adding more smaller turbines that lead to a small increase in AEP but an even larger increase in the LCOE.

6.4 Limitations of this study

It is important to acknowledge the limitations of this study. Firstly, the assumption of a uniform square boundary for the wind farm layout oversimplifies real-world conditions, where geographical constraints and non-uniform boundaries prevail. It is important to note that the impact of these factors will vary significantly across different locations. The variation in water depth, boundaries, and other site-specific characteristics underscores the need for a

location-specific approach to wind farm design optimization. Adapting the analysis to the unique conditions of each location will result in more tailored and accurate outcomes.

Additionally, assuming a constant water depth throughout the wind farm neglects the influence of varying water depths on installation and operational costs [28]. In offshore wind farm projects, water depths can vary significantly within the project area, leading to variations in foundation types, installation methods, and maintenance procedures. These variations in water depth can have a significant impact on the overall cost of the wind farm and the feasibility of different layout designs [7].These simplifications may impact the accuracy of the cost model employed in the optimization algorithms.

Furthermore, the simplifications made in the cost model employed in the optimization algorithms may affect the accuracy of the results. The cost model used in this study incorporates capital costs, operational costs, development costs, and annual expenditure costs. However, it is important to note that the cost calculations in this thesis are based on 2017 euro rates and may not accurately reflect the current costs in reality. To improve the accuracy of the cost model, it would be beneficial to update it with current cost data and consider more detailed cost components specific to the region and time of the project [83].

6.5 Future research

Future research should consider incorporating more realistic constraints and site-specific information to enhance the accuracy and applicability of wind farm layout optimization. Geographical constraints such as land topography, land use regulations, and environmental considerations should be taken into account when designing wind farm layouts. Advanced modeling techniques, such as Geographic Information Systems (GIS), can be used to incorporate these constraints into the optimization process [31]. Moreover, incorporating detailed information on water depths and their impact on installation and operational costs would provide a more realistic assessment of wind farm feasibility and cost-effectiveness [28]. In conclusion, this study conducted a thorough comparison between the Particle Swarm Optimization (PSO) and Random Search algorithms in the context of wind farm layout optimization.

Bibliography

[1] Ahmed G Abo-Khalil et al. "Dynamic modeling of wind turbines based on estimated wind speed under turbulent conditions". In: *Energies* 12.10 (2019), page 1907.

[2] Mersal Al Halabi. "Comparing wind farm production data to engineering wake model simulations". Master's thesis. University of South-Eastern Norway, 2023.

[3] Cristina L Archer and Mark Z Jacobson. "Evaluation of global wind power". In: *Journal of Geophysical Research: Atmospheres* 110.D12 (2005).

[4] Muhammad Arshad and Brendan O'Kelly. "Offshore wind-turbine structures: A review". In: *Proceedings of the Instituion of Civil Engineers – Energy* 166 (November 2013), pages 139–152. DOI: 10.1680/ener.12.00019.

[5] Christian Bak et al. "The DTU 10-MW reference wind turbine". In: *Danish wind power research 2013*. 2013.

[6] Shimaa Barakat, Haitham Ibrahim, and Adel A Elbaset. "Multi-objective optimization of grid-connected PV-wind hybrid system considering reliability, cost, and environmental aspects". In: *Sustainable Cities and Society* 60 (2020), page 102178.

[7] R. Barthelmie et al. "Modelling and Measuring Flow and Wind Turbine Wakes in Large Wind Farms Offshore". In: *Wind Energy* 12 (July 2009), pages 431 –444. DOI: 10.1002/we.348.

[8] RJ Barthelmie et al. "Meteorological aspects of offshore wind energy: Observations from the Vindeby wind farm". In: *Journal of Wind Engineering and Industrial Aerodynamics* 62.2-3 (1996), pages 191–211.

[9] Rebecca Jane Barthelmie and LE Jensen. "Evaluation of wind farm efficiency and wind turbine wakes at the Nysted offshore wind farm". In: *Wind Energy* 13.6 (2010), pages 573–586.

[10] Majid Bastankhah and Fernando Porté-Agel. "A new analytical model for wind-turbine wakes". In: *Renewable energy* 70 (2014), pages 116–123.

[11] Majid Bastankhah and Fernando Porté-Agel. "Experimental and theoretical study of wind turbine wakes in yawed conditions". In: *Journal of Fluid Mechanics* in press (2014).

[12] Lucas Bauer. *Vestas V80-2.0*. 1998. URL: https://en.wind-turbine-models.com/turbines/19-vestas-v80-2.0?picture=DP71tE3FB28.

[13] Ben Benuwa et al. "A Comprehensive Review of Particle Swarm Optimization". In: *International Journal of Engineering Research in Africa* 23 (April 2016), pages 141–161. DOI: 10.4028/www.scientific.net/JERA.23.141.

[14] Pietro Bortolotti et al. *IEA Wind TCP Task 37: Systems engineering in wind energy-WP2. 1 Reference wind turbines*. Technical report. National Renewable Energy Lab.(NREL), Golden, CO (United States), 2019.

[15] Tony Burton et al. *Wind Energy Handbook*. John Wiley and Sons, 2011.

[16] Marloes Caduff et al. "Wind power electricity: the bigger the turbine, the greener the electricity?" In: *Environmental science & technology* 46.9 (2012), pages 4725–4733.

[17] Naima Charhouni, Mohammed Sallaou, and Khalifa Mansouri. "Realistic wind farm design layout optimization with different wind turbines types". In: *International Journal of Energy and Environmental Engineering* 10 (2019), pages 307–318.

[18] Ying Chen et al. "Wind farm layout optimization using genetic algorithm with different hub height wind turbines". In: *Energy Conversion and Management* 70 (2013), pages 56–65. ISSN: 01968904. DOI: 10.1016/j.enconman.2013.02.007.

[19] Souma Chowdhury et al. "Optimizing the arrangement and the selection of turbines for wind farms subject to varying wind conditions". In: *Renewable Energy* 52 (2013), pages 273–282.

[20] Souma Chowdhury et al. "Unrestricted wind farm layout optimization (UWFLO): Investigating key factors influencing the maximum power generation". In: *Renewable Energy* 38 (1 February 2012), pages 16–30. ISSN: 09601481. DOI: 10.1016/j.renene.2011.06.033.

[21] S. Christiansen et al. *Horns Rev 1: A Case Study of Offshore Wind Farm*. Technical report. Risø National Laboratory, 2006.

[22] Yiwen Dai. *Mixed integer-discrete-continuous optimization for wind farm design*. 2021. URL: www.vindenergi.dtu.dk.

[23] Abdul Salam Darwish and Riadh Al-Dabbagh. "Wind energy state of the art: present and future technology advancements". In: *Renewable Energy and Environmental Sustainability* 5 (2020), page 7.

[24] Kalyanmoy Deb et al. "A fast and elitist multiobjective genetic algorithm: NSGA-II". In: *IEEE Transactions on Evolutionary Computation* 6.2 (2002), pages 182–197.

[25] Pedro Santos Valverde Technology Development et al. *Offshore Wind Farm Layout Optimization-State of the Art*. 2014, pages 23–29. URL: http://www.isope.org/publications.

[26] Andrej Dobnikar et al. "A niched-penalty approach for constraint handling in genetic algorithms". In: *Artificial Neural Nets and Genetic Algorithms: Proceedings of the International Conference in Portorož, Slovenia, 1999*. Springer. 1999, pages 235–243.

[27] Katherine L Dykes et al. *IEA Wind Task 37: Systems Modeling Framework and Ontology for Wind Turbines and Plants*. Technical report. National Renewable Energy Lab.(NREL), Golden, CO (United States), 2017.

[28] Hugo Díaz and Carlos Guedes Soares. "Review of the current status, technology and future trends of offshore wind farms". In: *Ocean Engineering* 209 (June 2020). DOI: 10.1016/j.oceaneng.2020.107381.

[29] Russell Eberhart and James Kennedy. "A New Optimizer Using Particle Swarm Theory". In: *Proceedings of the Sixth International Symposium on Micro Machine and Human Science* (1995), pages 39–43.

[30] US Department of Energy DOE OFFICE OF INDIAN ENERGY. *Levelized Cost of Energy (LCOE)*.

[31] Andries Petrus Engelbrecht. *Computational intelligence: an introduction*. John Wiley and Sons, 2007.

[32] M Dolores Esteban et al. "Riprap scour protection for monopiles in offshore wind farms". In: *Journal of Marine Science and Engineering* 7.12 (2019), page 440.

[33] Euronews. *European countries sign declaration to make North Sea wind power hub*. Online news article. 2023, April 24. URL: https://www.euronews.com/my-europe/2023/04/24/european-countries-sign-declaration-to-make-north-sea-wind-power-hub.

[34] Ju Feng and Wen Zhong Shen. "Design optimization of offshore wind farms with multiple types of wind turbines". In: *Applied Energy* 205 (November 2017), pages 1283–1297. ISSN: 03062619. DOI: 10.1016/j.apenergy.2017.08.107.

[35] Ju Feng and Wen Zhong Shen. "Optimization of wind farm layout: a refinement method by random search". In: *Proceedings of the 2013 International Conference on Aerodynamics of Offshore Wind Energy Systems and Wakes, Copenhagen, Denmark*. 2013, pages 17–19.

[36] Ju Feng and Wen Zhong Shen. "Solving the wind farm layout optimization problem using random search algorithm". In: *Renewable Energy* 78 (June 2015), pages 182–192. ISSN: 18790682. DOI: 10.1016/j.renene.2015.01.005.

[37] Ju Feng, Wen Zhong Shen, and Ye Li. "An optimization framework for wind farm design in complex terrain". In: *Applied Sciences* 8.11 (2018), page 2053.

[38] Jana Fischereit et al. "Comparing and validating intra-farm and farm-to-farm wakes across different mesoscale and high-resolution wake models". In: *Wind Energy Science* 7.3 (2022), pages 1069–1091.

[39] GWEC and IRENA. "Global Wind Report 2020". In: (2021). Accessed: June 6, 2023. URL: https://gwec.net/global-wind-report-2020/.

[40] M Gaumond et al. "Evaluation of the wind direction uncertainty and its impact on wake modeling at the Horns Rev offshore wind farm". In: *Wind Energy* 17.8 (2014), pages 1169–1178.

[41] Dolf Gielen et al. "The role of renewable energy in the global energy transformation". In: *Energy strategy reviews* 24 (2019), pages 38–50.

[42] Angel G Gonzalez-Rodriguez et al. "Multi-objective optimization of a uniformly distributed offshore wind farm considering both economic factors and visual impact". In: *Sustainable Energy Technologies and Assessments* 52 (2022), page 102148.

[43] Javier Serrano González et al. "Optimal wind-turbine micro-siting of offshore wind farms: A grid-like layout approach". In: *Applied energy* 200 (2017), pages 28–38.

[44] Neeraj Gupta. "A review on the inclusion of wind generation in power system studies". In: *Renewable and sustainable energy reviews* 59 (2016), pages 530–543.

[45] Antonio Herrera and Sierra Eduardo García Pérez. *Wind farm owner's view on rotor blades-from O&M to design requirements*. 2013.

[46] A Honrubia-Escribano et al. *Analysis of wind turbine simulation models: Assessment of simplified versus complete methodologies*. Technical report. National Renewable Energy Lab.(NREL), Golden, CO (United States), 2015.

[47] Weicheng Hu et al. “A novel approach for wind farm micro-siting in complex terrain based on an improved genetic algorithm”. In: *Energy* 251 (2022), page 123970.

[48] Sherif M Ismael, Shady HE Abdel Aleem, and Almoataz Y Abdelaziz. “Optimal sizing and placement of distributed generation in Egyptian radial distribution systems using crow search algorithm”. In: *2018 International Conference on Innovative Trends in Computer Engineering (ITCE)*. IEEE. 2018, pages 332–337.

[49] M Janga Reddy and D Nagesh Kumar. “Evolutionary algorithms, swarm intelligence methods, and their applications in water resources engineering: a state-of-the-art review”. In: *H2Open Journal* 3.1 (2020), pages 135–188.

[50] Niels Otto Jensen. “A note on wind generator interaction”. In: *Technical report* (1983).

[51] Ellen Jump, Alasdair Macleod, and Tom Wills. “Review of tidal turbine wake modelling methods: state of the art”. In: *International Marine Energy Journal* 3.2 (2020), pages 91–100.

[52] James Kennedy and Russell Eberhart. “Particle swarm optimization”. In: *Proceedings of IEEE International Conference on Neural Networks* (1995), pages 1942–1948.

[53] James Kennedy and Russell Eberhart. “Swarm intelligence”. In: *Morgan Kaufmann* (2001).

[54] Scott Kirkpatrick, C Daniel Gelatt Jr, and Mario P Vecchi. “Optimization by simulated annealing”. In: *science* 220.4598 (1983), pages 671–680.

[55] Elektra Kleusberg. “Wind-turbine wakes-Effects of yaw, shear and turbine interaction”. PhD thesis. KTH Royal Institute of Technology, 2019.

[56] Atul Khan Kumar. “Muhammad and Pandey, Bishwajeet.(2018)”. In: *Wind Energy: A Review Paper. Gyancity Journal of Engineering and Technology* 4 (), pages 29–37.

[57] WIRE Laboratory. “Wind Farm Layout Optimization”. In: *https://www.epfl.ch/labs/wire/research/wind-farm-layout-optimization-2/* (2023).

[58] Gunner C Larsen, Henrik Aa Madsen, and Torben J Larsen. “A simple stationary semi-analytical wake model”. In: *Proceedings of European Wind Energy Conference and Exhibition*. 2009.

[59] Gunner Chr Larsen et al. “TOPFARM-next generation design tool for optimisation of wind farm topology and operation”. In: (2011).

[60] Jens HM Larsen et al. “Experiences from Middelgrunden 40 MW offshore wind farm”. In: *Copenhagen offshore wind conference*. Copenhagen Denmark. 2005, pages 1–8.

[61] Zhenyu Lei et al. “An adaptive replacement strategy-incorporated particle swarm optimizer for wind farm layout optimization”. In: *Energy Conversion and Management* 269 (2022), page 116174.

[62] Simon B Leonhard, Claus Stenberg, Josianne G Støttrup, et al. *Effect of the Horns Rev 1 offshore wind farm on fish communities: follow-up seven years after construction*. Danish Energy Authority, 2011.

[63] Li Li et al. “Comparison and validation of wake models based on field measurements with lidar”. In: January 2016, 66 (6 .)–66 (6 .) DOI: 10.1049/cp.2016.0587.

[64] Jinxin Liu et al. “Particle Swarm Optimization Algorithm with Adaptive Inertia Weight and Its Application in Wind Farm Layout Optimization”. In: *Renewable Energy* 109 (2017), pages 133–144.

[65] Jane Marsh. “The History of Wind Energy in the United States”. In: (2021). URL: `https://environment.co/the-history-of-wind-energy-in-the-united-states/`.

[66] Seiied Mohsen Masoudi and Mehdi Baneshi. “Layout optimization of a wind farm considering grids of various resolutions, wake effect, and realistic wind speed and wind direction data: A techno-economic assessment”. In: *Energy* 244 (2022), page 123188.

[67] Parwadi Moengin. “Penalty Methods in Constrained Optimization”. In: *Lecture Notes in Engineering and Computer Science* 2169 (March 2008).

[68] Louis de Montera et al. “High-resolution offshore wind resource assessment at turbine hub height with Sentinel-1 synthetic aperture radar (SAR) data and machine learning”. In: *Wind Energy Science* 7.4 (2022), pages 1441–1453.

[69] L Mora-Lopez et al. “Wind energy in the 21st century: Economics, policy, technology and the changing electricity industry”. In: *Renewable and Sustainable Energy Reviews* 65 (2016), pages 381–394.

[70] GPCDB Mosetti, Carlo Poloni, and Bruno Diviacco. “Optimization of wind turbine positioning in large windfarms by means of a genetic algorithm”. In: *Journal of Wind Engineering and Industrial Aerodynamics* 51.1 (1994), pages 105–116.

[71] N. Moskalenko, Krzysztof Rudion, and Antje Orths. “Study of wake effects for offshore wind farm planning”. In: October 2010, pages 1 –7.

[72] H E Neustadter and D A Spera. *Method for Evaluating Wind Turbine Wake Effects on Wind Farm Performance*. 1985. URL: `http://solarenergyengineering.asmedigitalcollection.asme.org/`.

[73] Konstantinos E Parsopoulos, Michael N Vrahatis, et al. “Particle swarm optimization method for constrained optimization problems”. In: *Intelligent technologies–theory and application: New trends in intelligent technologies* 76.1 (2002), pages 214–220.

[74] Mads M Pedersen et al. “DTUWindEnergy/PyWake: PyWake”. In: *Zenodo [code]* 10 (2019).

[75] Juan-Andrés Pérez-Rúa and Nicolaos Antonio Cutululis. “A framework for simultaneous design of wind turbines and cable layout in offshore wind”. In: *Wind Energy Science* 7.2 (2022), pages 925–942.

[76] Marija Petrović-Ranđelović, Nataša Kocić, and Branka Stojanović-Ranđelović. “The importance of renewable energy sources for sustainable development”. In: *Economics of Sustainable Development* 4.2 (2020), pages 15–24.

[77] A Petrović and Ž Đurišić. “Genetic algorithm based optimized model for the selection of wind turbine for any site-specific wind conditions”. In: *Energy* 236 (2021), page 121476.

[78] Ajit C Pillai et al. “Application of an offshore wind farm layout optimization methodology at Middelgrunden wind farm”. In: *Ocean Engineering* 139 (2017), pages 287–297.

[79] Ajit C Pillai et al. “Offshore wind farm layout optimization using particle swarm optimization”. In: *Journal of Ocean Engineering and Marine Energy* 4 (2018), pages 73–88.

[80] A. K. Qin, V. L. Huang, and P. N. Suganthan. "Differential evolution algorithm with strategy adaptation for global numerical optimization". In: *IEEE Transactions on Evolutionary Computation* 13.2 (2009), pages 398–417.

[81] REN21. *Renewables 2022 Global Status Report*. Accessed: June 6, 2023. 2022. URL: https://www.ren21.net/gsr-2022/.

[82] Bosko Rasuo and Aleksandar Bengin. "Optimization of Wind Farm Layout". In: *FME Transactions* 38 (January 2010).

[83] Pierre-Elouan Réthoré et al. "TOPFARM: Multi-fidelity optimization of wind farms". In: *Wind Energy* 17.12 (2014), pages 1797–1816.

[84] Rafael Valotta Rodrigues et al. "A surrogate model of offshore wind farm annual energy production to support financial evaluation". In: *Journal of Physics: Conference Series*. Volume 2265. 2. IOP Publishing. 2022, page 022003.

[85] Rafael Valotta Rodrigues et al. "Speeding up large wind farms layout optimization using gradients, parallelization, and a heuristic algorithm for the initial layout". In: *Wind Energy Science Discussions* 2023 (2023), pages 1–30.

[86] Silvio Rodrigues et al. "A multi-objective optimization framework for offshore wind farm layouts and electric infrastructures". In: *Energies* 9.3 (2016), page 216.

[87] B. Sanderse. *Aerodynamics of wind turbine wakes Literature review B. Sanderse*.

[88] Umair Shahzad. "Application of machine learning for optimal wind farm location". In: *Journal of Electrical Engineering, Electronics, Control and Computer Science* 8.3 (2021), pages 9–20.

[89] Shubhkirti Sharma and Vijay Kumar. "A comprehensive review on multi-objective optimization techniques: Past, present and future". In: *Archives of Computational Methods in Engineering* 29.7 (2022), pages 5605–5633.

[90] Chandra Shekar and M. Shivakumar. "Multi-objective wind farm layout optimization using evolutionary computations". In: *International Journal of Advances in Applied Sciences* 8 (December 2019), page 293. DOI: 10.11591/ijaas.v8.i4.pp293-306.

[91] Farm Show. *World's first windfarm*. 1981. URL: https://www.farmshow.com/a_article.php?aid=4771.

[92] Siemens Gamesa Renewable Energy. *Why we need the European wind industry and how to safeguard it*. White paper. n.d. URL: https://www.siemensgamesa.com/en-int/-/media/siemensgamesa/downloads/en/explore/journal/siemens-gamesa-europe-wind-energy-security-white-paper.pdf.

[93] Poul Sørensen et al. "Power fluctuations from large wind farms-Final report". In: (2009).

[94] Sami Yamani Douzi Sorkhabi et al. "The impact of land use constraints in multi-objective energy-noise wind farm layout optimization". In: *Renewable Energy* 85 (2016), pages 359–370.

[95] David A. Spera. *Wind Turbine Technology: Fundamental Concepts in Wind Turbine Engineering*. ASME Press, 2010.

[96] Pradhnya Tajne. "Wind Energy Timeline–from Persian Windmills Crushing Grains to Vesta's Wind Turbines Churning Out 8 MW of Output". In: *Altenergymag. Com* (2015).

[97] PyWake Development Team. *PyWake: Open-source wind farm wake modeling tool*. https://github.com/TNWindPower/PyWake. Accessed: 2023-06-07.

[98] Jared J Thomas et al. "A comparison of eight optimization methods applied to a wind farm layout optimization problem". In: *Wind Energy Science Discussions* 2022 (2022), pages 1–43.

[99] Zilong Ti, Xiao Wei Deng, and Hongxing Yang. "Wake modeling of wind turbines using machine learning". In: *Applied Energy* 257 (2020), page 114025.

[100] Santosh Tiwari, Georges Fadel, and Kalyanmoy Deb. "AMGA2: improving the performance of the archive-based micro-genetic algorithm for multi-objective optimization". In: *Engineering Optimization* 43.4 (2011), pages 377–401.

[101] "Twenty years of offshore wind farm development in Denmark". In: (2022). URL: https://ens.dk/sites/ens.dk/files/Vindenergi/offshore_wind_development_final_june_2022.pdf.

[102] Dinh Quang Vu et al. "Evaluation of resource spatial-temporal variation, dataset validity, infrastructures and zones for Vietnam offshore wind energy." In: *Vietnam Journal of Sciences, Technology and Engineering (Serie C)* 62.1 (2020), pages 03–16.

[103] Asim Imdad Wagan, Muhammad Mujtaba Shaikh, Riazuddin Abro, et al. "Wind turbine micrositing by using the firefly algorithm". In: *Applied Soft Computing* 27 (2015), pages 450–456.

[104] *Wind Turbines: Bigger & Better*. URL: https://www.energy.gov/eere/articles/wind-turbines-bigger-better.

[105] Yu-Ting Wu and Fernando Porté-Agel. "Modeling turbine wakes and power losses within a wind farm using LES: An application to the Horns Rev offshore wind farm". In: *Renewable Energy* 75 (2015), pages 945–955.

[106] Yuan-Kang Wu et al. "Economics-and reliability-based design for an offshore wind farm". In: *IEEE Transactions on Industry Applications* 53.6 (2017), pages 5139–5149.

[107] Wing Yin Kwong et al. "Multi-objective wind farm layout optimization considering energy generation and noise propagation with NSGA-II". In: *Journal of Mechanical Design* 136.9 (2014), page 091010.

[108] Jianhong Zhang and Hao Wang. "Development of offshore wind power and foundation technology for offshore wind turbines in China". In: *Ocean Engineering* 266 (2022), page 113256.

[109] Chen Zheng. "Surrogate-Assisted Evolutionary Algorithms for Wind Farm Layout Optimisation Problem". PhD thesis. University of Waikato, 2016.

[110] Pegah Ziyaei et al. "Minimizing the levelized cost of energy in an offshore wind farm with non-homogeneous turbines through layout optimization". In: *Ocean Engineering* 249 (2022), page 110859.

{2.7182818284}ϑφερτυθιοπσδφγηξκλ